DYNAMIC SIMULATOR FOR A GRINDING CIRCUIT

By

Vaibhav Srivastava

A Thesis Submitted in Partial Fulfillment of the Requirements

for the Degree of

Master of Science

in

Mineral Preparation Engineering

University of Alaska Fairbanks

August 2017

APPROVED:

Rajive Ganguli, Committee Co-Chair
Tathagata Ghosh, Committee Co-Chair
Guven Akdogan, Committee Member
Margaret Darrow, Chair
Department of Mining and Geological Engineering
Douglas Goering, Dean
College of Engineering and Mines
Michael Castellini, *Dean of the Graduate School*

Abstract

The grinding circuit is a primary and indispensable unit of a mineral processing plant. The product from a grinding circuit affects the recovery rate of minerals in subsequent downstream processes and governs the amount of concentrate produced. Because of the huge amount of energy required during the grinding operation, they contribute to a major portion of the concentrator cost. This makes grinding a crucial process to be considered for optimization and control. There are numerous process variables that are monitored and controlled during a grinding operation. The variables in a grinding circuit are highly inter-related and the intricate interaction among them makes the process difficult to understand from an operational viewpoint.

Modeling and simulation of grinding circuits have been used by past researchers for circuit design and pre-flowsheet optimization in terms of processing capacity, recovery rate, and product size distribution. However, these models were solved under steady approximation and did not provide any information on the system in real time. Hence, they cannot be used for real time optimization and control purposes. Therefore, this research focuses on developing a dynamic simulator for a grinding circuit. The Matlab/Simulink environment was used to program the models of the process units that were interlinked to produce the flowsheet of a grinding circuit of a local gold mine operating in Alaska. The flowsheet was simulated under different operating conditions to understand the behavior of the circuit. The explanation for such changes has also been discussed.

The dynamic simulator was then used in designing a neural network based controller for the semi-autogenous mill (SAG). A two-layer non-linear autoregressive (NARX) neural network with feed to the mill as exogenous input was designed using data generated by the simulator for a range of operating conditions. Levenberg-Marquardt (LM) and Bayesian Regularization (BR) training algorithms were used to train the network. Comparison of both algorithms showed LM

performed better provided the number of parameters in the network were chosen in a prudent manner. Finally, the implementation of the controller for maintaining SAG mill power to a reference point is discussed.

Dedicated to

My Beloved Mother, Father, Brother

and

Advisors for their undying love and support.

Table of Contents

Page

List of Figures

Page

List of Tables

Page

List of Appendices

Page

Acknowledgements

According to Bhagavad Gita, a Guru is described as the "dispeller of darkness" and is considered as the supreme source of knowledge. My Gurus have been a guide to me in my research. I would first like to express my deepest gratitude to all my Gurus, Dr. Guven Akdogan, Dr. Rajive Ganguli and Dr. Tathagata Ghosh for their valuable support and guidance over the span of my studies. They have helped me at every stage of my study and inspired me towards the success of this investigation. They have allowed me to grow both personally and professionally and served as a constant source of motivation. I have learned much more from them than simply doing research. I would also like to thank the faculty members of the courses which I took during my Master's program. Their contribution in developing knowledge related to the subject and its applicability towards my research cannot be ignored.

I would further like to extend my thanks to Department of Labor (DOL) for supporting this research financially. Special thanks to supporting mines who have been a partner in the project and helped by sharing the necessary data and information related to their mine.

I am grateful to my mother, father and brother who never doubted my abilities, trusted me and stood by my side in my every endeavor. I was blessed to have numerous friends during the course of my stay in Fairbanks. The experience with them both good and bad have helped me to become the individual who I am today. Their encouragement and constant motivation have helped me to excel in other areas of life. Finally, I am obliged to the International Programs of University of Alaska Fairbanks (UAF), Graduate School, Department of Mining and Geological Engineering and other communities of UAF who treated me as a family member and made me feel at home. Even though living miles away from my home I never felt like an alien in this place. Thanks to good the people of Fairbanks.

Thank you everyone, thank you very much.

CHAPTER 1 INTRODUCTION

Grinding is an essential and an unavoidable step of a mineral processing plant. It is the last stage in the process of size reduction and plays a major role in the production of metal. The objective of a grinding process is to liberate valuable minerals from impurities. The size of the product from grinding influences the recovery rate of the mineral in the subsequent downstream process. Both, under-grinding and over-grinding can slow the recovery rate of mineral and hamper the quality of the concentrate produced.

Grinding also accounts for up to 50 percent of the entire energy consumed by a mineral processing plant. This makes it one of the most cost-intensive processes of a mineral plant. Thus, it is essential to control and optimize the grinding process. However, grinding ore is not achieved using a single process unit; instead, it is done in stages as primary and secondary grinding utilizing multiple process units. In modern grinding circuits the primary grinding is done using autogenous or semi-autogenous mills (AG/SAG) whereas a ball mill is used for secondary grinding. The circuit also constitutes multiple size classification units such as screen or hydrocyclone. The process units chosen are arranged in a desired configuration to achieve required performance decided at the design stage. Thus, the operation of the grinding becomes much more complex involving numerous variables and it becomes difficult for engineers and operators to control the process. Because the process units are inter-related to each other the performance and process variables of a process unit are influenced by the previous one, increasing further intricacy.

Grinding operations are continuous and are aimed to treat a huge amount of solids every hour. To ensure such high productivity the operations are heavily automated and controlled to prevent any process upset or equipment failure. The degree of automation applied depends upon the complexity of the process. Any operational failure in a processing unit not only results in stoppage of the particular unit but

may also lead to stopping the entire operation. The operations are controlled by control system architecture, which consists of actuators, operating under a supervisory control. The controllers operate on the basis of control objective defined when designing the controllers. Operators are equally responsible for managing the process. The role of operators in the plant varies from site-specific maintenance, sampling, to process monitoring. The control room operators make decisions in assigning set points of many operating variables based on their experience. It is common for an operator to make decisions using manual control bypassing the supervisory or expert control systems. Thus, it is essential for both operators and control engineers to have an understanding of the process.

Modeling and simulation of the grinding process was done for understanding the underlying mechanism of the process. These models were also made available to engineers and researchers in various simulation packages and were further used for:

- Equipment sizing
- Flowsheet designing and optimization
- Process diagnosis
- Economics analysis

The extensive usage of the models led to their continuous refinement and pressed the researchers to develop more sophisticated models. Despite the huge applicability, the popularity of the existing models and simulation packages is now fading. The major reason attributed for this is that most of the models are limited to the steady state approach. Steady state simulation predicts the performance of the system at equilibrium and under ideal conditions. The steady state simulator responses are based on the assumption that there are no changes in the system with time or all-time derivatives are equal to zero. They fail to describe the time dependence and true dynamics of the system. Thus, they cannot be used in studying the operational behavior of such highly automated and controlled processes. With

current advancement in sensor technology and an upsurge in the degree of automation in the industry, there is an increased demand for a dynamic simulation approach. The dynamic simulation has been effectively used in other process industries for:

- Studying complex nonlinear behavior of processes
- Transient response of a system when subjected to change
- Offline evaluation of control strategies for process optimization
- Operator training

The applicability of a dynamic simulation approach in mineral processing can help in studying the actual performance of the system over time. It can provide information about time varying non-linear characteristics of the system. This can help to simulate multiple scenarios for operator training and in the development of various control systems. Therefore, this work focuses on simulating grinding circuits using a dynamic approach and studying different condition of a grinding circuit with time. A library of models of different process units related to a grinding circuit was developed and used to construct the flowsheet of a local gold mine in operation. The data from the mine was later used to estimate the parameters and predict the response of key operating variables. Finally, application dynamic simulation was presented in the development of a neural network based controller for a SAG mill.

1.1 Circuit Description

The grinding circuit considered for the study was of a gold mine operating in Alaska. The circuit of the mine is designed to process 80-120 tons per hour of high grade gold ore. The circuit consists of primary and secondary grinding stages along with multiple classification units (Figure 1). A SAG mill is used for primary grinding which is fed by means of a belt conveyor, transporting coarse ore from a bin. Water is added to the mill along with the ore to maintain a solid concentration of around 65-75 percent weight-by-weight (w/w) within the mill. The size reduction

in the mill is achieved by the means of impact and attrition between the ore particles, ore and steel balls. The ground ore then undergoes classification through a discharge grate and trommel screen which retains the grinding media and allows fine particles and water to be discharged to a sump. The SAG discharge is then pumped to a ball mill feed box for the secondary grinding stage.

Further size reduction is achieved in an overflow ball mill. The ball mill product is then discharged on a single deck vibrating screen. The undersize of the screen is sent to the gravity circuit for recovery of gold while the oversize and gravity circuit rejects are reported to the cyclone feed pump box. The cyclone feed pump box is diluted with water which further feeds the slurry to the cyclone cluster. The feed stream to cyclone cluster is classified on the basis of size and is discharged into two streams as overflow and underflow. The overflow stream consists of fine particles which are reported to the flotation circuit for subsequent beneficiation, while the underflow stream consisting of coarse particle is reported back to the ball mill for further grinding.

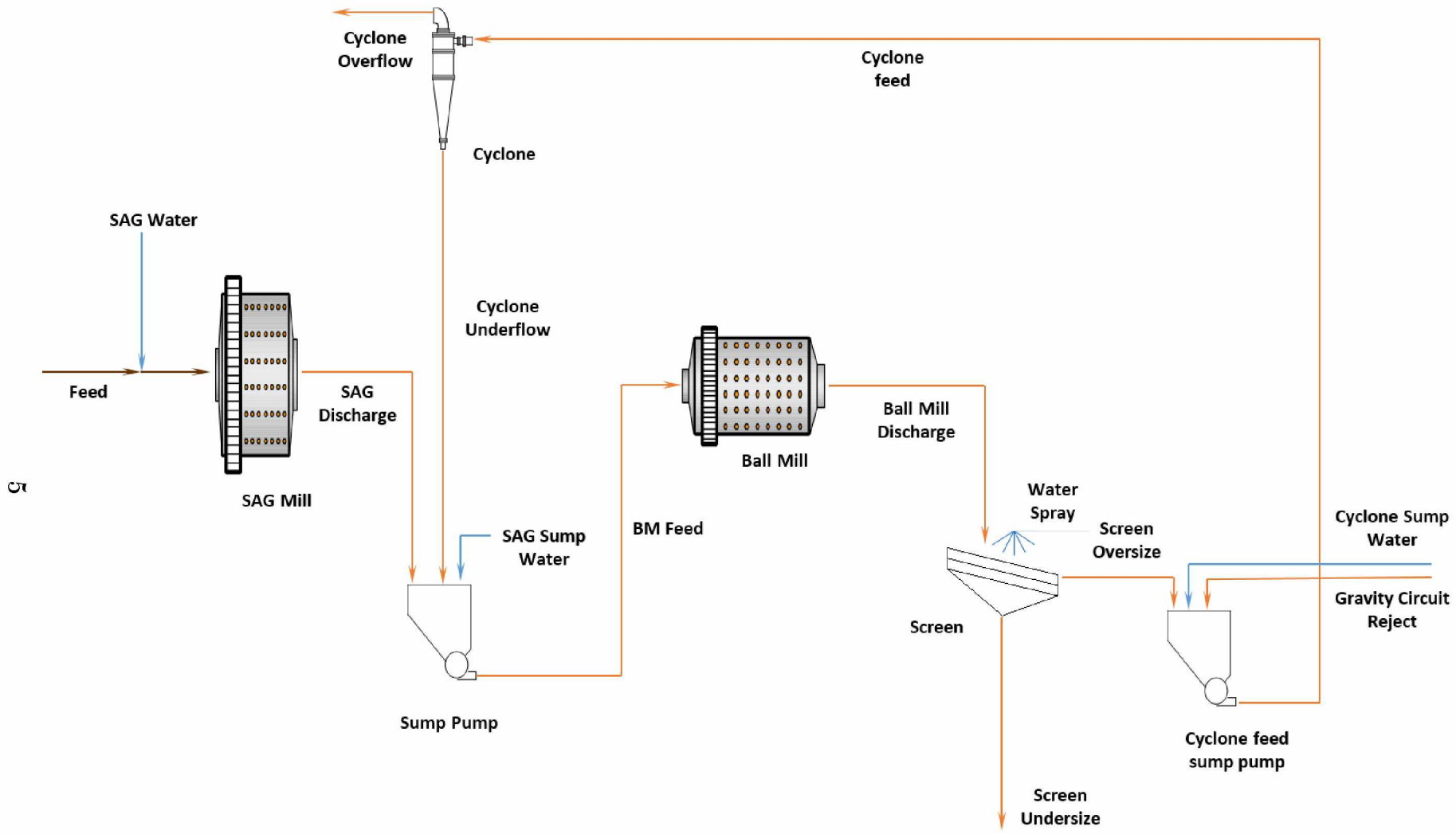

Figure 1: Flowsheet of the gold mine used for this study

1.1.1 Convention Used

The circuit shown in Figure 1 consists of multiple process units and streams entering and leaving the process units. The stream lines represent the flow of material (solid, water and slurry) from one unit to another and carry the information regarding the properties of the material. In the case of the grinding circuit the properties are the particle size distribution, mass flow rates of materials, volumetric flow rates of materials, pulp density, and specific gravity of ore and water. Because of large numbers of similar types of variables to be monitored it becomes quite difficult to keep a track of variables. To avoid such confusion, we will use the following nomenclature for representing stream properties:

- The process unit will be presented as a superscript to a particular property, e.g. feed entering the SAG mill will be represented as f^{SM}.
- The material name will be written as subscripts, e.g. solid entering the SAG mill will be represented as f_s^{SM}, where s indicates solids.

Table 1 summarizes the naming convention that will be used throughout this document for different units, materials and their properties.

Table 1: Abbreviations and Symbols Used

Process Unit	***Index***
Semi-Autogenous Mill	SM
Ball Mill	BM
Screen	SC
Hydrocyclone	Hy
Ball Mill Feed Sump-Pump	SPBM
Cyclone Feed Sump Pump	SPHY
Material	
solids	s
water	w
slurry	sl
Properties	
feed tph	f
product tph	p
mill content, t	m
feed flow rate solids m^3/hr	Q_{f_s}
Product flow rate solids m^3/hr	Q_{p_s}
feed flow rate water m^3/hr	Q_{f_w}
Product flow rate water m^3/hr	Q_{p_w}
80 % Passing size	P_{80}
% weight by weight	w/w
% volume by volume	v/v
specific gravity to be followed by subscript of material	ρ_{sl} (for soilds)

1.2 Objective

Grinding is a complex process consisting of numerous process variables, monitored and controlled during the operation. The variables of a grinding circuit are inter-related with each other and intricate interactions among them make the process more complex and difficult to understand. The process is affected by changes in input and operating conditions which alter the performance of the system. In order to understand complex behavior of the process with time a dynamic simulation approach is needed.

Therefore, the intent of this research is to develop a dynamic simulator module for a grinding circuit. The simulator module will be used in studying and analyzing time dependent behavior of the grinding plant. This will help in understanding the operation of the grinding circuit under different conditions over time and will aid in developing methods for improving the process.

The dynamic simulation approach will help in answering question such as:

- What are the effects of changing input variables and disturbance on the response of the circuit?
- How can a dynamic simulation be used in the mineral industry?
- What factors are responsible for the dynamic behavior of a grinding circuit?

In this work, the major focus is answering the first two questions. The circuit response is explained under different operating conditions followed by development of a neural network based controller for a SAG mill. The objective of the research can be laid out as:

- Development of a library of dynamic mathematical models of different process units of a grinding circuit in a MATLAB/SIMULINK environment.
- Construction of a flowsheet using a model library of a local gold mine operating in Alaska.

- Data Collection and pre-processing for model parameter estimation and validation.
- Application of dynamic models to analyze and understand complex interaction among various process variables by introducing changes in manipulated variables commonly encountered in a mill processing plant.
- Application of a dynamic simulator in controller design to control key response variables essential from the process viewpoint to ensure smooth operation.

1.3 Thesis Outline

Chapter 2 presents a literature review on research pertaining to this area to provide a background of existing models of grinding circuits, their applicability and usage in steady state simulation packages. The dynamic model development of various process units and their parameter estimation along with the approach adopted to develop the simulator module is described in Chapter 3. The model library is then used to construct the grinding circuit flowsheet of the operating gold mine. The flowsheet is then validated using real plant data. Chapter 4 presents the application of the dynamic model in studying different scenarios commonly encountered in a mill plant. The disturbance in the form of changes in throughput, feed size distribution, etc. were introduced and the effects on the response variables were analyzed. After developing an understanding of the process, the application of the dynamic simulator for controller development is presented in Chapter 5 along with conclusions and a scope for future work.

CHAPTER 2 BACKGROUND

The intent of this chapter is to review the evolution of models of the grinding circuit with reference to the process units presented in Figure 1. The chapter commences with a brief introduction on the workings of different devices of the grinding circuit and identifies key response variables associated with them. The description of different models of the process units are then reviewed and the estimation of their parameters are discussed. Further discussion on control strategies commonly employed for the grinding circuits is also presented.

2.1 Mills

A tumbling mill is a device used for achieving fine size reduction in the mineral industry. A tumbling mill consists of a cylindrical steel shell supported on both ends by trunnion bearings. The mill shell is rotated via a drive assembly connected to the girth gear bolted on one end, commonly referred as the drive end. Size reduction takes place as a result of impact, attrition and abrasion due to movement of charge which is a mixture of ore and grinding media. There are different types of mills used in the mineral industry. They are categorized on the basis of their design and the mode of operation. Conventional mills such as rod and ball mills have larger lengths as compared to their diameter and use rods or balls for grinding. Modern mills such as AG and SAG have a larger diameter compared to the length and use both ore and balls for grinding. The design difference and operating conditions are responsible for different types of breakage mechanism taking place inside the mill. For rod and ball mills attrition is dominant because of larger length and less diameter, whereas in AG/SAG impact is more dominant. Likewise, for rod and ball mills the grinding media comprise the major portion of the charge in the mill, whereas ore constitutes the major portion of charge as grinding media in AG/SAG mill.

Both types of mill are used in combination to achieve the required degree of size reduction. However, because of the high capacity and improved performance,

modern mills are preferred in industry. Currently, AG/SAG mills are widely used for primary grinding and have replaced conventional secondary-tertiary crushing stages which were followed by rod mills, while the ball mill has held its place for secondary grinding. Despite the economic advantage, challenge lies in operating these devices. The challenge is in the form of fluctuation in power draw, bearing pressure, etc. When these exceed beyond operating conditions, it leads to stoppages. The cause for these fluctuation is the variability in the nature of ore. This has led to monitoring different variables during a mill operation. The variables monitored are the combination of mechanical and process variables. The mechanical variables are not essential from a mineral preparation engineer's viewpoint but are monitored to ensure safety and prevent equipment damage. The number of such variables are less and are not of prime concern to us. Figure 2 shows an example snapshot from a distributed control system (DCS) of a mill plant from where the mill operational variables are monitored and controlled. The variables such as trunnion bearing temperature can be categorized into mechanical variables.

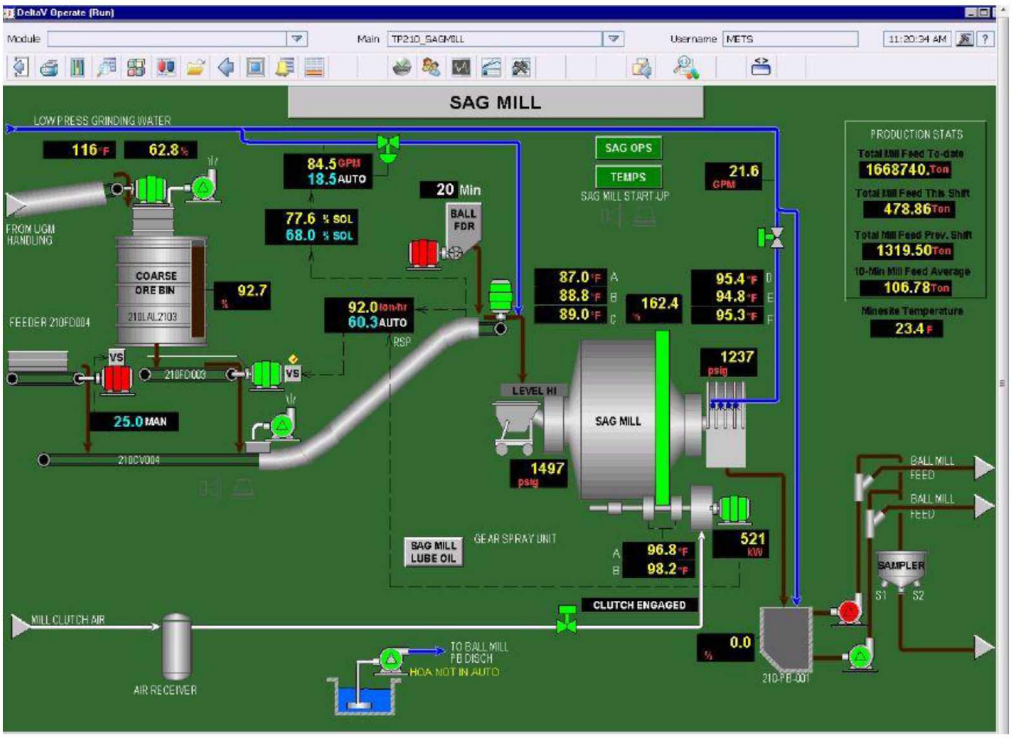

Figure 2: DCS Snapshot of SAG Mill

Shifting focus to other process variables, as the objective of grinding is size reduction, it is self-explanatory that particle size distribution is an important variable. The other I/O variables specific to the mill are summarized in Table 2:

Table 2: List of I/O variables

Variables	Type (I/O)	Measured
Feed Mass Flow rate (tph)	I	Yes
Feed size distribution (% age)	I	*
Water Volumetric Flow rate (m^3/hr or gpm)	I	Yes
Ball charge (t)	I	**
Mill Speed (rpm)	I	Yes
Mill Power (kW)	O	Yes
Bearing Pressure/ Mill Weight (psi/t)	O	Yes
Mill discharge size distribution (% age)	O	*
Solids Discharge Mass Flow rate (tph)	O	**
Water discharge volumetric flow (m^3/hr or gpm)	O	**
Mill Load (t)	O	**

* Measured at some places depends upon degree of automation of plant (size distribution for coarse particles are measured using image analysis and for fine sized particles using laser diffraction)

** Inferred or measured indirectly using soft sensors.

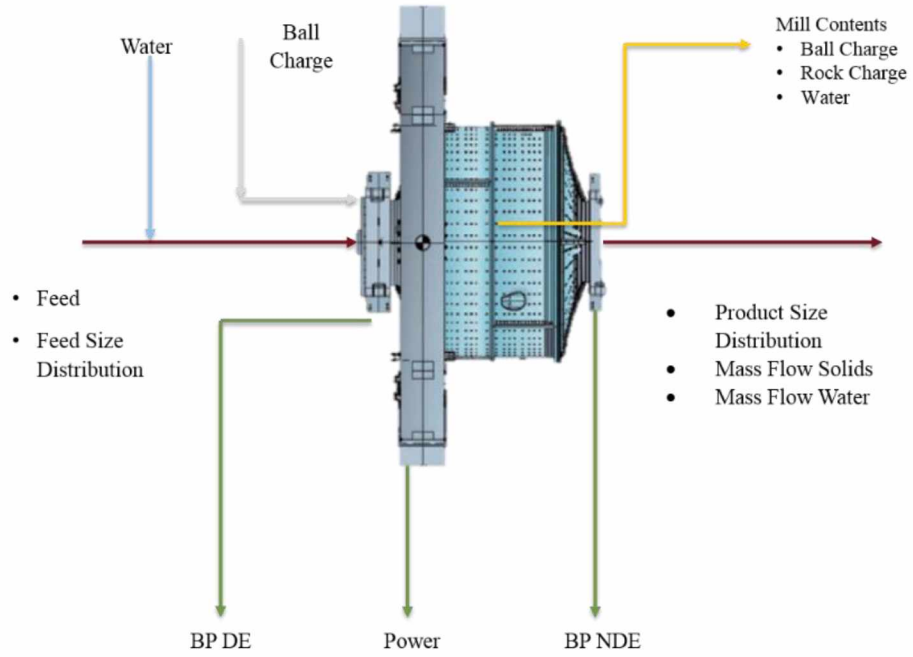

Figure 3: Schematic of tumbling mills showing different I/O variables

The models developed to predict output variables are described in the following section:

2.1.1 Mill Discharge Particle Size Distribution

It has been of great interest since 1867 to predict the energy required for size reduction and size distribution of product resulting from breakage. The first model was proposed by Rittinger to predict the specific energy required to achieve a particular degree of size reduction (von Rittinger, 1867). He proposed this energy depends upon the surface area generated from breakage of particles. Later in 1885, Kick suggested that the specific energy required is dependent on the reduction in volume of particles (Kick, 1885). His theory was held until 1952 when the relationship was modified by Bond to particle size (Wills & Finch, 2015). There existed controversies among three theories until Hukki (1961) showed that all of them were limited to specific size ranges. The most general form of all three relationships can be expressed as:

$$dE = -K \cdot dx/x^n \quad (1)$$

where, E is the specific energy (i.e. energy per unit mass), x is the particle size, K is a constant, and n is an exponent indicating the order of process.

The equation reduces to all three forms depending upon the value of n. However, the Bond theory still holds its practical demand in ball mill selection because it links the experimental work conducted by him in defining K (as work index) from industrial data for different ore types. It can also be extrapolated to a wide range of ball mills operating in industry (Lynch & Bush, 1977).

The common feature of all the above models was they tried to predict size reduction to energy supplied, but this is not usually the case. The major portion of the energy supplied to tumbling mills goes into rotating the mill and grinding media. The remaining portion is lost in the form of heat and sound generated during grinding. Only one-tenth of the energy is utilized in grinding. Another aspect which the models didn't cover was they were unable to describe the size reduction process like breakage of ore particles, distribution of breakage products in different size range, and effects of operating variables.

The first attempt to describe the size reduction process was by Epstein (1948). He statistically described breakage as a repetitive process of two events taking place within the mill:

1. Probability of breakage of particles to be selected for breakage described by a selection function, and
2. Distribution of products in different size ranges arising as a result of breakage, which was described by the appearance function.

This led to the development of different approaches to model the grinding process and to predict the size distribution of products arising from breakage. These models were:

- Matrix Model
- Kinetic Model
- Perfect Mixing Model

2.1.1.1 Matrix Model

In the matrix approach for describing the breakage process, feed and product size distribution were represented by a column vector of size n, where n is the number of discrete size ranges for both the feed and the product. The transformation from feed to product during a grinding operation was then expressed as:

$$p = X \cdot f \tag{2}$$

where X is the transformation matrix which provides information on breakage events within the size reduction device. This breakage event, as mentioned earlier, is a combination of two events repetitively taking place inside a comminution device:

1. Probability of selection of particle for breakage defined as selection function (S)
2. Breakage distribution product arising from breakage defined by breakage distribution function (B)

Thus, considering both the events mass balancing around a comminution device with no classification reduces Eq (2) to the following form:

$$p = B \cdot S \cdot f + (I - S) \cdot f \tag{3}$$

The first component on the right-hand side (RHS) of Eq (3) represents the transformed product arising from breakage, whereas the second component represents the particles which didn't undergo breakage.

The above model describes size reduction in its simplest form and is easy to use. However, the major problem lies in the characterization and determination of the selection function and breakage distribution function. Both the parameters are

dependent upon machine and mineral characteristics, but no information in evaluating the parameters was provided. Different experimental techniques and functional forms were proposed later by different researchers, and will be discussed in more detail in the next sections. The matrix approach of modeling laid the initial foundation of comminution modeling. However, it is rarely used because of its simplistic form and failure to provide the description of parameters. The model form is also time invariant and does not provide time dependency of the system.

2.1.1.2 Kinetic Model

The shortcoming of the matrix model was it could not explain the formation or the change in product with time. The limitation led to the development of the kinetic approach of modeling size reduction. Sedlatschek and Bass (1953) using experimental tests showed that grinding can be described as a rate process and follows the first order law. Extensive work was then done from 1940 to 1970 to characterize breakage and selection parameters by using continuous functional forms or discrete forms so as to completely describe size reduction. It is difficult to list the all of the references in this thesis. Austin (1971), in his review, presented the variety of approaches followed by various researchers and attempts to list similarities and differences between them. However, the model formulation was based on population balance (i.e. mass balance) and can be stated as:

For a discrete size class i, the rate of change in mass of particles in size range i is because of:

1. Rate of disappearance of particles from coarser size j (j > i) to size i is given by

$$k_j w_j(t) W \tag{4}$$

2. Rate of appearance in size i from size j

$$b_{ij}k_j w_i(t)W \tag{5}$$

3. Rate of disappearance from size i

$$k_i w_i(t)W \tag{6}$$

Thus, the overall process in mathematical form is expressed as:

$$\frac{dw_i(t)}{dt} = \sum_{\substack{j=1 \\ i>1}}^{i-1} b_{ij}k_j w_i(t) - k_i w_i(t) \tag{7}$$

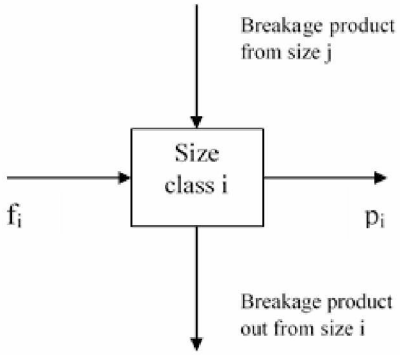

where k_i is the breakage rate for size i, $w_i(t)$ is the mass fraction in size i, W is the sum of weights in all sizes, and b_{ij} is the discretized breakage distribution function from size j to i.

The parameters breakage distribution function (B) and selection function (S) are determined from batch grinding tests conducted on particles in different size intervals. The test involves batch grinding of monosize samples and then using the following form of Eq (7) followed by log transformation to estimate the selection function:

$$\frac{dw_i(t)}{dt} = -k_i w_i(t) \tag{8}$$

Several such test conducted on different types of ore yielded the following functional form of selection function:

$$k_i = A\left(\frac{x_i}{x_O}\right)^{\alpha}\left[\frac{1}{1+(x_i/\mu)^m}\right] \tag{9}$$

where x_i is the upper size of the size range in consideration, x_o is standard size, A, m and μ are the parameters related to grinding conditions, and α represents material characteristics.

Similarly, the breakage distribution function was evaluated using back calculation methods. A functional form derived for the breakage function was (L. G. Austin & Luckie, 1972; Klimpel & Austin, 1977):

$$B(x_i) = 1 - [1 - (\frac{x_i}{x_j})]^{n_1}[1 - (\frac{x_i}{x_j})^2]^{n_2}[1 - (\frac{x_i}{x_j})^3]^{n_3} \quad (10)$$

where $B(x_i)$ is the cumulative mass fraction finer than xi, and n_1, n_2 and n_3 are constant depending upon particle shape and density.

The kinetic approach to model grinding proved to be useful and was simulated for a wide range of operating conditions, such as fully mixed and plug flow. However, the predictive capabilities of the model were limited to fine grinding, and rod and ball mill operation, and cannot be used for an AG/SAG mill. The interdependence of breakage rate and distribution functions and failure to incorporate the change in breakage rate due to change in milling conditions were the model's limitations. There was a need for a standard procedure for breakage distribution function estimation, which was later covered by the perfect mixing model.

2.1.1.3 Perfect Mixing Model

This model was regarded as a variant of the kinetic method and utilized the first principle approach of mass and volume balance to characterize mill content. Mill contents were then solved for the mill products (Napier-Munn, 1996). The underlying assumption for the model was that the contents of the mill were perfectly mixed. The rate of change of mill content was then described by the sum of physical events causing it to change, which can be listed as (Whiten, 1974):

1. Rate of fresh feed entering the mill, f;
2. Removal rate of material for breakage, R·s;

3. Distribution of breakage product A·R·s;
4. Flow of material out of the mill given by p, which is dependent on the discharge rate of mill contents.

The overall rate can be represented by following equations:

$$\frac{\partial s}{\partial t} = A \cdot R \cdot s - R \cdot s + f - p \tag{11}$$

$$p = D \cdot s \tag{12}$$

where s is mill content. Eq (11) can be solved assuming mill contents as a continuous function of size or discrete size class. However, Whiten did not provide any information on estimation of parameters and stated that parameters A, R, and D can be a function of time, feed or mill content. The uniqueness of the model lies in its simplicity to simulate a wide range of comminution devices. Assuming steady state conditions when the rate of change in mill content is 0 (i. e. $\frac{\partial s}{\partial t} = 0$) simplifies the model to Eq (13). The product size distribution can then be estimated without knowledge of the mill contents (Eq (14)).

$$(D + R - A \cdot R) \cdot s = p \tag{13}$$

$$p = DR^{-1}(DR^{-1} + I - A)^{-1} \cdot f \tag{14}$$

The steady state approximation reduces the model to a simple form which can be solved using Excel. Also decoupling of the breakage rate and breakage distribution function led to its wide usage for SAG/AG/BALL mills. Later standard test procedures were developed to estimate the parameters.

2.1.2 Power Draw

Power draw is the most important variable monitored continuously during a mill operation. Power draw provides a measure of the rate at which the energy is supplied to the mill for grinding operation. Most of the energy supplied during the grinding process goes into rotating the mill and mill charge, while some amount is

lost in overcoming friction in drive assemblies, shaft, heat, and sound. The amount of energy supplied during the operation determines the fineness of the product and is affected by changes in feed and operating conditions. Hence, it is required to maintain the power between desired set points so as to effectively utilize the energy. Operating mills more than their rated power may result in overgrinding. Exceeding operating power more than the rated power may also lead to a breakdown or motor failure which must be avoided.

Mill power draw is affected by numerous factors. Modeling power consumed by the mill has helped to understand the complex behavior of the milling process on power draw. It has aided in improving mill design parameters, the selection of an optimum operating point, and the design of efficient control systems. Initial attempts to predict power drawn by ball and rod mills was made by Bond (1961) and was based on a torque arm balance of mill charge. The charge was assumed to take the shape as shown in Figure 4. This is true in the case of ball and rod mills as the media charge more or less remains constant and is not much affected due to change in feed.

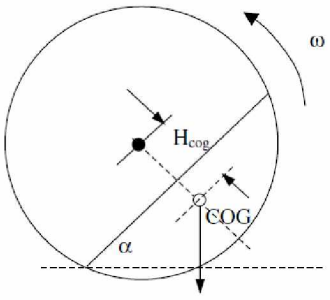

Figure 4: Power draw based on Torque arm balance (Napier-Munn, 1996)

However, charge motion varies with mill speed, media and conditions inside the mill. A correlation between charge position in terms of toe and shoulder angle was evaluated and Eq (15) was developed to determine the power consumed by the ball mill:

$$K_{W_b} = 4.879D^{0.3}(3.2 - 3V_p)fc_s\left(1 - \frac{0.1}{2^{9-10fc_s}}\right) + S_S \quad (15)$$

where K_{wb} is kilowatt per ton of balls, D is mill diameter, fcs is fractional critical speed, and V_p is the fraction of mill volume filled with ball, and S_s is ball size factor evaluated using following expression:

$$S_s = 1.102\left(\frac{B-12.5D}{50.8}\right) \quad (16)$$

where B is ball diameter (mm). A similar equation exists for the rod mill but the difference lies in its parameters. More details of which can be found in Mular and Bhappu (1978). However, the above model was based on an empirical approach and showed deviations for operating conditions different from the data set used for modeling. Another limitation was it cannot predict power draw for AG/SAG mills because of continuous variation in mill charge during the operation.

Later, a semi-phenomenological model based on charge behavior was attempted by Moys (1993) for South African mills operating at 90 to 92 percent of critical speed. The model was developed for the selection of different liner designs and provided a new approach to power draw modeling. A more theoretical approach was later presented by Morrell (1996) by applying an energy conservation principle to mill charge. The model used simplified assumptions to characterize mill charge on shape, motion, and velocity. The advantage of the model was it could be used for Ball, SAG, and AG mill power for a wide range of operating conditions. The model divides the mill power into two components which can be expressed as:

$$P_{Gross} = P_{No\ Load} + kP_{Charge} \quad (17)$$

where $P_{No\ Load}$ is power consumed by an empty mill in [kW], P_{Charge} is power consumed by the rotating charge, and k is a lumped parameter to account for heat loss and loss due to friction.

The second component of Eq (17) describes the power consumption by the charge by evaluating kinetic and potential energy of the charge. This approach evaluates three properties of the charge, summarized in Figure 5:

1. Charge shape: The assumption of charge shape used by Bond (1961) was very simplistic (Figure 4) for estimating power draw. Morrell (1992) used a glass mill along with tracers and photographic images and determined the shape of the charge at different mill filling and mill speeds. He observed that the charge actually in contact with the mill which and those hitting the mill toe constitute major portion of mill power. Those in flight constitute only about 3-5 percent of mill power and can be ignored for modeling purposes. Figure 6 shows the crescent shape of the charge which affects mill power while the mill is in motion and is referred as an active charge. This shape was taken into account for modeling purposes.

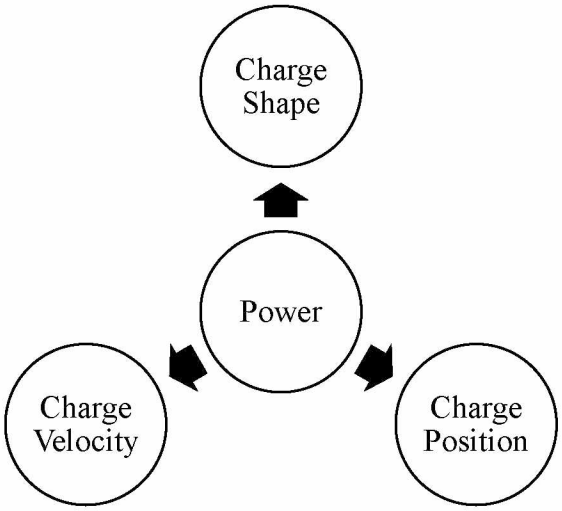

Figure 5:Charge Components

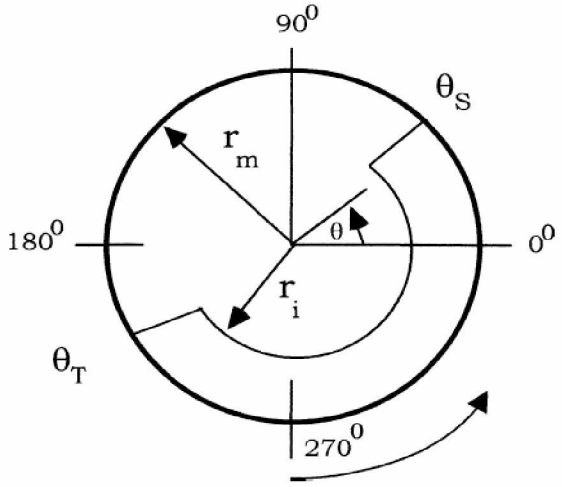

Figure 6: Charge Shape for Grate Discharge Mills

2. Charge position: After determining the charge shape it was essential to know the position to which charge rises inside the mill. The position can be used in evaluating the potential energy within the charge. Charge position was measured in terms of angular position, shoulder angle (θ_S ; maximum

angle to which charge rises) and toe angle (θ_T) point of impact of charge. The effect of mill filling and critical speed on charge position was then determined. It was observed that both mill filling and mill speed were directly related to charge position. Higher shoulder and low toe angle were reported with an increase in both variables. The empirical equation describing shoulder and toe angle position with respect to mill speed and filling were given by:

$$\theta_T = A\left(1 - e^{B(\emptyset_c - \emptyset)}\right) + \pi/2 \quad (18)$$

$$\theta_S = \frac{\pi}{2} - (\theta_T - \frac{\pi}{2})(E + FJ_t) \quad (19)$$

where Θ_T is the toe angle in radians, Ø is mill operating speed, expressed in terms of fraction of critical speed, $\emptyset_c$ is experimentally determined fraction of critical speed at which centrifuging begins and is also a function of mill filling (J_t) of form $C + DJ_t$, A and B are functions of mill filling (J_t), and E and F are functions of Ø. A, B, C, D, E and F are estimated by fitting data from laboratory mills using simple linear regression.

3. Charge velocity profile: The velocity profile of the charge which indicates the tangential velocity of charge at different radial position from the center was also determined. The velocity profile was used in evaluating the kinetic energy of the charge. It was evaluated assuming no slip condition within the charge. Because the velocity of charge varies from center to periphery, the velocity profile was normalized with respect to the speed of mill shell. The normalized velocity along with normalized radial position was used to evaluate the angular velocity at different mill fillings. The relationship was expressed in terms of rotational rate and was given by:

$$V_r = 2\pi r N_r \quad (20)$$

$$N_r = N_m r_m (r - r^*)/r(r_m - r^*) \quad (21)$$

$$r^* = zr_i \tag{22}$$

where N_r is the rotational rate, r_i is the distance of charge from center, r_m is the mill radius, and r* is the normalized radial position at point of zero rotational rate.

After charge characterization, the energy conservation was applied by considering an element of length L and width dr to within active charge. The sections were integrated to the entire charge profile. The different energies determined for the sections were:

1. Rate of increase in potential energy when charge travels from toe to shoulder position

$$PE = \rho_c V_r L dr g h \tag{23}$$

$$h = r(sin\theta_s - sin\theta_T) \tag{24}$$

2. Rate of change in kinetic energy of charge

$$KE = V_r^3 \rho_c L dr/2 \tag{25}$$

Assuming energy contained in charge is conserved and is not lost by impact to mill or as sound and heat, then the overall rate of change of energy is given as:

$$P_t = \int_{r_i}^{r_m} (\rho_c V_r L g r(sin\theta_s - sin\theta_T) + V_r^3 \rho_c L dr/2) dr \tag{26}$$

Using Eq 26 and substituting values of V_r and N_r yields:

$$P_{net} = \frac{\pi g L_m N_m r_m \left[2r_m^3 - 3zr_m^2 r_i + r_i^3(3z-2)\right] \left[\rho_c(\sin\theta_s - \sin\theta_T) + \rho_p(\sin\theta_T - \sin\theta_{TO})\right]}{3r_m - 3zr_i} + L\rho_c\left(\frac{N_m r_m \pi}{r_m - zr_i}\right)^3 \left[(r_m - zr_i)^4 - r_i^4(z-1)^4\right] \tag{27}$$

Eq (27) estimates the power consumed by the mill charge in the cylindrical section. However, it cannot be used for the mill with conical ends or large diameter mills with conical ends as the charge in the conical section consumes power and that

should be evaluated. Using a similar approach the power consumed by the conical end was evaluated and is given by:

$$P_c = \frac{\pi g L_m N_m r_m \left[r_m^4 - 4r_i^3 r_m + 3r_i^4\right]\left[\rho_c(\sin\theta_s - \sin\theta_T) + \rho_p(\sin\theta_T - \sin\theta_{TO})\right]}{3(r_m - z r_i)} + \frac{2\pi^3 N_m^3 L_d \rho_c}{5(r_m - r_t)}\left[r_m^5 - 5r_m r_i^4 + 4r_i^5\right] \quad (28)$$

After estimating the power consumed by the charge no load power was evaluated so as to get total power consumed by the mill. No load power is estimated by emptying the mill contents and running the empty mill and usually known at the mill commissioning stage. An empirical relationship was developed utilizing data of different mill size and no load power:

$$P_{No-Load} = 1.68D^{2.05}[\emptyset(0.667L_D + L)]^{0.82} \quad (29)$$

The power model was then validated utilising 45 different data sets of ball and SAG mills. The accuracy of the model was evaluated by determining the standard deviation of the predicted response which was 6.5, indicating high accuracy.

2.1.3 Bearing Pressure / Mill Load

Bearing pressure is a measure of the back pressure of a trunnion bearing lubrication system and is used for indirect measurement of mill weight. Bearing pressure along with load cell measurement data have been used in inferring mill load and total filling by researchers such as (Apelt, Asprey, & Thornhill, 2001). As the bearing pressure is positively correlated with mill filling, it is often used as a control variable for SAG/AG filling. However, Moys (1972) showed that bearing pressure is also affected by the bulk density of the charge, angle of repose, etc. Because it's a mechanical variable it can be highly unreliable as it is dependent on mechanical conditions. Models of the bearing pressure are based on the simple linear approach using the data of mill filling. No fundamental model exists to predict the variable but is still a key variable for monitoring and control purposes.

2.2 Size Classification Units

Sizing in the mineral industry is employed to ensure that the product meets the specific size requirement for the subsequent beneficiation process or the downstream process. Sizing is also used to grade material into different size ranges depending upon the process requirements. However, in grinding circuits the role of a sizing device is to act as a gatekeeper and ensure ore had been grounded to the targeted size. Sizing is usually performed with the aid of screens and classifiers. The choice of sizing device is based on the size at which material is to be classified. For coarse material, greater than 16 mesh (1 mm) screens are used. However, for material finer than 16 mesh the efficiency of the screens decreases drastically due to the effect of blinding and slower separation rate so the use of a hydrocyclone is preferred.

Sizing devices can be operated in an open circuit or in closed circuit with the comminution device. In a closed-circuit operation crushed/ground material is passed through the sizing device, the oversize of which is recirculated back for further size reduction while undersize is reported to the other units. In an open circuit, the materials after classification are directly reported to other units without any recirculation. The classification in closed circuit ensures size reduction is achieved with minimum energy requirements by preventing the overgrinding of material. Thus, the sizing device plays a crucial role in determining the energy efficiency of the plant, essential for grinding which already is known for its energy requirements.

Models of a sizing device were developed to predict the size distribution of the resulting products by encapsulating the mode operation of the device. As both screen and hydrocyclone have a different mode of operation the model varies in their formulation. However, the concept still remains the same; the models are designed to predict cut size of separation so that they can be utilized in an efficiency-curve equation.

Table 3 lists the I/O variables common to both devices and are essential from a performance assessment viewpoint. The other operating variables are discussed in specific equipment details in the subsequent section.

Table 3: I/O variables common to screen and cyclone

Variables	Type (I/O)	Measured
Feed mass flow rate (tph)	I	Yes
Feed size distribution (% age)	I	**
Water volumetric flow rate in feed (m^3/hr or gpm)	I	Yes
Oversize stream mass flow rate	O	*
Oversize stream size distribution	O	**
Water volumetric flow rate in oversize stream or flow split	O	*
Undersize stream mass flow rate	O	*
Undersize stream size distribution (% age)	O	**
Water volumetric flow rate in undersize stream	O	*

* Measurement depends upon degree of automation of plant (size distribution for coarse particles are measured using image analysis and for fine size using laser diffraction)

** Measured on daily or shift basis

2.2.1 Screen

Screens are fabricated surfaces made of metal or rubber in the form of bars, woven wire or punched plate, etc., which allow material smaller than its aperture size to pass through it, while coarser is retained on the surface. There are different types of

screens and they can be classified on the basis of design, mode of operation and their usage. Table 4 lists different methods of classification of the screens used in the mineral industry.

Table 4: Classification of screen

Design	Mode of operation	Usage
➢ Perforated or Punched plates ➢ Woven wire ➢ Wedge wire ➢ Grizzly bars	➢ Vibrating ➢ Static	➢ Sizing/Grading ➢ Scalping ➢ Media Recovery ➢ Dewatering

They are the simplest operating device in a mill plant. The screen models developed by previous researchers are based on the different constructs of probability and kinetics. The focus of these models lies in predicting the product size distribution, tonnage of material in the products and the screen efficiency.

The most popular model for the screen is the performance model which is based on partition analysis. Partition number determines the probability of particles reporting to different streams, i.e. oversize and undersize in the case of screen. Partition numbers are evaluated to determine the amount of material in the feed reporting to different streams. There are different variations of partition number models and can be used both for screen and hydrocyclone; however, they should be modified accordingly before their use. The most widely used model based on partition analysis for the screen was developed by (Whiten, 1973, 1974):

$$E(x) = \exp[-TRNf_o(1-\frac{x}{d})^2] \quad (30)$$

where $E(x_i)$ is the probability of particle to report to oversize stream, TRN is the efficiency parameter, f_o is the fractional open area, d is the screen aperture size, and x_i is respective particle size.

An extended version of the partition model was later developed by Whiten which was applicable to all classifying device i.e. screen, hydrocyclone, etc. The model was called as Whiten's model for reduced efficiency curve and was derived by fitting a function to performance analysis data of various classification devices. The model also accounted the separation inefficiency arising due to material bypass. The model equation was given by:

$$E(x_i) = \frac{e^{\propto x_i} - 1}{e^{\propto x_i} + e^{\propto} - 2} \tag{31}$$

where $E(x_i)$ is the Probability of particle to report to oversize stream, α is the efficiency Parameter, and x_i is the reduced size x_i/x_{50}.

2.2.2 Hydrocyclone

A hydrocyclone is a fluid flow operating device that utilizes centrifugal force to promote the separation process. Due to simplicity in structure cyclones are the most widely used devices in processing industry for separating particles below 300 microns. Figure 7 is a schematic of hydrocyclone showing different components of a cyclone design. It consists of four major components; the feed inlet, the cylindrical section, apex and the vortex finder.

When the slurry is fed to a cyclone the particles within the slurry are subjected to an outward centrifugal force and an inward drag force (Figure 8). As a result, the particles based on their settling rates are segregated within the cylindrical section. The centrifugal force accelerates the settling rate of particles. The faster settling particles, which are coarser in size and have high specific gravity, move towards the periphery and are discharged from the apex, while the slow settling particles which are finer in size and have less specific gravity are trapped at the center. Because of

a zone of low pressure in the center the finer particles are discharged from the vortex finder thereby achieving the separation.

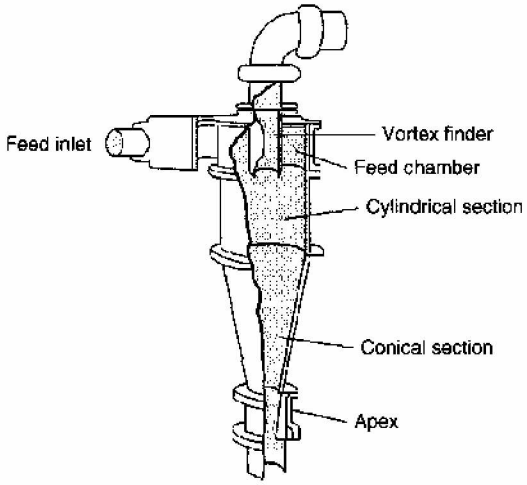

Figure 7: Schematic of hydrocyclone

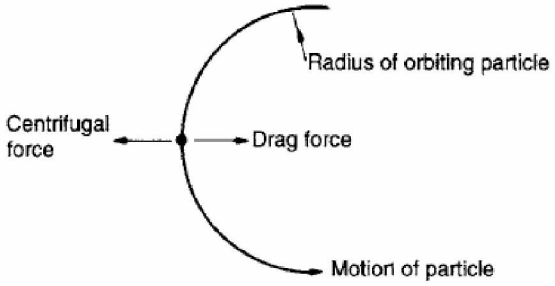

Figure 8: Forces acting on Particle (Wills & Finch, 2015)

There are many operational variables of prime importance which control the cyclone performance. The common variables monitored in an industry are:

- Feed Percent Solids
- Feed Flow rate
- Feed Pressure

The mentioned variables are used for adjusting the cut/separation size and thus the performance of the cyclone. Online monitoring of cyclone performance is difficult as overflow and underflow particle size distribution are rarely measured. However, most of the cyclone model are focused on utilizing the above-mentioned operational variables to predict the cut size, flow split and efficiency parameters. They are then utilized in an efficiency function such as described in Eq (64) to predict the size distribution of product streams.

There are a variety of models for the hydrocyclone. They are based on the theoretical approach of fluid flow, empirical approach and semi-empirical approach

(a combination of both). Chen, Zydek, and Parma (2000) in their review compared all the available models of different formulations and stated that none of the models can be employed to most of the cyclones. Because of the complex nature of two-phase fluid flow and different flow conditions during the operation, it is difficult to develop a single model for a cyclone. Based on this review and also the applicability of existing hydrocyclone models it can be stated that an empirical model performs well in the mineral industry. The three most popular empirical models are discussed below.

2.2.2.1 Lynch & Rao

This model is of purely empirical construct and was developed by Lynch and Rao (1975) based on different experimental studies conducted using limestone. Experiments were conducted using different designs and operating conditions similar to that of a plant to derive a relationship with d_{50c}, feed flow rate, and flow split. This relation is derived was:

$$log d_{50c} = 4.18D_o - 5.43D_u + 3.04D_i + 0.0319f_s - 3.6Q_f - 0.0042(\% + 420) + 0.0004(\% - 53) \quad (32)$$

where, f_s is the percent solid by mass in feed, Q_f is volumetric flow rate of feed (m^3/s), D_i, Du, D_o are cyclone inlet, apex and vortex diameter respectively (m), and $d50_c$ is the cut size (µm).

The cyclone used during the study was Krebs, therefore, the model should be carefully used when applied to another cyclone. Also, the model needs to be scaled for when applied to other material. The following correction factor should be used when the model is applied to another mineral of different density:

$$(d_{50c})_1/(d_{50c})_2 = [(\rho_{s1} - p_l)/(\rho_{s2} - p_l)]^{0.5} \quad (33)$$

where 1 and 2 are in reference to minerals of density p_{s1} and p_{s2}, respectively. The d_{50c} is used in the Whiten efficiency curve model to predict product size distribution.

2.2.2.2 Nageswararao Model

This model was developed using similar approach, by conducting experiments on Krebs cyclone of diameter ranging from 102-381 mm with limestone as the test material. The model is of the phenomenological construct and had undergone modification during the years of its usage. It is used as a prime model in many simulation packages such as JKSimMet, Limn, etc., (Napier-Munn, 1996). The model considers the effect of centrifugal forces and hindered settling with other fluid flow parameters to describe cyclone performance. Table 5 list design and the fluid parameter which were considered for modeling (Nageswararao, Wiseman, & Napier-Munn, 2004).

Table 5: List of design and fluid parameters (Nageswararao et al. 2004)

Design	Fluid
• Cyclone Diameter, Dc • Reduced vortex finder, Do/Dc • Reduced spigot, Du/Dc • Reduced inlet, Di/Dc • Reduced length Lc /Dc • Cone angle, θ	• Euler's and Froude numbers • Hindered settling factor, λ

The model was formulated using dimensional reasoning on above parameters assuming design parameters follow a monomial power function relationship. The parameters were evaluated using an extensive database of Lynch and Rao (1975) and Nageswararao. The model equations are given by:

$$\frac{d_{50c}}{D_c} = K_{D0} D_c^{-0.65} (D_o/D_c)^{0.52} (D_u/D_c)^{-0.47} (D_i/D_c)^{-0.5} (L_c/D_c)^{0.2}\ \theta^{0.15}\ \lambda^{0.93} (P/\rho_p g D_c)^{-0.22} \quad (34)$$

$$R_f = K_{W0} (D_o/D_c)^{-1.19} (D_u/D_c)^{2.4} (D_i/D_c)^{0.5} (L_c/D_c)^{0.22}\ \theta^{-0.24}\ \lambda^{0.27} (P/\rho_p g D_c)^{-0.53} \quad (35)$$

$$R_v = K_{V0}(D_o/D_c)^{-0.94}(D_u/D_c)^{1.83}(D_i/D_c)^{0.25}(L_c/D_c)^{0.22}\ \theta^{-0.24}\ (P/\rho_p g D_c)^{-0.31} \quad (36)$$

where K_{Do} is the constant incorporating feed characteristics, K_{Wo} is the constant in water recovery relationship, K_{Vo} is the constant in slurry volume recovery relationship, R_f is the recovery of water to underflow, R_v is the volumetric yield of feed slurry to underflow, g is acceleration due to gravity constant, and ρ_p is pulp density

The variable λ is defined as:

$$\lambda = C_v/(1 - C_v)^3 \quad (37)$$

C_v is volumetric fraction of solids in feed slurry.

2.2.2.3 Plitt's Model

Plitt's model is based on a similar approach and predicts the $d_{50c,}$ pressure drop, flow split and efficiency of separation. The data is then utilized in an efficiency equation curve derived by (Plitt 1976; Reid 1971). This model had been extensively used and can be modified to a wide range of operating condition by carefully adjusting the model constant. The efficiency equation used in Plitt's model is given by:

$$E(u_i) = 1 - e^{-ln2\frac{d}{d_{50c}}} \quad (38)$$

The model describes most of the situation very well but relies on Plitt's efficiency curve equation and fails to explain all the different shapes of the reduced efficiency curve (Nageswararao, 1999).

Based on our discussion so far it is evident that the grinding process is highly complex with numerous process units. Because of so many processes simultaneously taking place and the continuous nature of the operation, mill plants use a high degree of automation. The degree of automation also depends upon the complexity

of the process, required production rates and types of equipment used. Generally, high capacity plants and cost intensive processes use higher degrees of automation. The automated plants employ controllers to manage any process. Therefore, the next section focuses on discussing the control techniques employed in mineral plants.

2.3 Control System in Grinding Circuits

The objective of a mineral processing plant is to produce the metal concentrate in a most economical manner. This is ensured by application of different control strategies being developed by the industries to optimize the process parameters and minimize downtime. The control strategies which are applied monitor the state of the system, response variables, and adjust the operating conditions of the equipment and process in case of any deviation. The change implemented is subjected to a performance index determined on plant requirements. As mineral processing operation involves numerous processes simultaneously taking place as a chain of events in a sequence, it becomes difficult to really define a plant-wide optimization/performance index. This also poses problems in deciding which specific variables to monitor and control.

Hence, the control task is disintegrated to specific processes, i.e. grinding, flotation, separation, etc., taking place in a mineral processing plant with separate objectives and control strategies for each process. For a grinding operation, the aim is to achieve an adequate degree of liberation. However, liberation is difficult to measure. Hence, the control task boils down to controlling product particle size distribution (Hodouin, 2011). However, care is also taken to prevent overgrinding of material. As grinding alone accounts for a significant amount of production cost, overgrinding results in extraneous energy consumption, hampers the recovery rate of mineral and creates unnecessary problems in dewatering circuits.

There are different control architectures which are used in mineral industry and are common to other process industries as well. The choice of controller and

architecture needed is dependent upon many factors such as the amount of information available about the process dynamics, disturbance within the process, interaction among the process variables, etc. Wei and Craig (2009) in their survey of 68 different milling circuits of different types (rod-ball, sag-ball, etc.) presented the control practices and technologies widely used for grinding circuits (Figure 9). According to their survey, propotional-integral-derivative (PID) controllers were at the top of the chain as they are easy to design and implement. However, over the last two decades, most of the grinding plants are now adopting multivariable controllers and model predictive controllers for more sophisticated process units such as AG/SAG. The reason for such a dramatic shift is because of complexity in operating these devices and their susceptibility to ore variability.

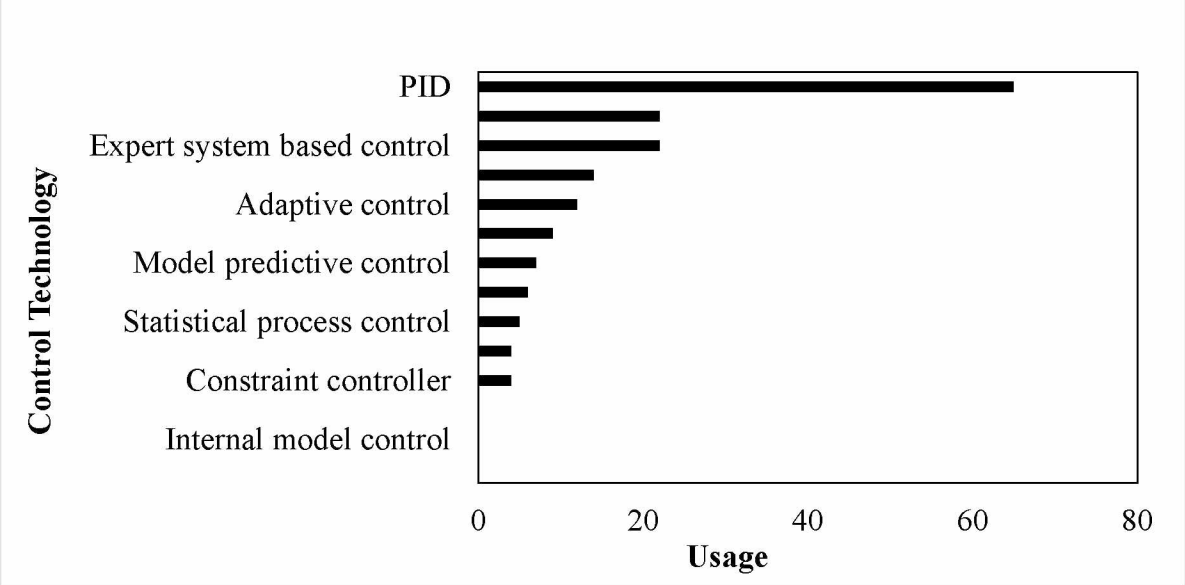

Figure 9: Control techniques used in mineral industry (Wei and Craig, 2009)

It is difficult to review and summarize all the control technologies in this study but the underlying principal and methodology of all control systems remain more or less the same. To understand the application of a control system the problem statement must first be summarized.

2.3.1 Control Problem

The major disturbances in a grinding circuit are feed particle size distribution and ore hardness. A conventional grinding circuit as shown in Figure 10 was treated as a two input-two output system assuming that pump-sump level is controlled by a local control loop, with two main control objectives.

1. Maintain product particles smaller than the desired size.
2. Maximize the recirculating load so as to minimize the energy consumed per ton of ore.

The manipulated variable of the system consists of fresh ore feed rate and water addition to the sump.

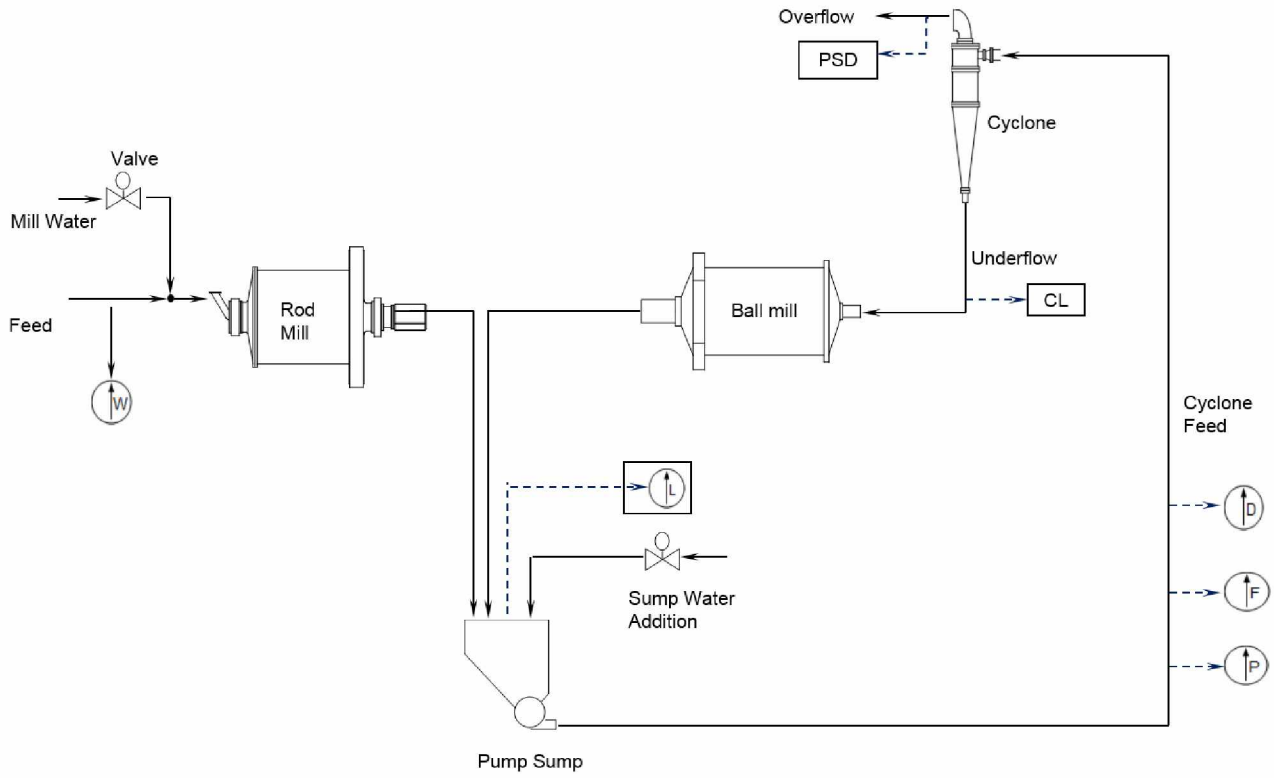

Figure 10: Conventional rod mill ball mill circuit

Any control strategy being developed is focused on finding the relationship between the manipulated and controlled variable. For the case presented above four different relationships exist:

- Feed affecting the product particle size distribution (PSD).
- Feed affecting the circulating load (CL)
- Sump water affecting the product PSD
- Sump water affecting the CL

The method employed to describe the above relations constitutes the type of control technology. If the relationships between all the manipulated and control variables are strong the process is called coupled and poses interaction problems among the controllers. Coupling is a common problem for grinding circuits.

The application of three different control technologies (PID, neural network and MPC for the circuit shown in Figure 10) was reviewed and is described below.

2.3.2 Decentralized PID

The decentralized PID is a typical form of PID controller used for the multivariable interacting process with feedback loops. Linear process models are developed by introducing step changes to the manipulated variables. The process models are of the form of a transfer function model usually of order one and two depending on the complexity of the process (Eq 39). Multiple single-input/single-output (SISO) loops are designed utilizing the process model to control the system. The network architecture is then decided based on I/O pairing and may involve a decoupler to control the effect of interaction.

$$y(s) = \frac{K_p\ e^{-\tau s}}{(T_p s+1)}\ u(s) \tag{39}$$

where Y(s) is the control variable, u(s) is the manipulated variable/also the controller output, K_p is process gain, τ is dead time, and T_p is the process time constant.

Figure 11 shows two typical decentralized PID loops used by (Pomerleau, Hodouin, Desbiens, & Gagnon, 2000) to compare it with the multivariable control scheme for such conventional circuits. Gij represents the transfer function relation between the i^{th} manipulated variable and j^{th} controlled variable derived using Eq (39), and G_{c1} and G_{c2} represent multi-loop controllers.

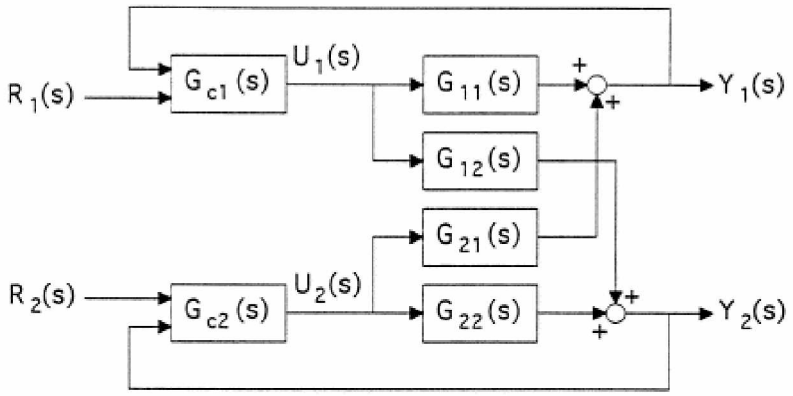

Figure 11: Decentralized PID (Pomerleau et al. 2000)

However, for all MIMO process such a controller poses a problem in tuning because of the presence of multi-loop and interaction which also limits the performance of the controller.

2.3.3 Neural Network Based Controller

Neural network based controllers employ the use of neural networks (NN) to approximate the relationship between I/O variables of a system. Because of the great ability to model any complex and non-linear relationship and adaptive nature they have been used widely in process control areas. Stange (1993) demonstrated the application of NN for a typical closed loop grinding circuit (Figure 10) in controlling the overflow size of a hydrocyclone classifier. He presented two control strategies. The first strategy involved the variables such as cyclone overflow percent solids, feed pressure and desired size in product as the set point was used to train the network (Figure 12). The network predicted the required feed percent solids

(amount of water that must be added) to maintain the product size set point (Figure 10).

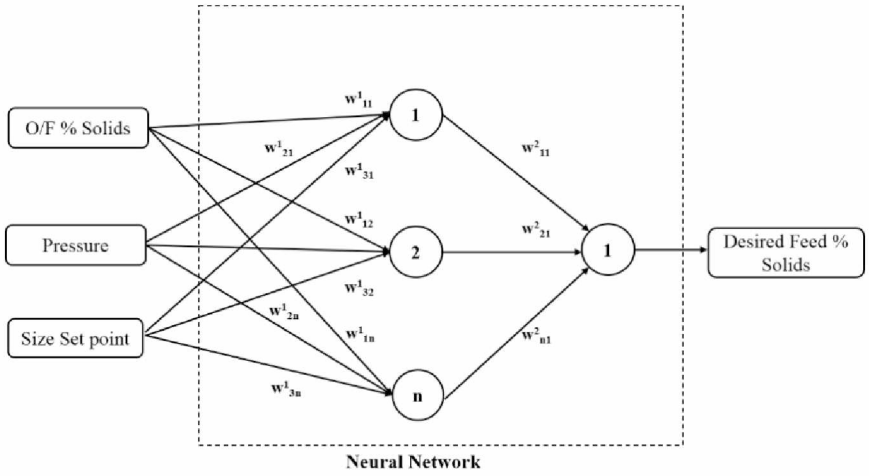

Figure 12: NN based model to control hydrocyclone overflow size; scheme 1

In the second strategy the overflow (o/f) percent solids, pressure and feed percent solids were used to predict overflow size (Figure 13). The feed percent solid was then adjusted (by varying water to the cyclone sump) as a part of the feedback loop. Steady state simulation runs were performed to generate data for a wide range of operating conditions for the variables shown in Figure 13 which were used to train the network.

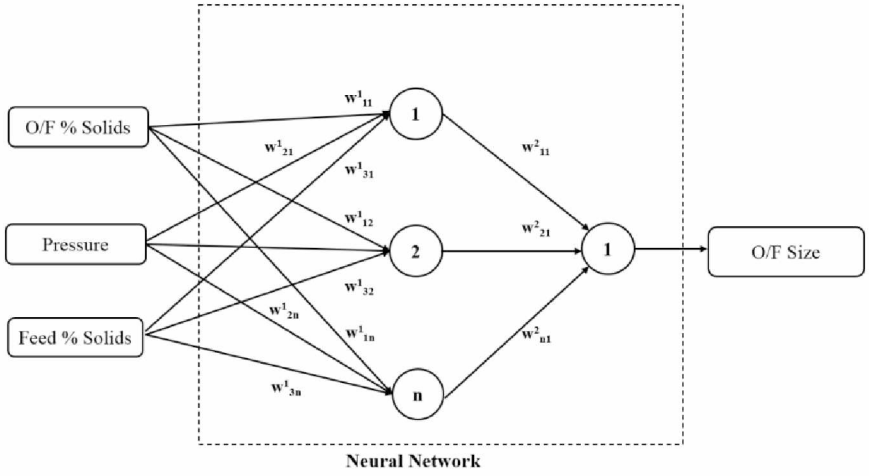

Figure 13: NN based model to control hydrocyclone o/f size scheme 2

In a similar attempt, Flament, Thibault, and Hodouin (1993) demonstrated different control strategies based on the neural network model. The DYNAFRAG grinding circuit simulator was used to develop neural network control strategies to control cyclone oversize by varying sump water addition. Three different neural network controllers developed were:

- Direct neural controller
- Inverse neural controller
- Inverse neural controller with weight adaptation

Past values of the response and manipulated variables (i.e., percent passing 200 mesh cyclone overflow size, water addition to the sump and circulating load) were used to develop the three different types of controllers mentioned above.

The application of NN has not been limited to controlling cyclone particle size but also has been applied to SAG mills for feed particle size distribution prediction. Pani and Mohanta (2015) demonstrated the application of time delay neural network (a class of NARX) to predict and fine-tune the measurement of feed particles size based on the previous measurement. As feed particle size is a major disturbance in the grinding circuit, prediction of it may aid in taking necessary control action beforehand.

The only limitation of NN is their dependency on the data on which they are trained. Hence poor data can result in a network failure. Therefore, the data set should be carefully chosen such that it captures the entire dynamics of the system.

2.3.4 MPC

Model predictive control is a control technique based on numerical optimization. Similar to multi-loop PID it requires step response model (transfer function relationship) to be derived in between the manipulated and control variable. The relationship is then utilized in a predictive control algorithm. The algorithm predicts the future plant responses using a system model and adjusts the

manipulated variable accordingly to optimize the performance with respect to a performance index. Figure 14 shows the MPC working philosophy in which the prediction at k^{th} time instance of all the control variables are made. The changes in the manipulated variable are implemented up to the control horizon so that the controlled variables follow the reference trajectory (desired set point).

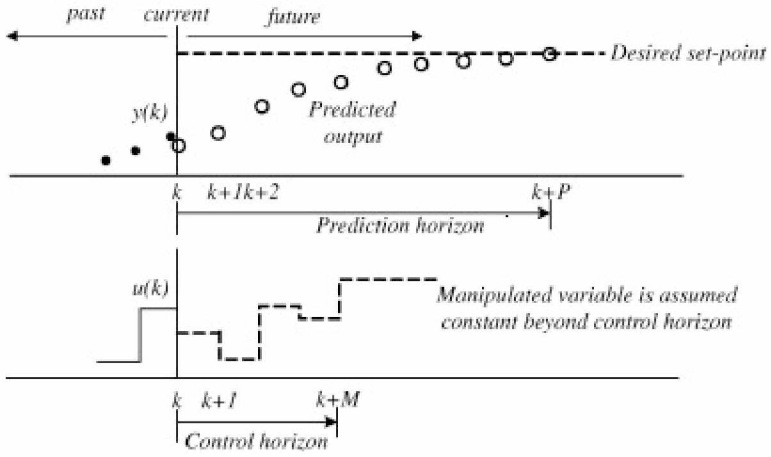

Figure 14: MPC Scheme (X.-s. Chen, Zhai, Li, & Li, 2007)

The major advantage of MPC is that it is simple to design and can control a system with a large number of input variables. MPC has found wide application in various chemical and process industries (Ramasamy, Narayanan, & Rao, 2005), but its application to mineral processing is limited and gaining momentum. Researchers have tried to incorporate the MPC scheme to grinding circuits and have found improved response in circuit performance using MPC scheme rather than conventional PID loops. The wide acceptance of MPC over conventional PID controllers is because it offers the following advantages:

1. It can easily be used to model and control any non-linear process of a MIMO system.
2. It predicts future behavior of the process with large time delays and time-varying characteristics.
3. Constraint on both manipulated and controlled variables can be managed easily.

4. The model mismatch problem is minimized.

X.-s. Chen et al. (2007) demonstrated the application of MPC to ball mills operating in a closed circuit with a hydrocyclone classifier. The circuit was similar to that shown in Figure 10, instead the ball mill was directly fed by the feeder. The authors reported that MPC leads to a smoother response of manipulated variables with stably maintaining the controlled variable. MPC application was also extended to individual process unit involving MIMO such as a SAG mill. Salazar et al. (2014) and Apelt and Thornhill (2009) applied the MPC strategy to a SAG mill to control mill power, fractional filling, and product flow rate by changing feed rate, water flow rate and mill operating speed. The MPC was able to reestablish the control in case of power fluctuation and showed better performance when compared to PID.

However, irrespective of the of type control technique employed in mineral industry, it is essential to have knowledge of the process for which control systems are being developed. Steady state modeling and simulation has proven to be useful tools in understanding process dynamics and to some extent in the development of control strategies. However, with an advancement in computational power, we should seek and progress toward the dynamic modeling approach.

Napier-Munn and Lynch (1992), imagined the future of comminution modeling as that which can be incorporated in dynamic simulation frameworks for the design of control system and operator training. Attempts made by Liu and Spencer (2004) to simulate a grinding circuit dynamically has gained a lot of attention. Similar attempts by Sbárbaro (2010) in developing a dynamic model library for comminution circuits for model based control system design has opened new gateways for practicing dynamic modeling. It is therefore our interest to explore more avenues of dynamic simulation approaches in the mineral industry. Most of the research pertaining to this area was limited to the steady state approach or was specific to a particular mine. The objective of this research is to produce a library of more generic and sophisticated models which should be easy to use, and to

demonstrate the application of developed dynamic models in understanding the grinding process and in the development of model-based control design.

CHAPTER 3 DYNAMIC MODEL DEVELOPMENT

Modeling a grinding process is a complex task as it involves multiple and interacting process units. The complexity increases due to the presence of two different phases, i.e., water and solids, which should be tracked during the simulation. In an industry, the process is also affected by startup procedure, controllers and natural variations making dynamic modeling much more difficult. To model such complex systems, it is essential to divide the modeling task into modules and subsystems. The circuit can be divided into smaller subsystems representing equipment. The equipment can be further subdivided into smaller subsystems to finally represent a model of different variables. All the subsystems at the end can be grouped to produce the flowsheet of the circuit (Figure 15).

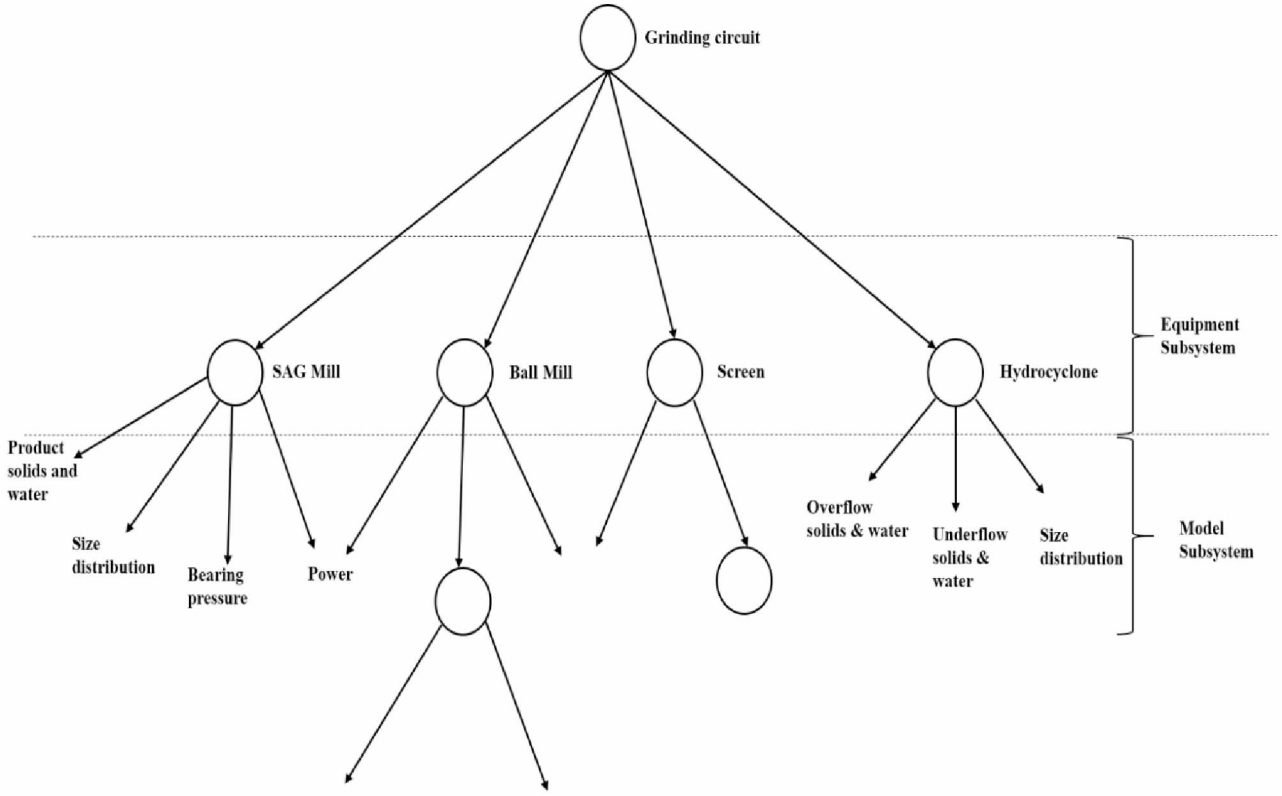

Figure 15: Typical representation of subsystems (adapted from Asbjörnsson, 2013)

The modular approach will make the modeling and programming task easy. It will also allow easy transfer of data from one equipment to another. The data contains information on variables:

- Size distribution
- Solid flow rate
- Water flow rate

It will also prove beneficial in the long run in adding a specific component to a model or new equipment in the flowsheet thereby increasing predictability of the simulator. Thus, the overall model development task can be outlined as:

1. Identification of different input and response variables associated with equipment.
2. Development of the models to predict the response variable of the equipment.
3. Estimation of model parameters from process and design data.
4. Validation of the model by simulating under the same operating conditions as that of the mill plant and comparing the results with actual measurements.

3.1 SAG Mill

Semi-autogenous (SAG) mills are a class of equipment used for primary grinding and are the most preferred piece of equipment in any modern mill plant design. The special feature which makes these devices popular is the reduced operating cost, less media consumption and the ability to treat a wide variety of ore types (Napier-Munn, 1996). However, they are complex in terms of their operation and control. To model SAG mills different process occurring within the mill should be taken into consideration. Figure 16 lists the main input and output variables associated with this equipment.

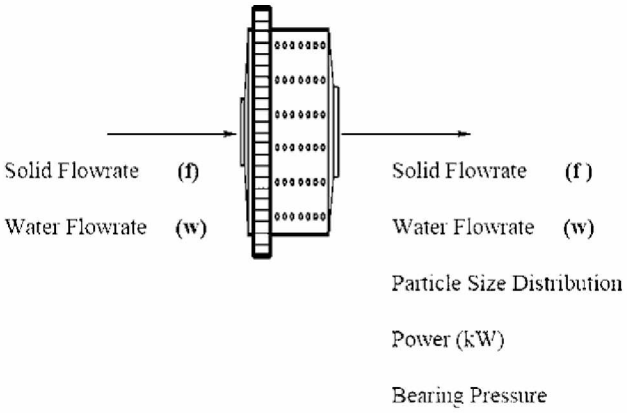

Figure 16: Schematic of a SAG mill listing I/O variables

The grinding process in a SAG mill can be divided into two major parts first being the size reduction occurring because of impact and abrasion, and second being the discharge of material out of the mill. To model this, Whiten's popular content based model was chosen. The model assumes grinding as rate process under perfect mixing conditions and utilizes a first principle approach of mass and volume balance to solve for mill content (Whiten, 1974). The information about the mill content is then latter used to solve for product, thus the model equation consists of two parts:

1. Rate of change in mill content due to incoming feed, breakage and distribution of breakage product in different size ranges given by:

$$\frac{\partial m^{SM}(t)}{\partial t} = AR^{SM}s^{SM} - R^{SM}s^{SM} + f^{SM} - p^{SM} \qquad (40)$$

where m^{SM} (t) is column vector (n x 1) representing mass of solid in discrete size fraction within the mill, f^{SM} is column vector (n x 1) representing mass of solid in discrete size fraction in feed, p^{SM} is column vector (n x 1) representing mass of solid in discrete size fraction, A is the appearance function or breakage distribution function (lower triangular) describing breakage distribution product in different size ranges, R^{SM} is breakage rate constant (diagonal matrix) indicating rate of breakage of particles, and t is the time

2. The transport of breakage products to the discharge stream is:

$$p^{SM} = D^{SM} \cdot m^{SM} \quad (41)$$

where D^{SM} is the discharge rate function (diagonal matrix) describing rate of discharge of breakage product.

To solve the above model, it is important to have information about the parameters. The three major parameters in the above model are the breakage rate constant (R), discharge rate (D) and appearance function (A). The parameters and their estimation are described in Figure 17 along with the model flow diagram depicting the simulation logic.

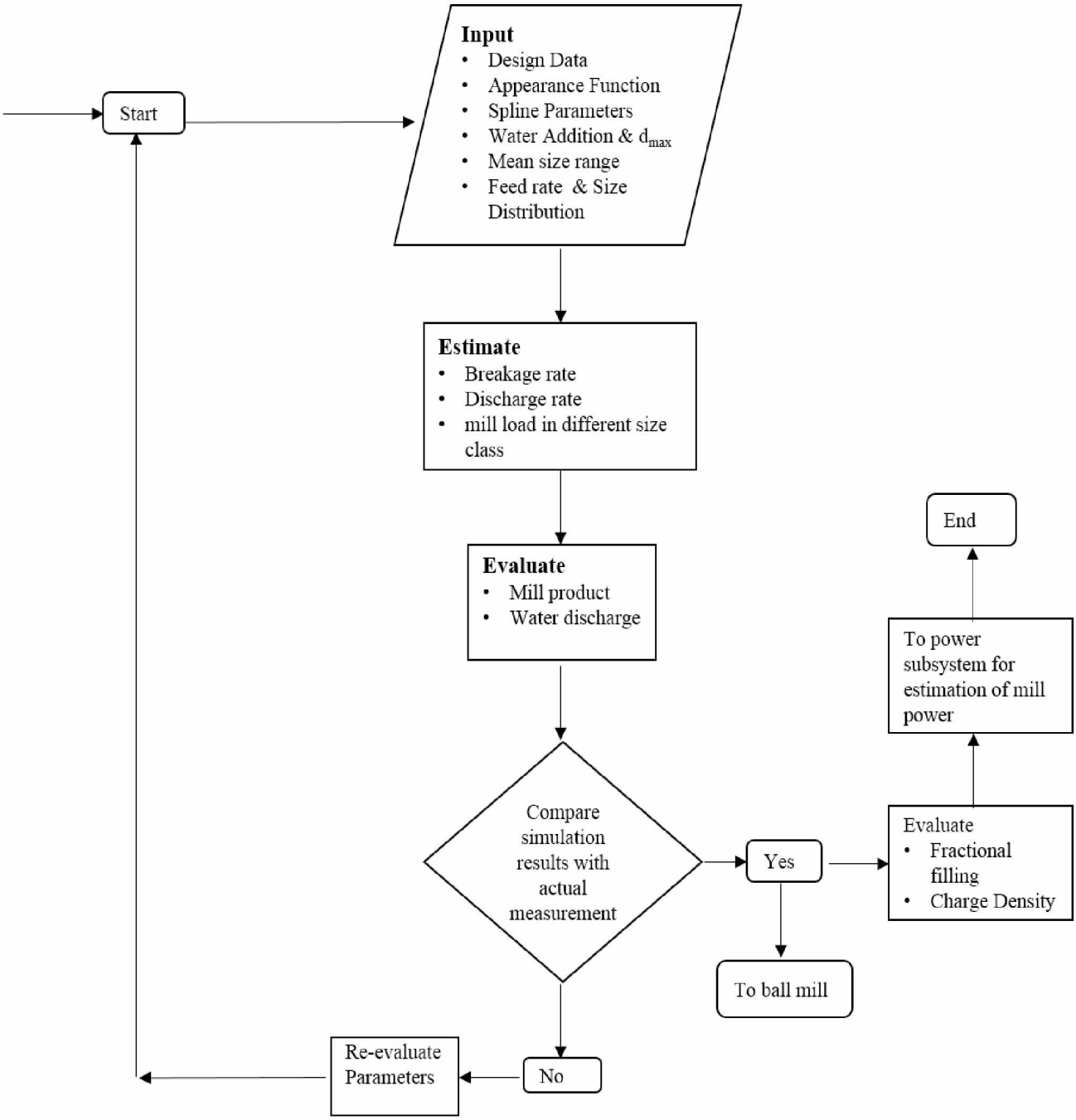

Figure 17: Model flow diagram for sag mill

3.1.1 Appearance Function

An appearance function in physical terms provides the description of the average size distribution of the products resulting from a single particle or multiple particle breakage. Standard experimental techniques which involve abrasion test and drop weight test developed at Julius Kruttschnitt Mineral Research Center (JKMRC) are used for estimating these parameters (Napier-Munn, 1996). The size distribution of products arising from these tests are measured as a function of specific energy supplied and are characterized in term of the size distribution index (t_{10}) parameter developed by Narayanan, (1986). However, for this study the breakage distribution function used was derived from the standard Broadbent–Calcott model rather than being derived from JKMRC procedures. The advantage is that the functional form of the appearance function encapsulates a wider size range rather than relying on laboratory tests conducted on a narrow size which sometime fail to resemble exact conditions encountered by the mill. The standard appearance function was derived using following function:

$$B(x_i) = 1.58(1 - e^{-\frac{xi}{xj}}) \tag{42}$$

where x_i is the size of breakage product, x_j is the size of particle being broken, and $B(x_i)$ is the cumulative mass fraction finer than x_i.

However, the major limitation to the standard appearance function is it is independent of ore type and fails to capture ore properties.

3.1.2 Discharge Rate

The discharge rate function essentially describes the transport of material out of the mill. For grate discharge mills this function is expressed in terms of a classification function lumped with a maximum discharge rate constant. Substituting a discharge rate function in Eq (41) results in the following form:

$$p^{SM} = d_{max}^{SM} C^{SM} m^{SM} \tag{43}$$

where $d_{max}^{SM}$is the maximum discharge rate constant, and C^{SM} is the classification matrix (diagonal matrix) of dimension n.

To solve Eq (43) for the discharge rate, the measurement of size distribution of mill product and content should be known, which is difficult in a continuous industrial operation. Since the grate of the mill behaves as a screen and as a classifying device, it was modeled using the Whiten function of reduced efficiency curve to calculate the partition number to discharge stream. The function is given by:

$$C^{SM}(i) = 1 - \frac{e^{\alpha x_i - 1}}{e^{\alpha x_i + e^{\alpha} - 2}} \tag{44}$$

and,

$$x_i = x_i / x_{50c} \tag{45}$$

where i is the size class in consideration, x_i is the mean size of size range in consideration, x_{50C} is the effective grate aperture size, and α efficiency parameter.

Solving Eq (44) gives the diagonal elements of a classification matrix with each element representing the probability of a particle to report to the discharge stream. The parameter d_{max} represents the maximum discharge for particles that behave like water in the mill (Valery and Morrell, 1995) and can be regarded as particles which are not subjected to classification or having partition number one.

3.1.3 Breakage Rate Constant

Breakage rate is the measure of selection rate of particles for breakage, or the frequency of collision of particles with grinding media and other rock charge. There exist no direct technique or instrumentation for measuring this quantity because of the large number of particles. However, measurement of impact distribution within the mill can provide a measure of the breakage rate constant. The most common technique employed by other researchers is using a back-calculation procedure provided data on appearance function, mill content, feed and product size distribution are known along with the mass flow rate of the respective stream. In

this model, the breakage rate constant was estimated as a lumped parameter using a back-calculation procedure at steady state condition. This is advantageous as it eliminates the measurement of mill load size distribution which is fairly impossible in an industrial operation, although efforts have made by researchers such as Morrell, (2004) to carry out this daunting task. Care should be taken when estimating the breakage rate constant matrix as it is dependent upon the factors such as mill speed. Hence, if the mill is being operated at different speeds, multiple sets of breakage rate values will be required (Valery and Morrell, 1995). The equations for estimating breakage rate were derived by setting Eq (40) to zero and further simplification reduces it to Eq (47):

$$0 = AR^{SM}m^{SM} - R^{SM}m^{SM} + f^{SM} - p^{SM} \tag{46}$$

$$p^{SM} = D^{SM}(R^{SM})^{-1}(D^{SM}R^{SM-} - I - A)^{-1}f^{SM} \tag{47}$$

The naming convention of variables described in Eq (47) is same as that of Eq (40) and I represent the Identity Matrix of size n.

The mill was simulated in the Limn© flowsheet processor using different feed and product size distribution data collected from mine. The generalized reduced gradient solver algorithm was used to minimize the sum of squared error cost function for product size distribution. The data obtained was of lumped parameter RD^{-1} from which the breakage rate matrix was evaluated.

3.1.4 Water Balance

Similarly, for water, the rate of change in mill water content is also described as a first order process:

$$\frac{\partial w^{SM}(t)}{\partial t} = w_f^{SM} - dw^{SM} \tag{48}$$

where w^{SM} is the mill water content (t/h), w_f^{SM} is the water in mill feed (t/h), and d is the rate constant. The constant d is equal to the discharge rate constant d_{max}^{SM} in Eq (43).

3.1.5 Power Draw

Mill power draw is the measure of the rate at which energy is supplied to the mill for size reduction and rotating the mill shell along with the charge. The model used for this purpose was one developed by Morrell (1996) because it is based on a theoretical construct of energy balance which considers charge shape, position, mill load and density inside the mill to estimate the power draw. The underlying assumption of this model is that slurry flow is through grinding media and there is no slurry pool formation within the mill. The model consists of two components; estimation of no-load power which is power consumed in rotating an empty mill, and power needed for charge, which is power consumed by charge motion and in size reduction (Eq 49).

$$P_{Gross} = P_{No\ Load} + kP_{Charge} \quad (49)$$

where, $P_{No\text{-}Load}$ is the power consumed by empty mill in [kW], P_{Charge} is the power consumed by rotating charge, and k is the calibration factor (default value of 1.26).

The charge motion is further divided into two categories based on shape of mill, the motion of charge in cylindrical section which is common to all mills and motion of charge in conical section for mills having conical ends. The model equation is given by:

$$P_{cyl} = \int_{r_i}^{r_m} (\rho_c V_r L g r (sin\theta_s - sin\theta_T) + V_r^3 \rho_c L dr/2) dr \quad (50)$$

$$P_{cone} = 2 \int_0^{L_i} \int_{r_i}^{r_m} [(2\pi N_m \rho_c r^2 g (sin\theta_s - sin\theta_T) + 4\pi^3 N_m^3 r^3 \rho_c)] dr dL_c \quad (51)$$

$$P_{No-Load} = 1.68(r_m/2)^{2.05} [\emptyset(0.667 L_D + L)]^{0.82} \quad (52)$$

where ρ_c is the mill charge density, ρ_p is the pulp density, L_D is the length of conical section (m), L is the length of cylindrical section (m), r_i is the charge inner surface radius (m), r_m is the mill radius (m), Θ_T is toe angle (radians), Θs is the shoulder angle (radians),$\emptyset$ is the mill operating speed expressed in terms of fraction of

critical speed, V_r is the tangential velocity of particles at a distance r (m/sec), and N_m is the mill speed in revolution per seconds.

The above model was solved by using information of mill charge obtained by simulating Eq (40) in real time. The data generated from Eq (40) was used to estimate charge position, density, mass which was used as input to estimate power required by the mill. When simulating the power model, it was assumed that the fractional fill of the balls within the mill remained constant.

3.1.6 Bearing Pressure

Bearing pressure is an indirect measurement of mill load mass and is used as a reference variable to monitor and control mill load and fractional filling in the mill. However, modeling of bearing pressure has not been given a great importance. The reason is that the bearing pressure is a measure of back pressure of the trunnion lubrication system which is often affected by conditions inside the mill and lubrication system of the mill (Ganguli, Dutta, & Bandopadhyay, 2006; Mular & Barratt, 2002). It has also been shown by Kawatra (2006) that there exists no direct correlation between bearing pressure and mill power which are mostly correlated in industries.

The bearing pressure for this case was modeled using Simple Linear Regression (SLR), in which the model was fitted using data of mill content derived using Eq (40) as predictor variables and bearing pressure as response. The model equation is given by:

$$\widehat{BP} = \beta_0 + \beta_1 x_1 \tag{53}$$

where $ß_0$ & $ß_1$ are the regression parameters, and x_1 is the mill load (t)

Underlying assumptions for fitting a SLR were then checked based on residuals of the fitted model. Hypothesis tests for non-constant variance and residual plot were done and analyzed which were in accordance to assumptions of the SLR models.

3.2 Screen

Industrial screens employed in grinding circuits are used for separating particles on the basis of size. Sometimes their role may vary such as to grade particles into different size ranges when multiple circuits are involved or to separate grinding media from the ore. However, irrespective of their use these devices are easy to operate and have no dynamics associated with them. The only input output variables are the mass flow rate of the feed, and the product streams and their related size distributions (Figure 18).

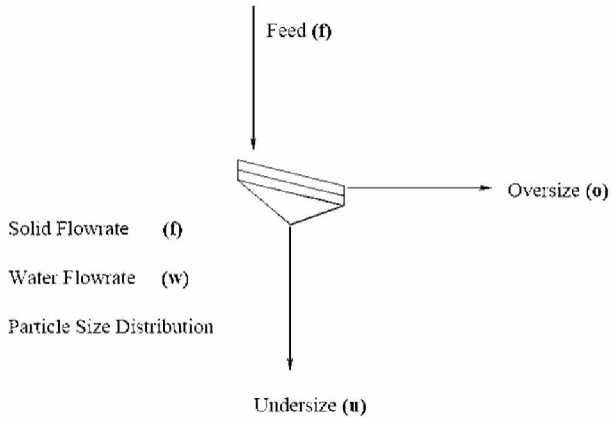

Figure 18: Schematic of a screen listing I/O variables

The usual performance model based on partition analysis was used to predict the probability of a particle in a given size range to report to a given stream, oversize and undersize in this case. The partition number then was used to evaluate the mass flow rate of solids and water in respective stream. The model equation is the same as used for the SAG mill discharge grate (Eq 44) to obtain a partition number for oversize stream; however, the parameters were different and were evaluated under steady state approximation utilizing mass conservation. The properties of the underflow stream were evaluated by subtracting the overflow mass distribution from feed:

$$u_s^{SC} = f_s^{SC}(I - C^{SC}) \tag{54}$$

3.3 Hydrocyclone

Hydrocyclones are the classification units used for separating particles at finer size when compared to screens. They are the key device in the grinding circuit, simple in operation and play a crucial role in determining performance of a circuit when measured in terms of product size. Despite their simple operation online monitoring of their performance is difficult which poses challenges in identifying any significant deviation from operating conditions. The different input and output variables monitored for a cyclone are illustrated in Figure 19.

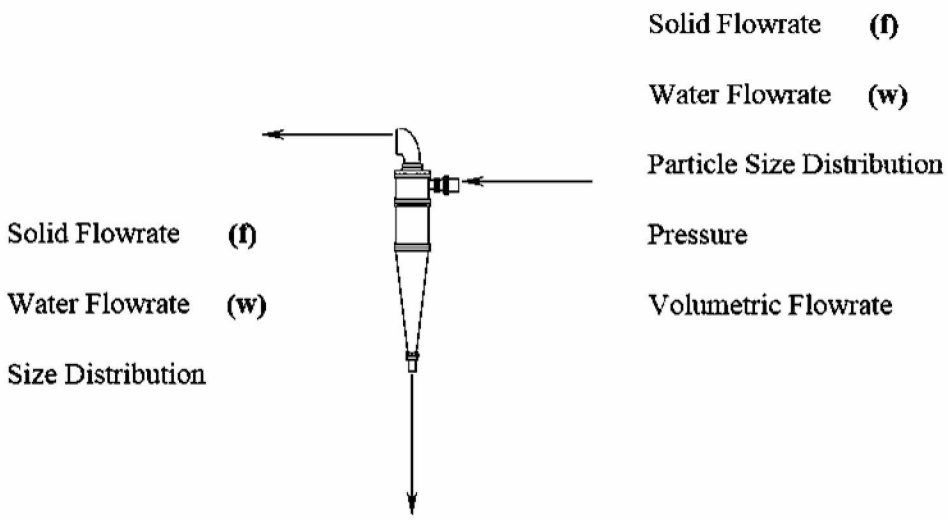

Figure 19: Schematic of a hydrocyclone listing I/O variables

To model a hydrocyclone an empirical method developed by Plitt was used. It considers design and operating variables such as cyclone dimensions and volumetric feed flow rate to predict d_{50c}, pressure and separation efficiency exponent. The predicted variables are used in the Plitt/Reid reduced efficiency models to evaluate mass flow rate and size distribution of overflow and underflow streams. The model is mathematically described as:

$$d_{50C} = \frac{F_1\ 39.7\ D_c^{0.46}\ D_i^{0.6}\ D_o^{1.21}\eta^{0.5}e^{0.063C_v}}{D_u^{0.71}h^{0.38}Q_f^{0.45}(\frac{\rho_s - 1}{1.6})^k} \quad (55)$$

where D_c, D_i, D_o, D_u are the diameters of cyclone cylindrical section, feed inlet, vortex and apex respectively (cm), H is the distance between the apex and vortex (cm), C_v is the percent solids in feed (v/v), k is the hydrodynamic exponent, ŋ is the liquid viscosity (cP), and Q_f is the volumetric flow rate of feed (l/min).

$$P = \frac{F_2 1.88 D_c^2 Q_f^{1.8} e^{0.0055 C_v}}{D_c^{0.37} D_i^{0.94} h^{0.28} (D_u^2 + D_o^2)^2} \tag{56}$$

$$S = \frac{F_3\ 3.29\ \rho_p^{0.24}\ (D_u/D_o)^{3.31}\ h^{0.54}\ (D_u^2+D_o^2)^{0.36} e^{0.0054 C_v}}{D_c^{1.1} P^{0.24}} \tag{57}$$

$$m = F_4\ 1.94\ (\frac{D_c^2 h}{Q_f})^{0.15} e^{-\frac{1.58\ S}{1+S}} \tag{58}$$

where F_1, F_2, F_3 & F_4 are constant with default value as 1. The reduced efficiency curve expression is given by

$$E_s^{Hy}(u_i) = 1 - \ e^{-ln2 \frac{d}{d_{50c}^{Hy}}} \tag{59}$$

where E_s^{Hy} is partition number to underflow stream.

3.4 Ball Mill

The ball mill was among the first devices to be considered for modeling by various researchers (Bond, 1961; Herbst & Fuerstenau, 1980). The models which are now being utilized for other mill modeling are actually the upgraded version of models which were developed initially for the ball mill. The design difference which separates ball mill from an AG/SAG mill lies is the aspect ratio. Aspect ratio is the diameter-length ratio which is less than or equal to one for a ball mill, and greater than one for the other mills. This design difference is responsible for altering the breakage mechanism within the mill. Longer length allows abrasion to be more dominant and allows more residence time resulting in finer product. For this study, the ball mill was modeled using Whiten's perfect mixing model. However, the model parameters such as breakage rate and discharge rate were derived separately for ball mill Eq (60).

$$\frac{\partial m^{BM}(t)}{\partial t} = AR^{BM}s^{BM} - R^{BM}s^{BM} + -p^{BM} \quad (60)$$

The feed to the ball mill was the combined product from the SAG mill and cyclone underflow Eq (61).

$$f^{BM} = p^{SM} + u^{hy} \quad (61)$$

Another design difference is the absence of a grate in ball mills. The absence of grate was taken into account in the ball mill model. Because no classification effect is taking place at the discharge end of the ball mill the Eq (43) classification matrix was assumed to be an identity matrix.

After developing the models for specific units, the models were programmed to develop the simulator framework, described in next section.

3.5 Present Programming and Simulation Framework

The models discussed so far involve matrix treatment of a huge amount of data every second and interaction among multiple process variables escalates computational requirement. So as to handle such large amounts of computation and upon reviewing various simulation platforms, it was decided to program models in Matlab/Simulink.

Matlab is a powerful simulation package which has built-in modules of scientific function and is equipped with non-linear system solver. The application of Matlab/Simulink has already been explored and tested by various researchers for comminution circuits such as (Liu and Spencer 2004, Salazar, Magne et al. 2009, Sbárbaro 2010).

In the present work programming of the models was done with an intent to develop more a generic simulator. The developed simulator was made flexible to simulate any number of particle size distributions, variable feed size distribution and using different design specifications of the equipment.

The programming task was divided into parts as per model hierarchy described in the previous sections. Models were programmed both as a S-function file and user defined Matlab function file which are imported during the simulation. The developed model library along with typical architecture for SAG mill are presented in Figure 20 and Figure 21.

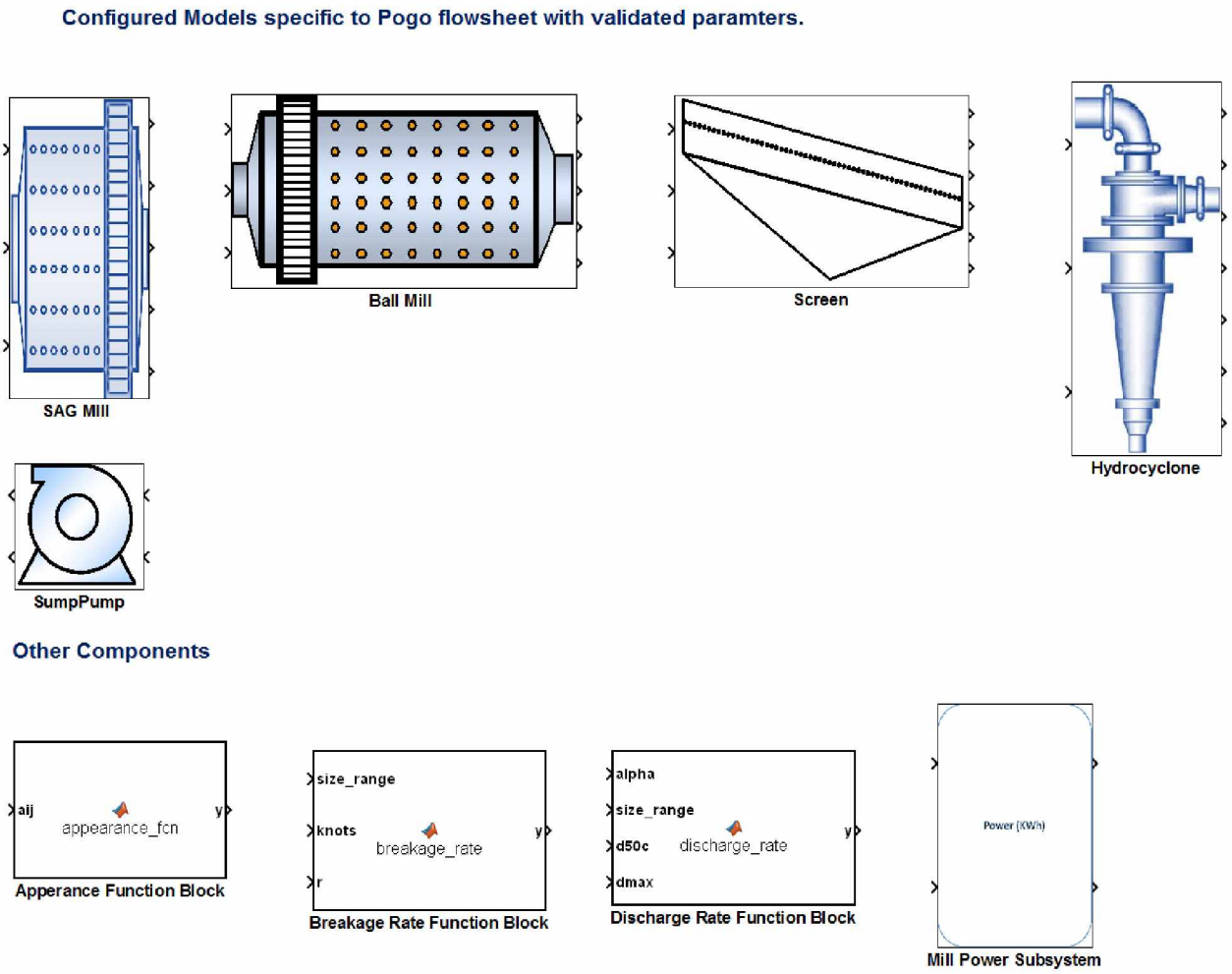

Figure 20: Model library of process units

In the SAG mill model architecture, the input variables such as size class, feed size distribution, throughput and water to the mill were passed as an input argument to the function files. The functions then calculated mill solid content, water and discharge which served as input to predict other response variables such as fractional filling, power draw and bearing pressure. Similarly, the properties of the

SAG mill discharge stream were surged to other ball mill as per flowsheet layout (Figure 22).

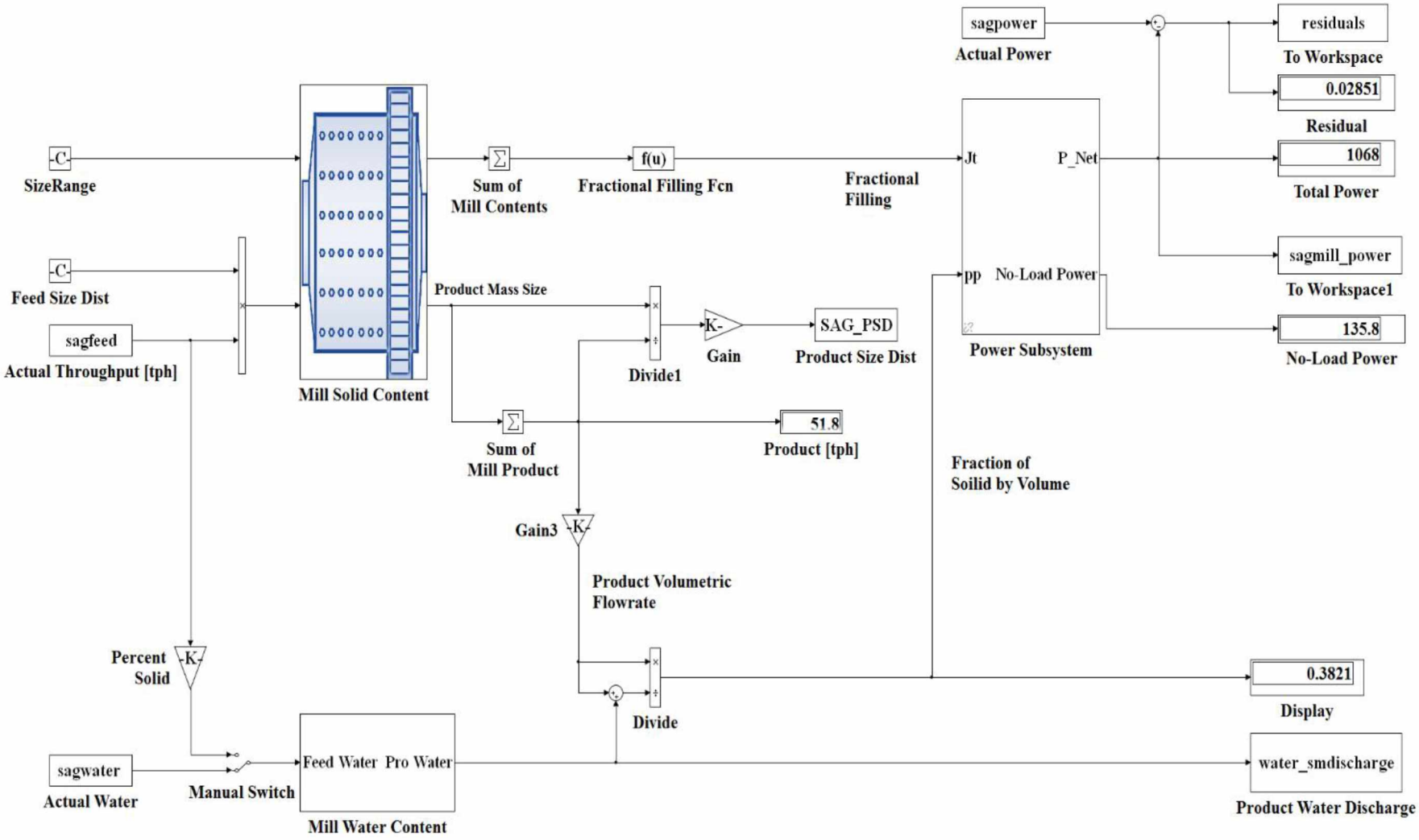

Figure 21: SAG Model Architecture

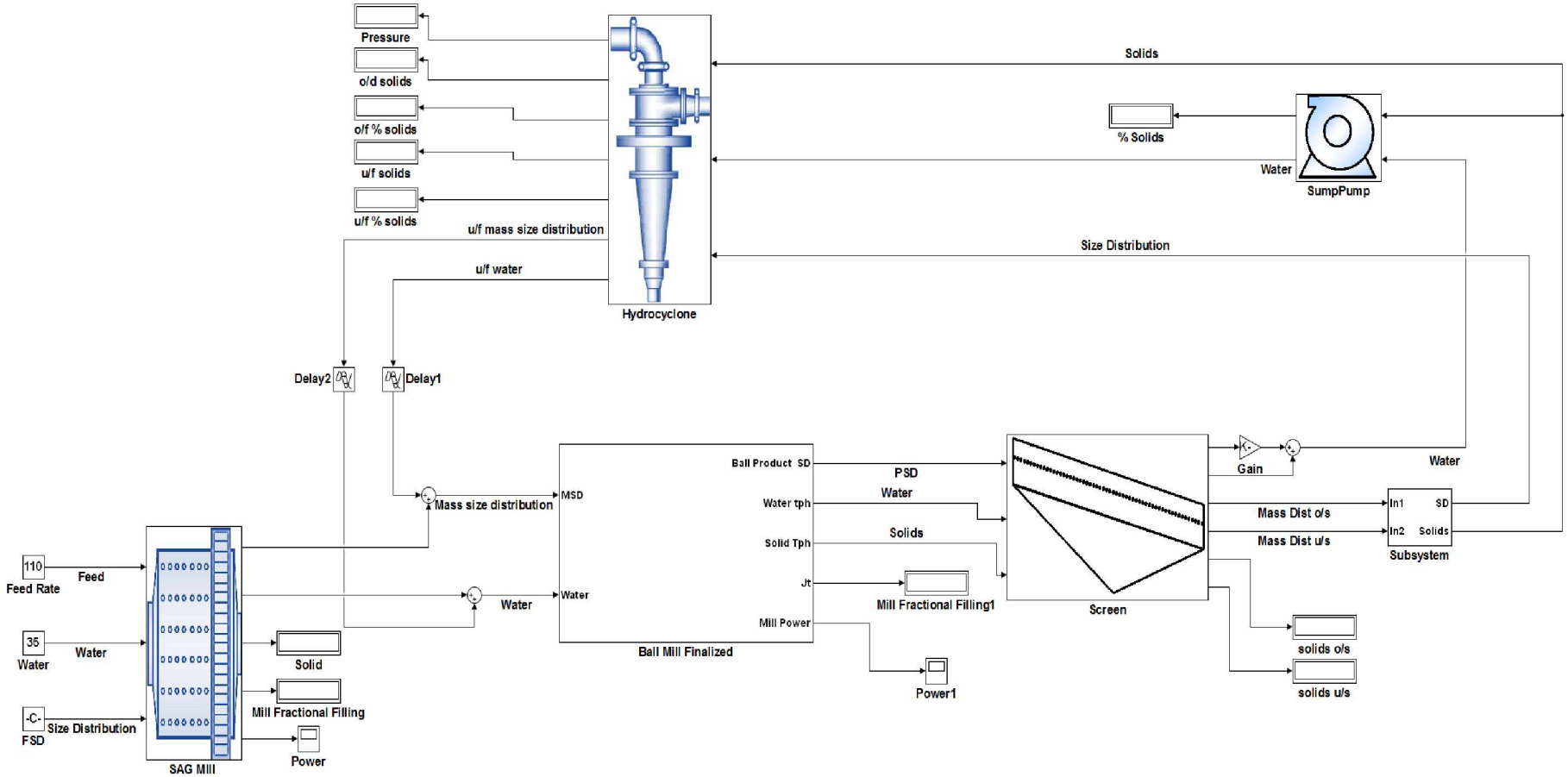

Figure 22: Circuit architecture in Simulink of present work

Because of the large number of modules associated with each process unit, the models were reduced to subsystems. Reduced subsystems were masked so as to provide controlled access to change the model parameters without actually changing them in the program. The program would directly inherit the parameters supplied through this masking. A typical example of a masked subsystem can be seen for the SAG mill in Figure 21 and Figure 22. Figure 21 shows open architecture of a SAG mill model which is reduced to a subsystem, as seen in Figure 22. The model parameter can be changed by double clicking the SAG icon which opens a new dialog box (Figure 23), a feature of masking.

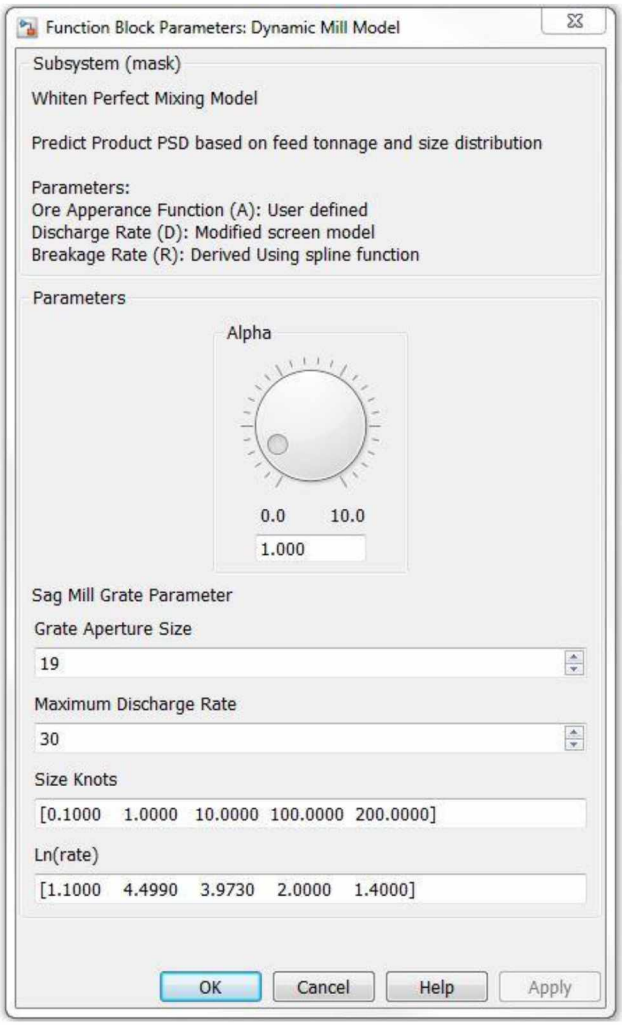

Figure 23: Masked SAG system

3.6 Data source and model validation in the present work

The data for model parameter estimation and validation was obtained by visiting the mill facility of the mine on various occasions. The data was classified into major categories as design data of different process units and operating process data.

3.6.1 Design data

The design data consisted of the dimensions of the different equipment and their components which are parts of different model structures. The role of the design data in a model structure is to incorporate the machine specific property. Examples of the design data include:

1. Mill dimensions SAG/Ball (diameter and length in meters).
2. Operating capacity of mill (tph).
3. Rated power of mill (kW).
4. Ball size (mm).
5. Screen size (dimension and aperture size) including angle of inclination.
6. Cyclone dimension and geometry

Appendix A provides detailed design specifications of different units used for modeling purposes.

3.6.2 Process data

The process data can be cataloged into two sections, one essential from an operational viewpoint while the other used is for performance analysis. As most of the mineral processing operations are continuous the monitoring and control of process is done from a centralized control system. The sensor measurements are collected in real time and sent to the Distributed Control System (DCS) of the plant. Necessary control actions are taken by the operators sitting in the control room or by the DCS to manage the process in case of any offset.

The second type of process data is not monitored continuously but is required by the engineers for evaluating the performance of the circuit. For a grinding circuit the performance is measured in terms of product particle size. Thus, size distributions of the streams entering and leaving the grinding and classification devices are important. The size distributions of different samples are used to evaluate the efficiency of any equipment. This type of process data is collected by sampling or surveying the circuit on a shift or monthly basis.

The operational data for the months of January 2015 and January 2016 were collected at a difference of 1-minute interval for the variables of the grinding circuit of the Pogo mill facility. The data was then analyzed for any missing values and zero values for the feed rate, which were removed. The zero value for the feed rate indicates the plant would have been under scheduled shutdown or unexpected breakdown. Survey data of the circuit conducted by the personnel of the facility were also obtained. This included information on SAG mill feed and discharge size distribution and ore impact breakage and abrasion parameters, work index, etc. (Appendix A).

The models of the equipment were validated by simulating each model under the same conditions as that of the mill plant. By same condition it is implied that input variables to the model were the same at which the plant was operating. This was done by using a data source block. The data source block in Simulink imports the I/O process data of the plant pre-loaded to Matlab workspace to the Simulink model of the unit in consideration (Figure 24).

Figure 24: Typical Source Block Used for Validation

Model response and the actual measurement were then compared (Figure 25). If the difference was significant the parameters were revaluated and the process was repeated. Model responses for which the information was not available were validated indirectly. For example, the SAG mill content based model estimates solid content inside the mill, but mill solid content cannot be measured. However, the mill solid content was used to derive product size distribution, hence, the product size distribution was compared with the actual measurement. Another question is that product size distribution measurements are not continuous with time so how do they validate the time dependency of the model? Such problems were resolved by comparing data on the variables which were measured continuously. Mill power is derived entirely using information from mill solid content and the power measurement is continuous. Hence, operating the mill at the same feed rate and water flow rate while comparing power measurements indirectly validates mill solid content model.

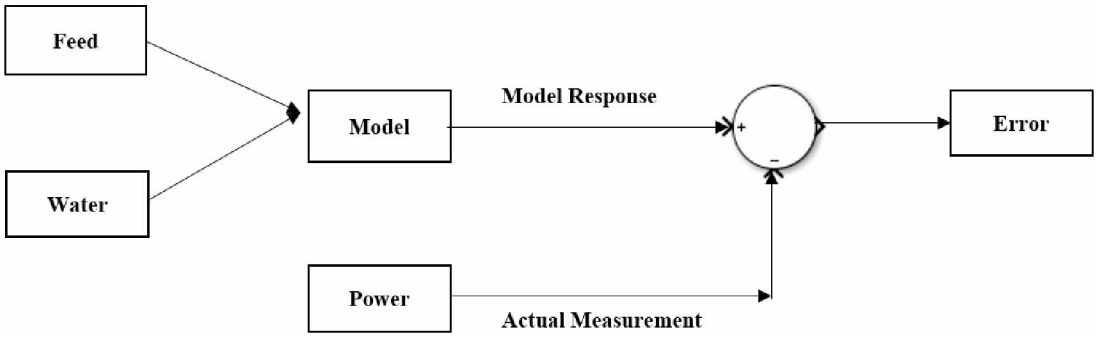

Figure 25: Model validation logic

Figure 26 shows the actual and predicted response of the SAG mill product size distribution when simulated for a feed size distribution data of the sample collected at the same time. The response of mill power draw was also compared. Figure 27 and Figure 28 show plot of predicted response and a plot of residuals respectively; which is the difference between observed mill power data and predicted mill power data from the model. It was found that mean value of residual was within 5.5

percent of maximum power drawn and residual lied in the range of ± 20 percent of maximum mill power.

When simulating models for validation the parameters representing feed properties such as feed size distribution and appearance function (Eq 62) were kept constant with time Eq (62).

$$\frac{\partial A}{\partial t} = 0 \;\&\; \frac{\partial \bar{f}}{\partial t} = 0 \tag{62}$$

where A is the appearance function, and $\bar{f}$ is feed size distribution.

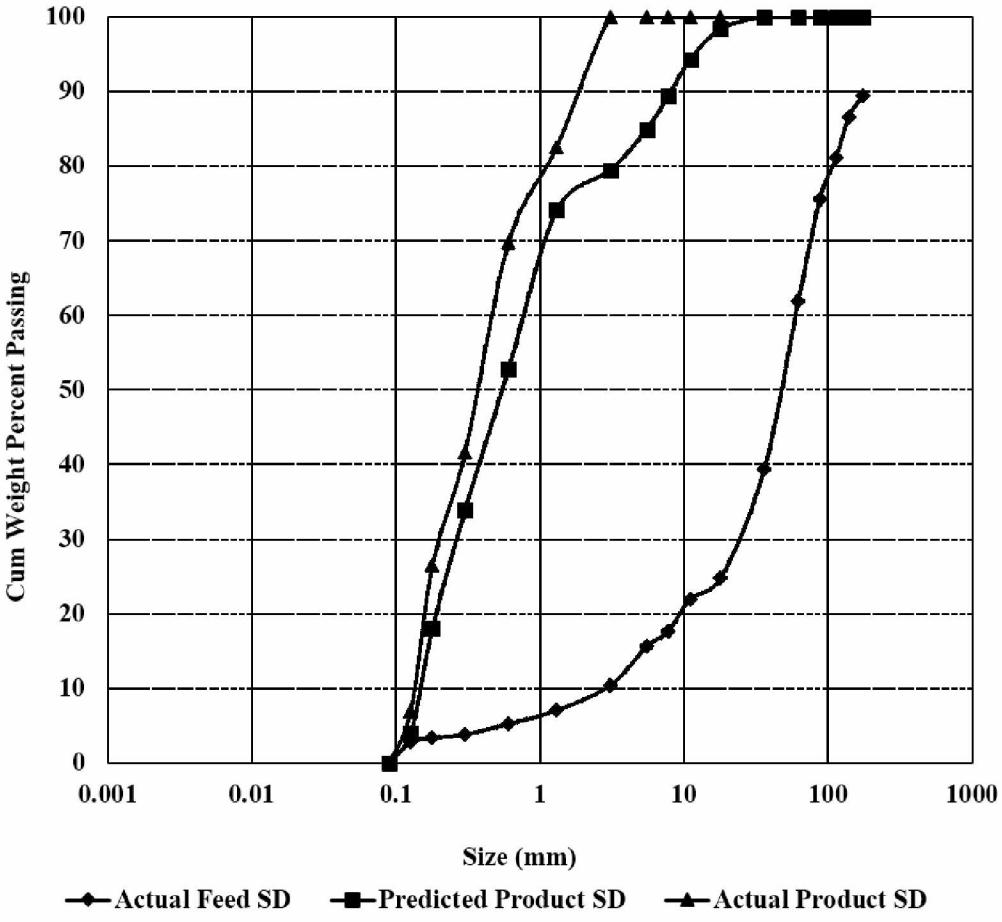

Figure 26: Feed and product size distribution for validation with model response

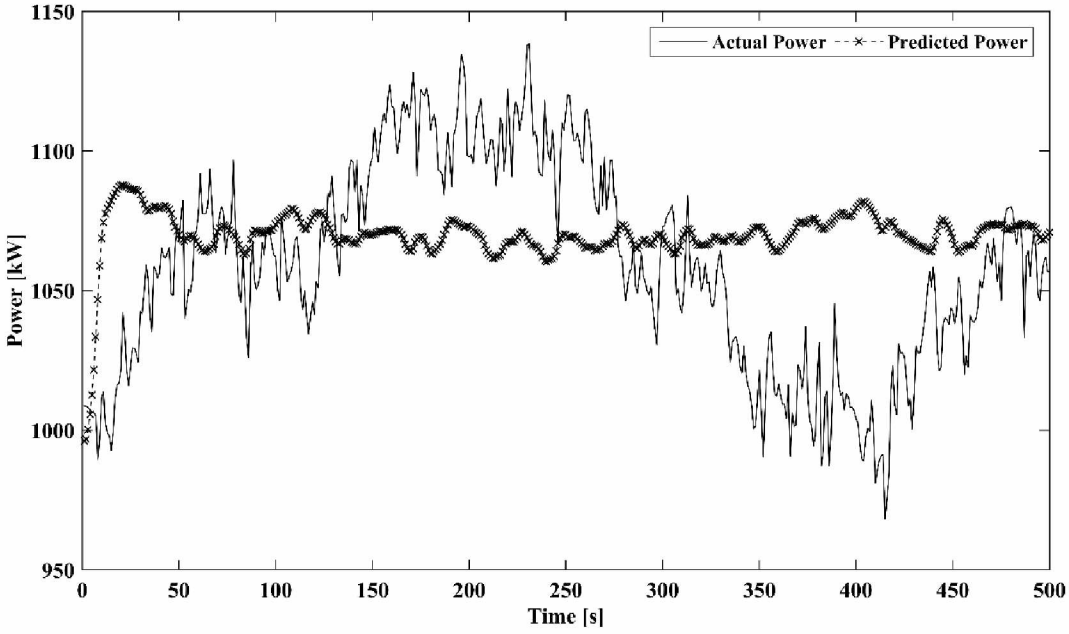

Figure 27: Response of simulator compared to actual power

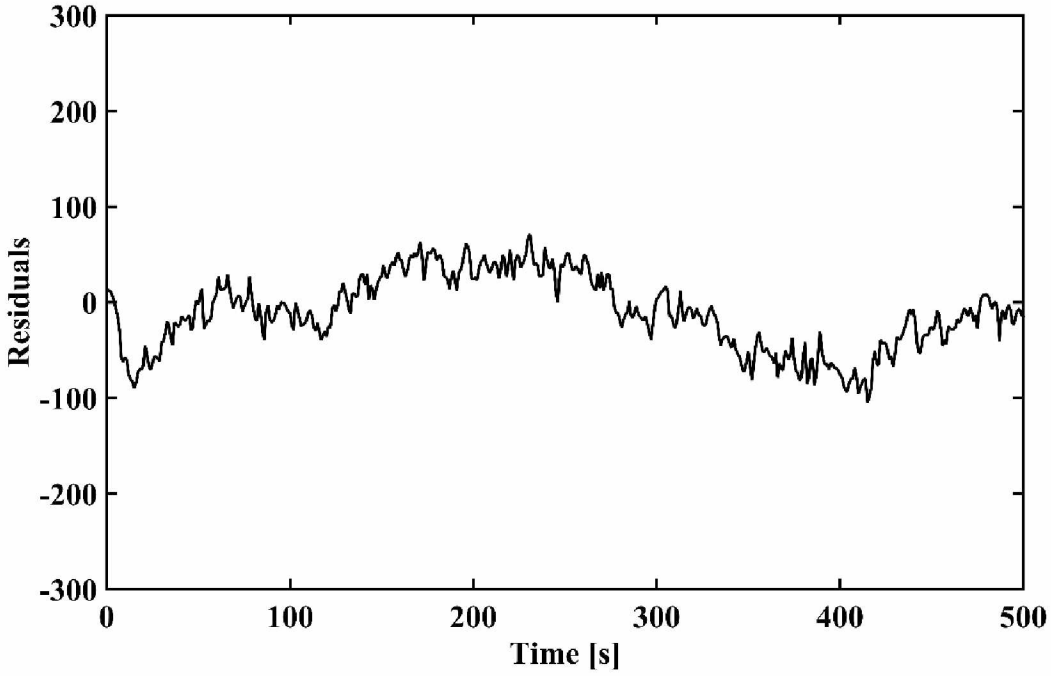

Figure 28: Residual plot

Similarly, for the hydrocyclone the data on variables such as feed slurry flow rate, percent solids, number of cyclones and pressure were available. First a set of data was used to estimate the parameter F2 in Eq (56), which came out to be 3.534 by minimizing the sum of square errors between the predicted response of pressure and actual measurement. The other set was then used to compare the model response of pressure when simulated at the same condition as that of plant (Figure 29).

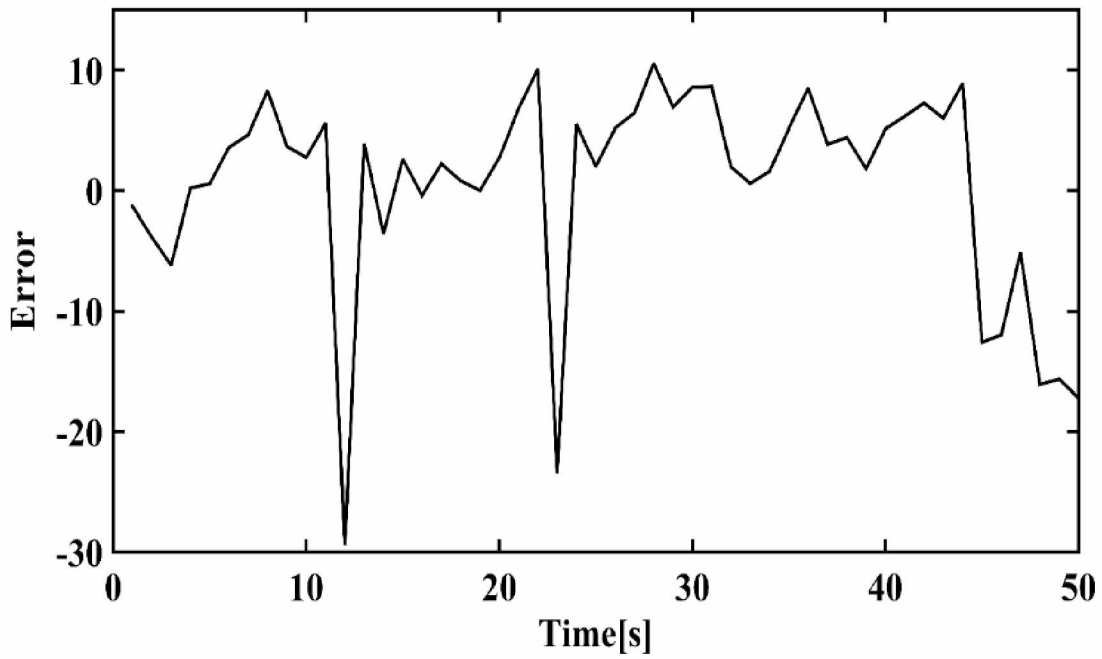

Figure 29: Difference in predicted and measured response for pressure

Because of unavailability of particle size distribution measurement of feed and product stream the d_{50c} was not validated. However, based on industrial documentation the cyclone should produce a cut size of 65 µm of P80 the comparison of which is presented in Figure 30.

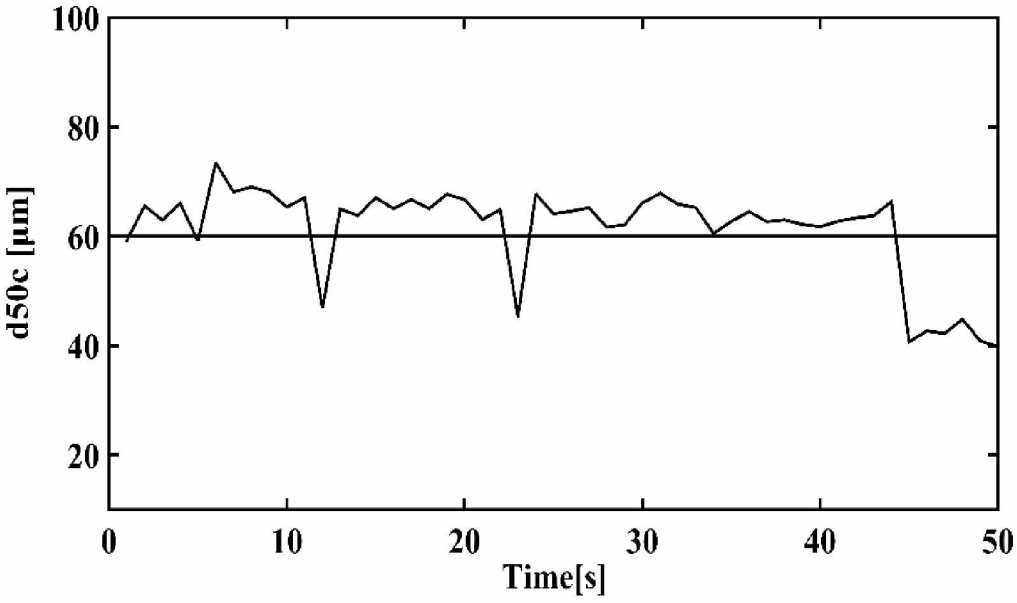

Figure 30: Predicted d50c response

CHAPTER 4 CASE STUDIES

The integrated models were then simulated under different conditions to present the simulation scenarios. The scenarios simulated are commonly encountered situations in an industry. The simulation scenario runs were performed by introducing step changes in manipulated variables and disturbance in the circuit. The changes were in the form of:

- Increase in feed rate to the circuit
- Increase in grind water to the SAG mill
- Increase in cyclone sump water
- Change in feed size distribution

The explanation of the effects of introduced changes has been discussed. The discussion presented is in two parts. The first part discusses the effect on the SAG mill while the other is for the entire grinding circuit. The reason the SAG mill as an individual unit was considered for the case study was because of its complex operation and susceptibility to disturbance and minute changes in operating conditions. While simulating each condition, white noise was lumped with input variables in the form of random numbers so as to produce an effect of noise associated with sensor measurement. The white noise added for feed and water were given by:

$$w_f \sim N(0,25) \tag{63}$$

$$w_w \sim N(0,1) \tag{64}$$

where w_f and w_w is noise associated with variance of 5 and 1, respectively. Four different scenarios simulated are discussed in subsequent sections.

Figure 31 shows the simulation progress from one process unit to another. The change in input variables of a particular unit gets propagated through the circuit.

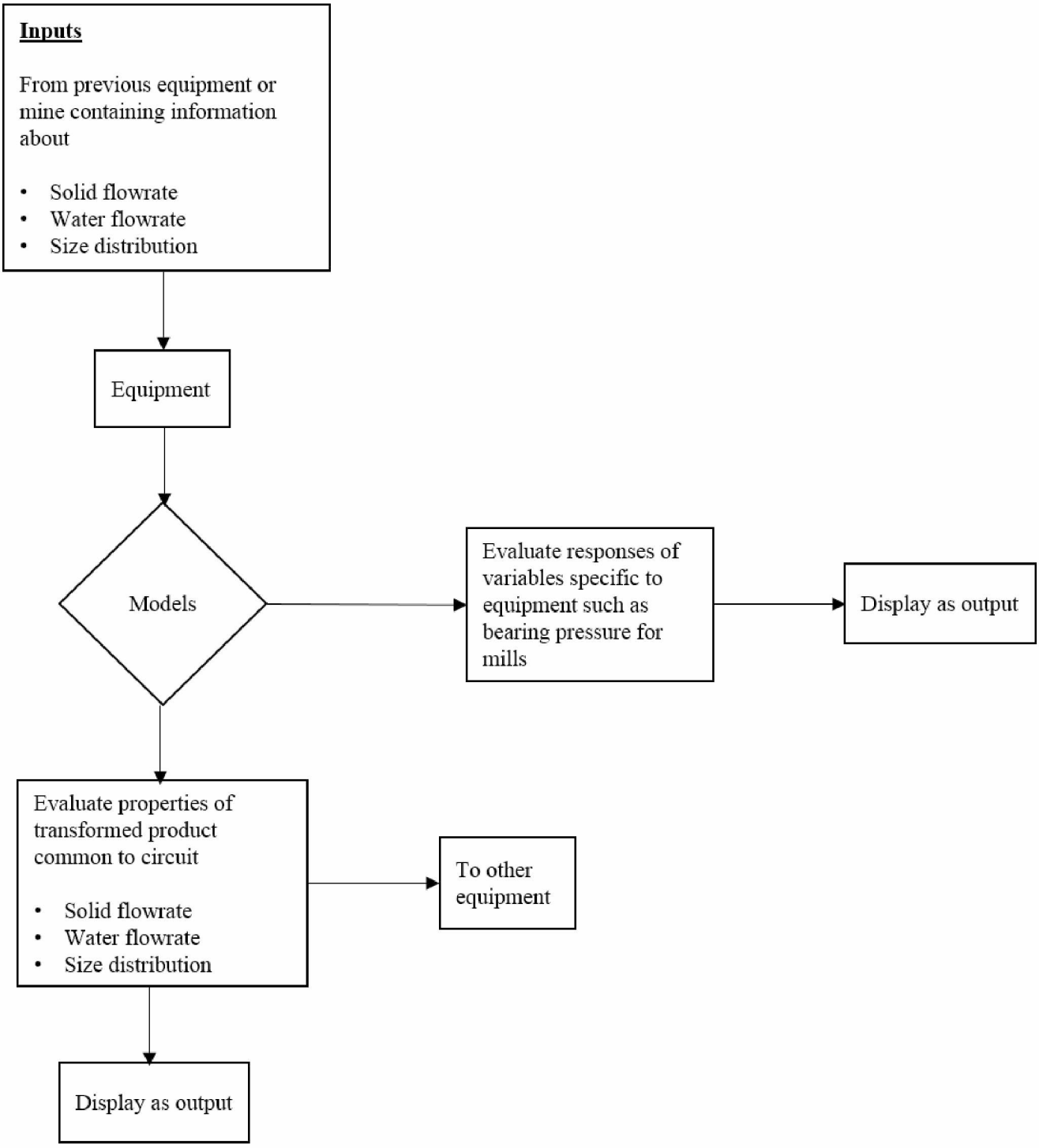

Figure 31: Simulation progress

4.1 Increase in feed rate

4.1.1 Effect on SAG mill

The circuit was initially operated at a feed rate of 100 tph keeping the volumetric flow rate of water and feed size distribution constant. A step change in feed was introduced at t = 100 s and feed was increased to 120 tph (Figure 32). It was observed that product discharge for the initial 20 s of simulation increased in an exponential manner from zero. This is well justified from a practical point of view, since it takes time to build up the mill content from the start-up, grinding the material and resulting in discharge. The time for the change in mill content is determined from rate constant. Rate constant is a combination of A, R and D, also referred to as the residence time distribution parameter in the conventional population balance model (Austin, 1971). The parameter is a vector with each element representing the rate constant for an individual size class. This change of mill content was also reflected in mill load in Figure 32 and as fractional filling in Figure 34.

The mill attained the equilibrium condition, and after t = 20 s it was observed that for a step increase in feed the mill attained equilibrium much earlier as compared to the initial start-up. A possible reason for this is the feed rate effects the rate of process which was small for small change in tonnage. Initially the mill consumed 680 kW, which was the no-load power mill at which mill was running without feed but with ball charge in it (0.1 fractional filling, Figure 34). As the feed was turned on power drastically increased to 1120 kW and later continued to drop as fractional filling of the mill attained a constant value up to t = 30 s. A sudden spike in power draw trend was also seen for step change (Figure 33) because of the increase in mill load which in turn had increased the charge density and fractional filling resulting in an increase in power draw. However, a minor increase in P_{80} value of product was observed before and after the change (Figure 35) which is because of an increase in the coarse material in feed to the mill. Also, a very minor increase in bearing

pressure was observed (Figure 33) which may be regarded as insignificant indicating the increase of coarse material inside the mill is very small in magnitude.

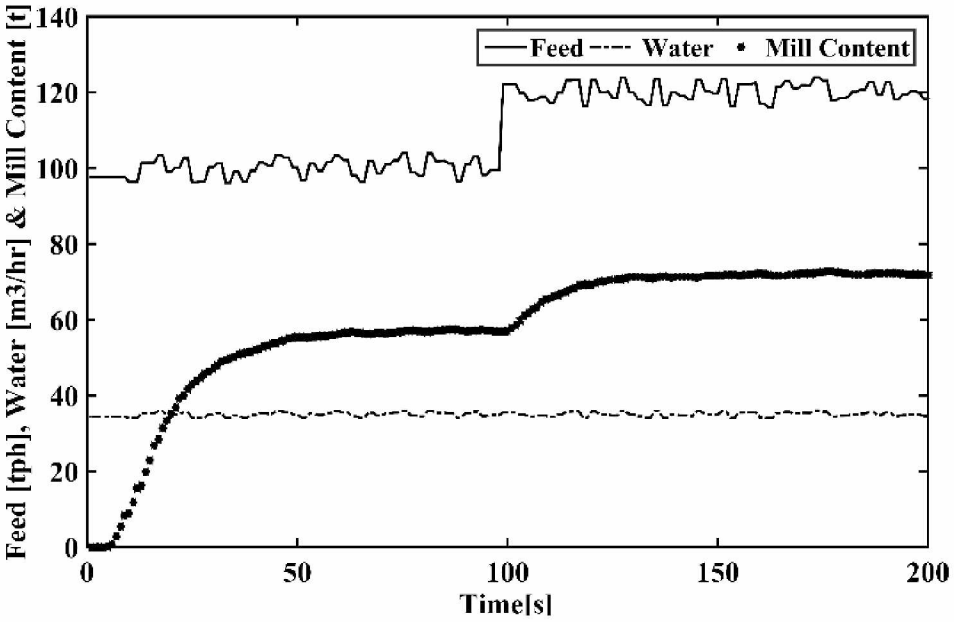

Figure 32: Change in feed and its effect on mill content

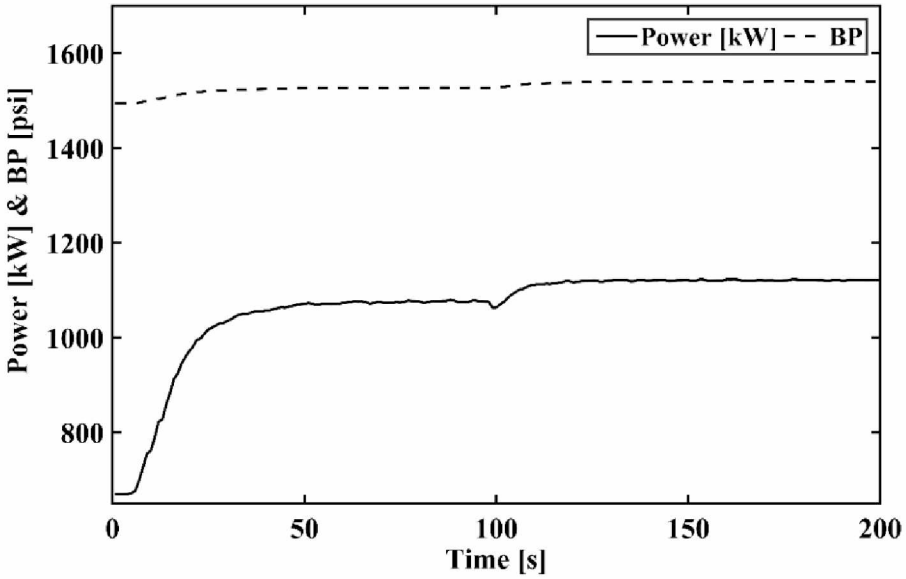

Figure 33: Effect of change in feed on SAG mill power and bearing pressure

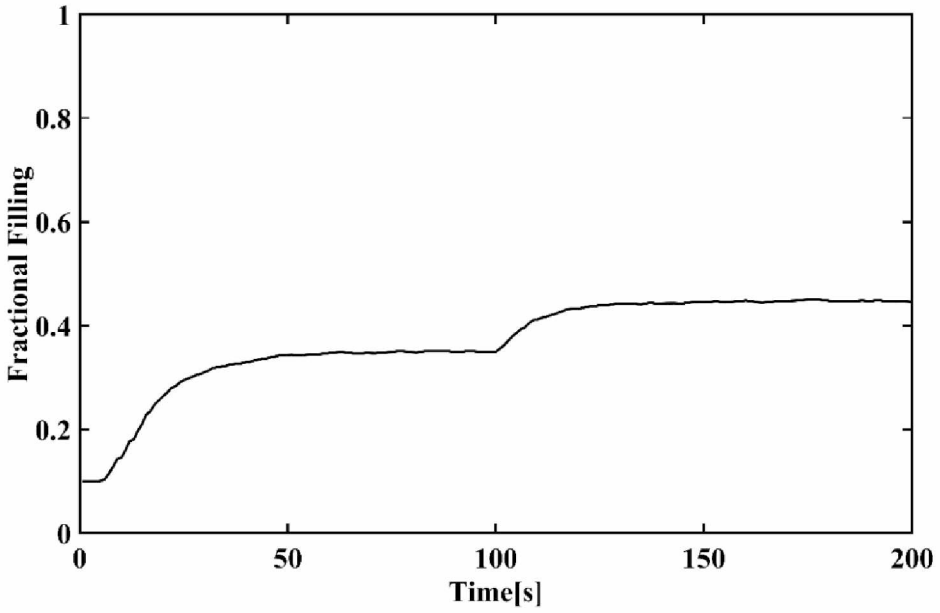

Figure 34: Effect of change in feed on fractional filling

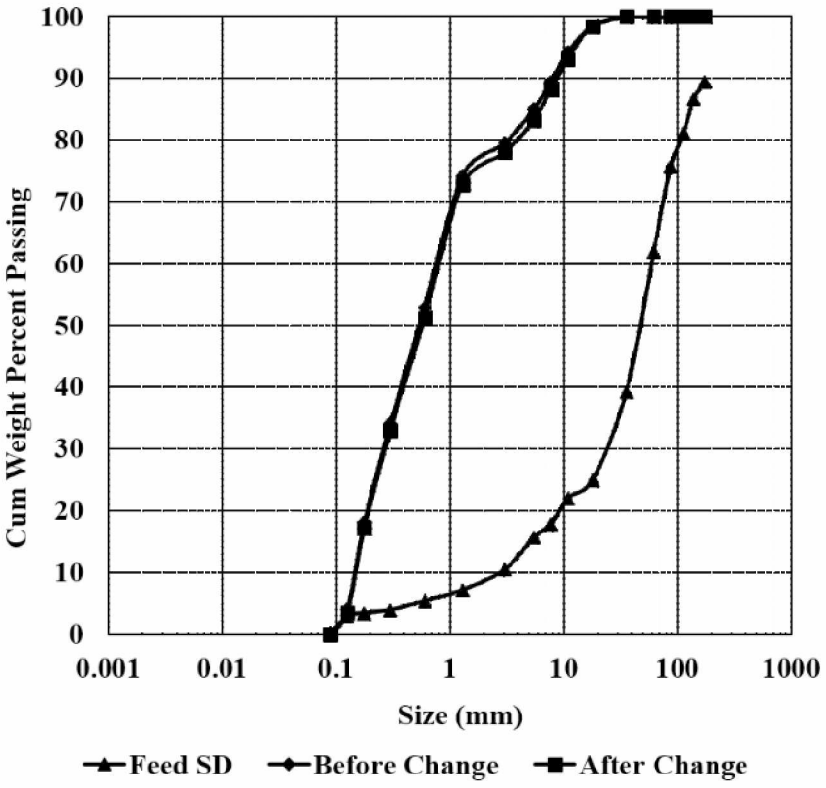

Figure 35: Effect of change in feed on SAG product particle size distribution

4.1.2 Effect on remaining circuit variables

The other circuit variables of prime importance include ball mill power, d_{50c} of hydrocyclone, recirculating load to ball mill and product size distribution of cyclone overflow. The increase in feed rate resulted in increase in ball mill power consumption. This increase was of 10 kW which was less when compared to the change in SAG mill power indicating the ball mill is less affected by changes in rock charge (Figure 36). Similarly, the d_{50c} (cut size) of the cyclone as observed increased from 72 µm to 82 µm (Figure 37). The increase in cut size can be explained as a result of two opposing changes taking place in the cyclone feed slurry. First is the increase in volumetric flow rate of slurry to the cyclone which should have resulted in a decrease of the cut size; but the increase in volumetric feed percent solids caused increases in cut size which dominated the effect of the previous decrease. Change in cut size in turn affected the cyclone overflow recovery which was increased and also evident from a decrease in recirculation (Figure 38). This increase was at the expense of an increase in overflow particle size distribution (Figure 39).

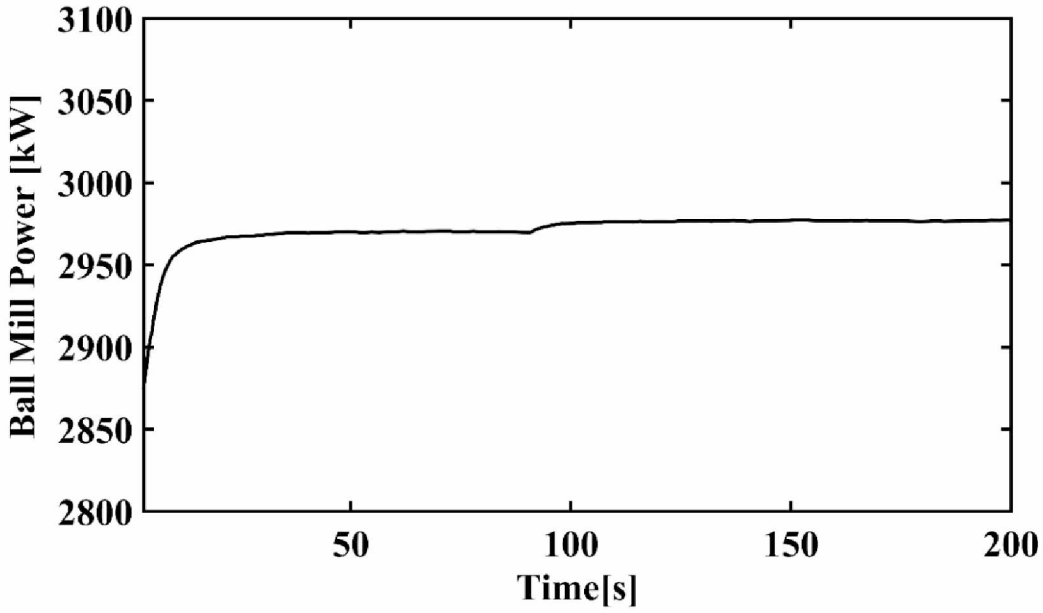

Figure 36: Effect of change in feed on ball mill power

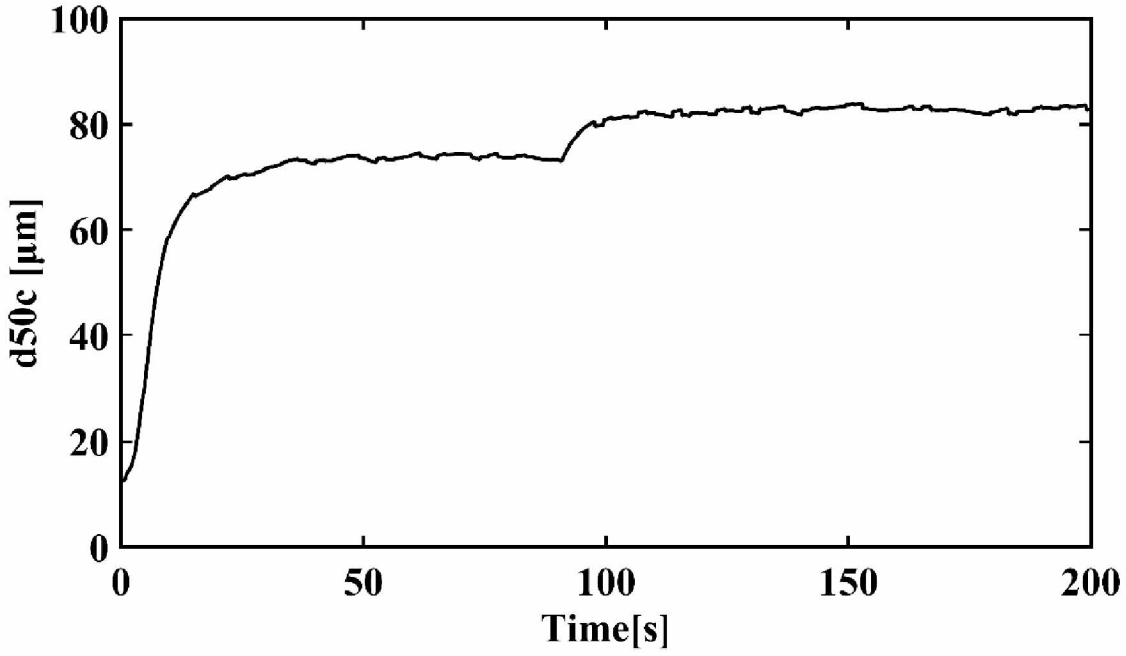

Figure 37: Effect of change in feed on d50c

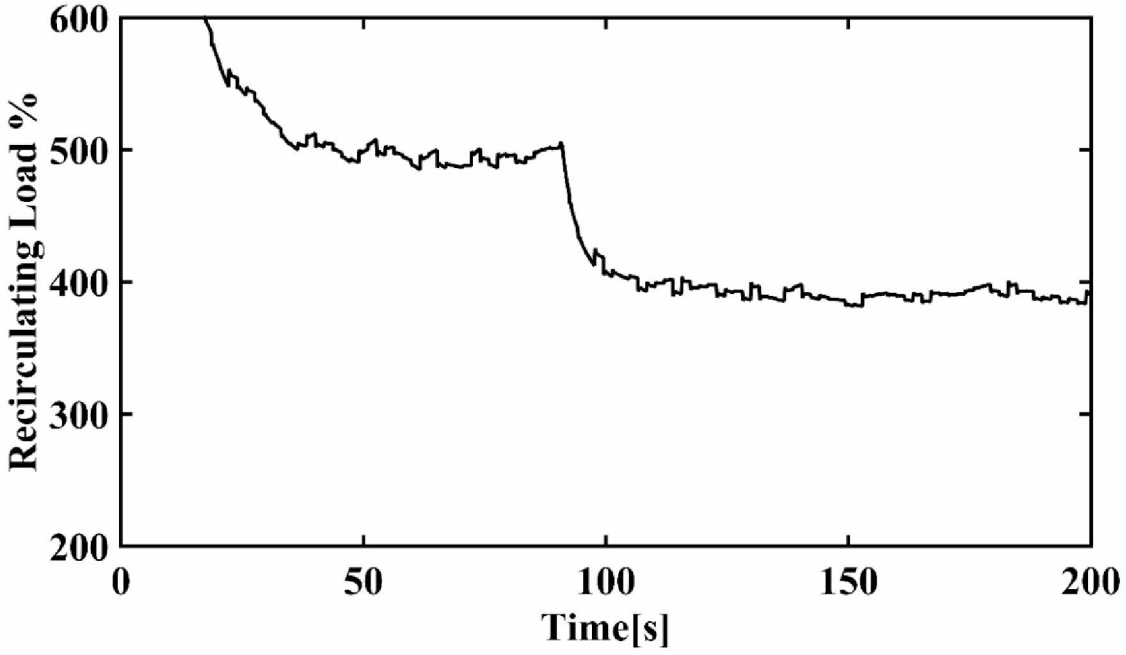

Figure 38: Effect of change in feed on recirculating load

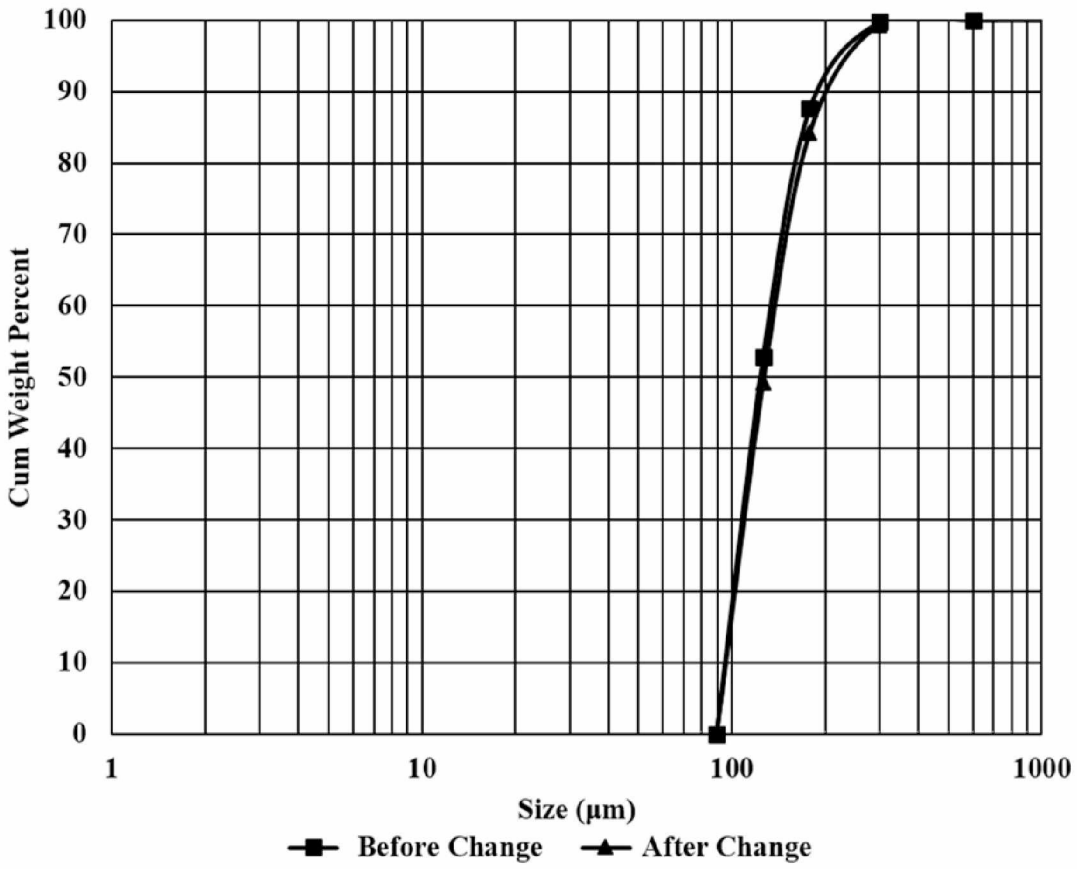

Figure 39: Effect of change in feed on cyclone overflow

4.2 Increase in mill feed water

4.2.1 Effect on SAG mill

Water is used as an important control variable to maintain mill power draw. It is the first defense mechanism used by various operators to control sudden increase in power. The effect of the change in water flow rate was studied by changing mill water from 30 m^3/hr to 50 m^3/hr. The change was introduced at t = 200 s (Figure 40). An instantaneous decrease in mill solid content was observed with a sharp decrease in mill power which later became constant (Figure 40 and Figure 41). There was no significant change in bearing pressure and product solid mass flow rate. The sudden increase in water flushes out finer solids which gives an immediate drop in power because of reduced mill charge density inside the mill.

However, the mill adjusts to this new condition and continues to operate at this new power. A reason for this is also because of an increase in discharge rate constant for finer size range d_{max} in Eq (43).

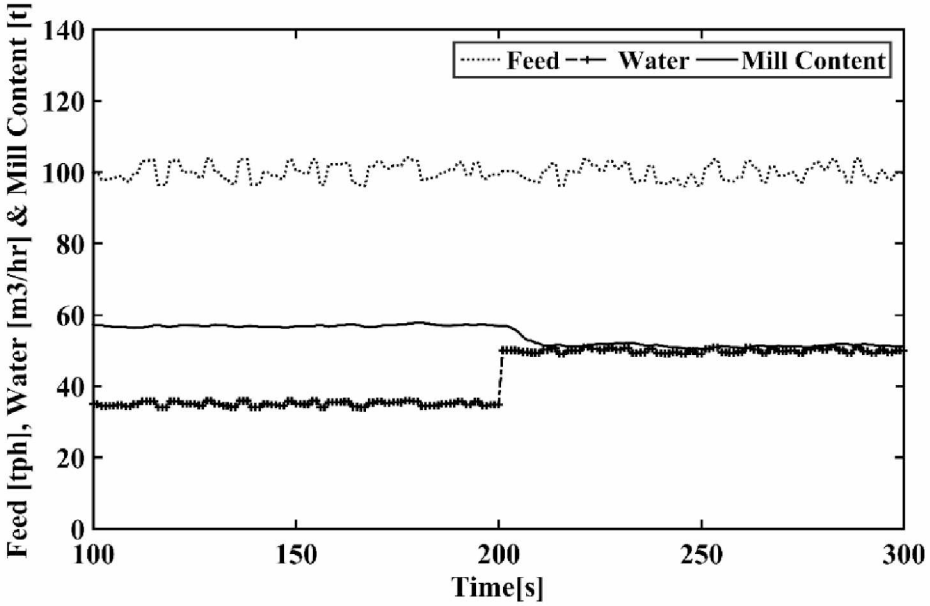

Figure 40: Effect of change in water on mill content

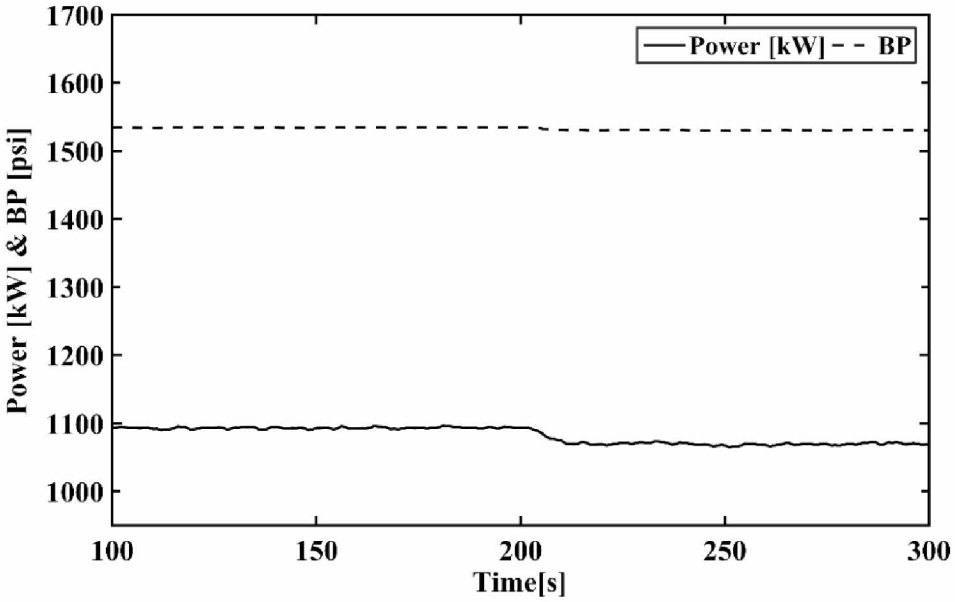

Figure 41: Effect of change in water on power and bearing pressure

4.2.2 Effect on remaining circuit variables

The increase in water flow rate to the SAG mill did not produce a significant effect on the remaining circuit variables. A decrease in 7 kW of power was observed for the ball mill which is not very significant for ball mill operation. Akin to ball power the $d50_c$ of the cyclone was not affected. A small spike in $d50_c$ was observed after which the cyclone adjusted to its original cut size (Figure 42). The small spike could be because of a sudden water surge which propagated to the circuit. However, an increase in recirculating load was observed indicating decreased recovery of solids to the overflow stream (Figure 43). The effect can be explained as: a water surge which propagated to the ball mill caused an increase in discharge rate of coarse material from the ball mill, also evident in the ball mill discharge size distribution (Figure 44). This coarse material during classification in hydrocyclone reported to underflow, thereby increasing recirculating load and also ball mill power.

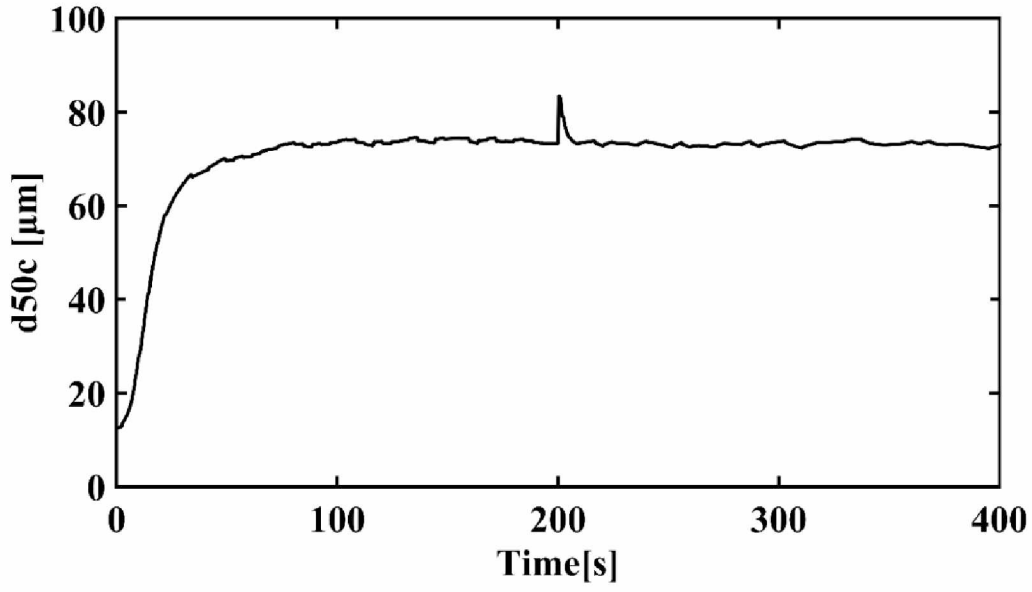

Figure 42: Effect of change in water on d50c

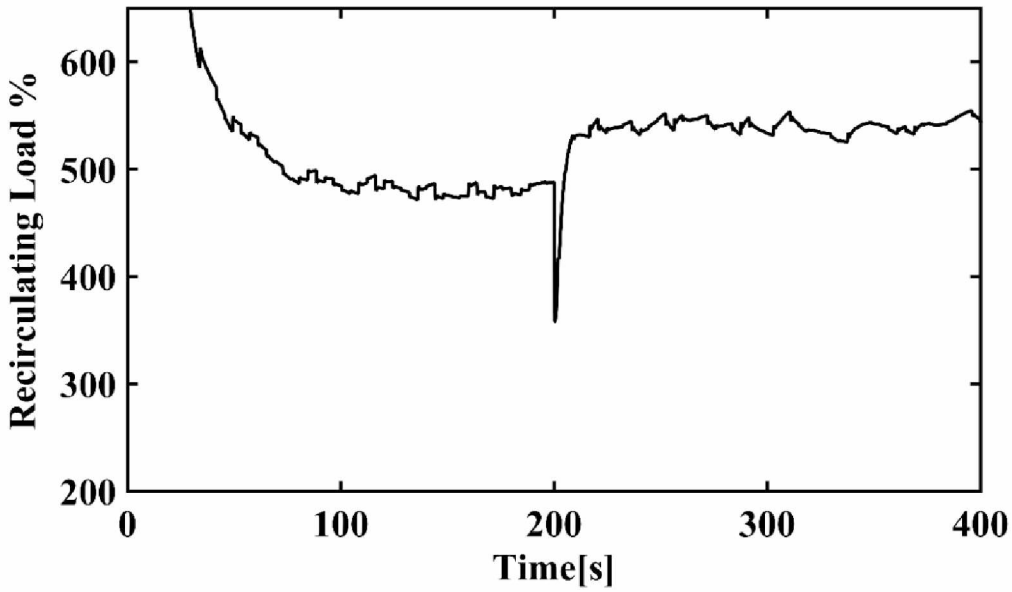

Figure 43: Effect of change in water on recirculating load

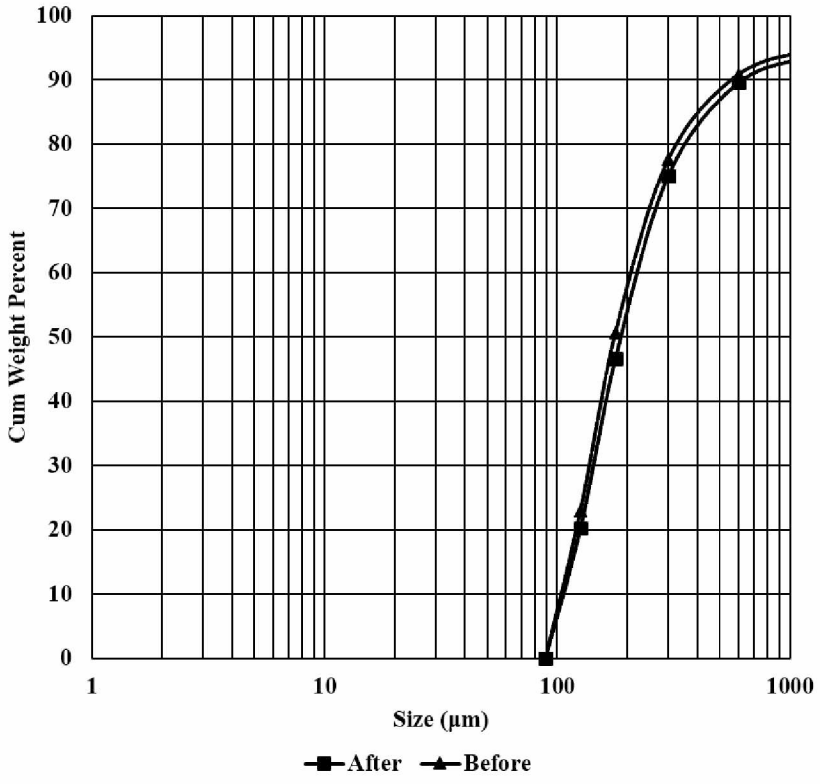

Figure 44: Effect of change in water on ball mill discharge size distribution

4.3 Change in feed size distribution

4.3.1 Effect on SAG mill

The feed size distribution is the most common variability associated with the ore and possible source of disturbance in the milling circuit. The change in feed size is more prominent where the ore is fed without any prior crushing stage or from a coarse ore bin because of segregation of the ore in the bin. The variability is less if the feed to the mill is a product of some prior crushing stage or proper care has been taken in blending to maintain a constant feed size distribution. The effect of change in feed size is most difficult to study and interpret. Because feed itself acts as grinding media in the SAG mill, it affects the load size distribution thereby altering the rate of breakage and discharge of mill content. Effect of change in feed size distribution was analyzed using the simulator where an increase in feed size from F_{80} of 107.52 mm to 169 mm was introduced at t = 50 s (Figure 45). An increase in total mill filling and power draw was observed due this change (Figure 46), because the increase in feed size increases the amount of coarser material in the mill content, increasing both the responses. This can also be interpreted as more energy is required to grind the coarser feed material to the targeted size. Also, a minor increase in product size distribution was observed. However, information about size distribution of the mill content in real time can be used a key control variable to maintain mill power. This can be achieved by using proper blending of feed to ensure a constant load size distribution in the mill, thereby reducing overall variability inside the mill.

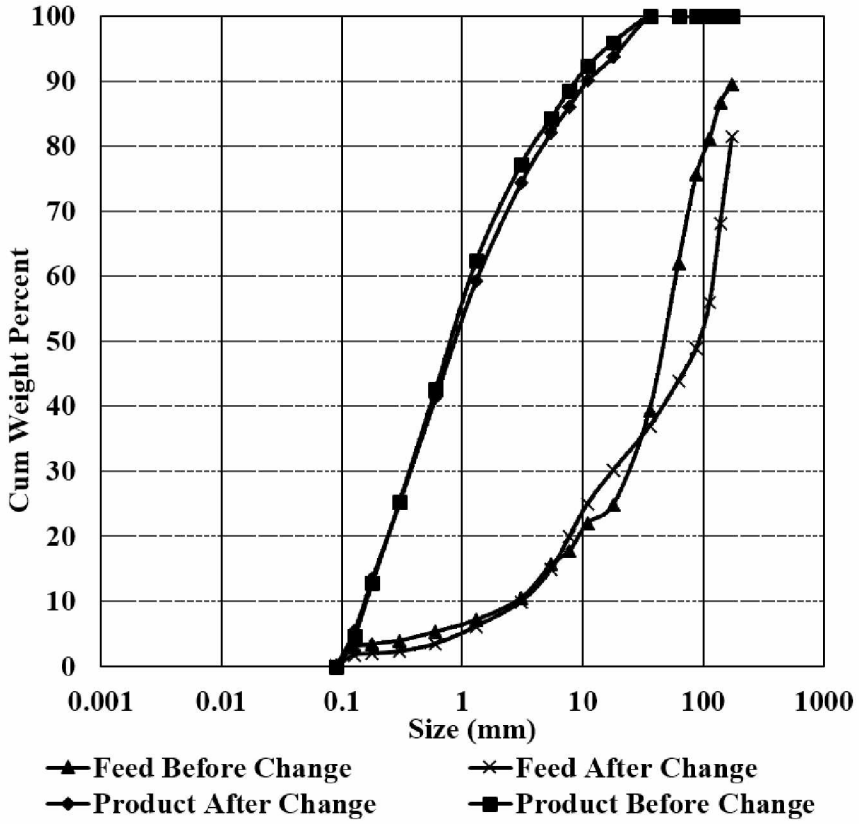

Figure 45: Change in feed size distribution

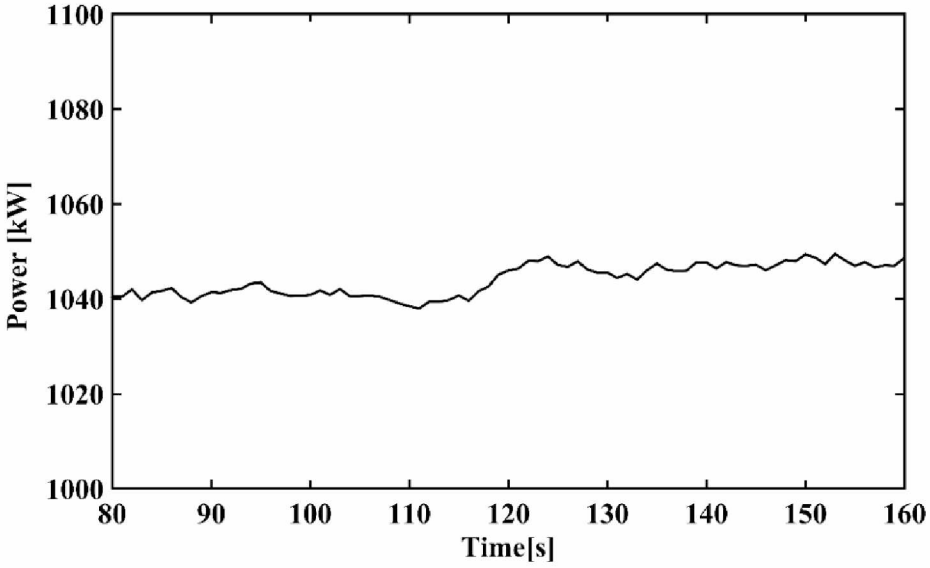

Figure 46: Effect of change in feed size distribution on mill power

4.3.2 Effect on remaining circuit variables

The effect of change in feed size distribution was only limited to the SAG mill and no change was observed for other variables. Despite the coarse product being discharged from the SAG mill; the ball mill was able to grind out the coarse material. This indicates the robustness of a conventional grinding circuit to disturbance in size distribution.

4.4 Increase in cyclone sump water

Sump water addition is an important control variable responsible for cyclone performance. Sump water is used to control the hydrocyclone feed percent solids and flow rate. Both variables significantly affect the cyclone cut size thereby altering the dynamics of the circuit. The effect of change in sump water was also studied. An increase in sump water was introduced at t = 150 s from 60 m^3/hr to 120 m^3/hr. The increase resulted in a decrease in the percent solids in feed to cyclone and increase in the flow rate. As a result of increase the d_{50c} of the cyclone decreased from 72 µm to 65 µm (Figure 47). This significant decrease resulted in finer separation with more particles reporting to underflow stream. This increased the recirculating load to 650 percent causing ball mill power to increase (Figure 49 and Figure 48).

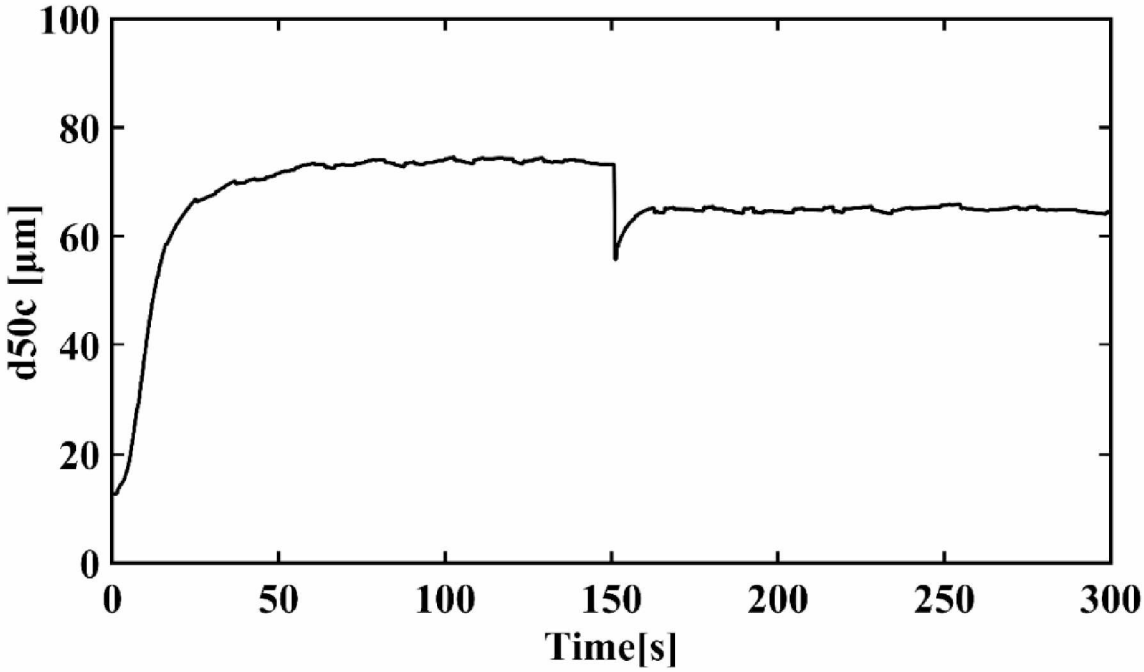

Figure 47: Effect of change in sump water on cyclone d50c

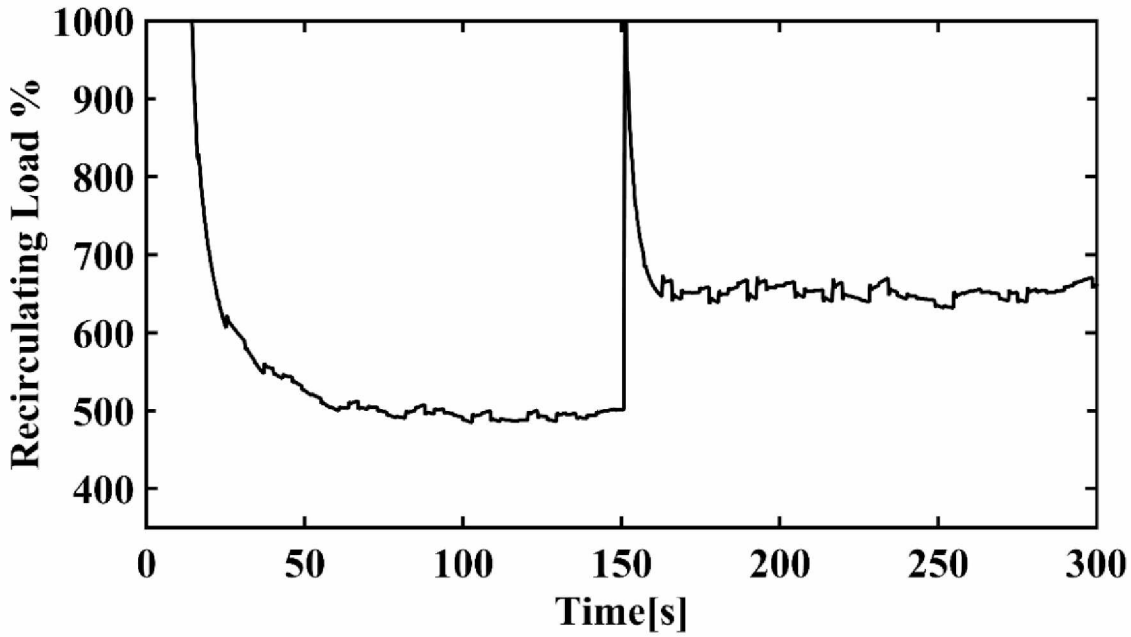

Figure 48: Effect of change in sump water on recirculation

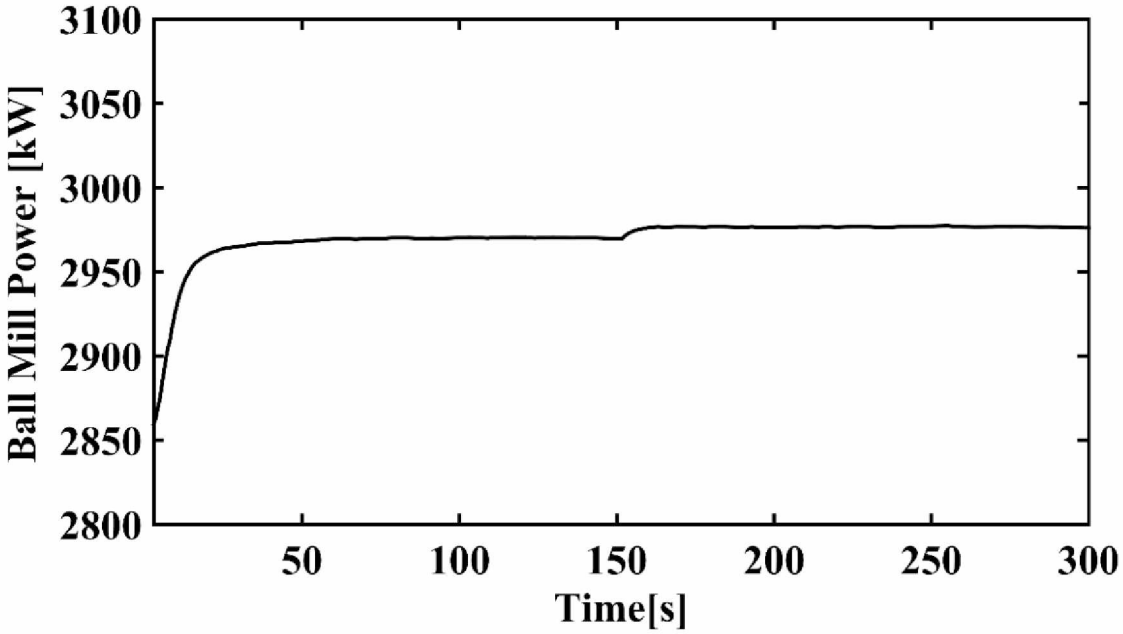

Figure 49: Effect of change in sump water on ball mill power

The dynamic simulation approach helped to analyze the effects of change in important variables of a grinding circuit. The simulation was able to capture real time dynamics observed in a mill plant. However, the cases presented were simplified versions in which a change in a single variable was introduced at one time. The simulator can also be used to analyze the effect of change in multiple variables. The dynamic simulation approach demonstrated that it can easily capture non-linear interaction in a multi-component system and has a great potential for other mineral processing processes. The application of the dynamic simulation approach is further extended by designing a neural network controller, which is discussed in the next chapter.

CHAPTER 5 APPLICATION AND CONCLUSION

The previous chapter detailed how dynamic simulation can be helpful in developing an understanding of the complex grinding process. The case study presented can be used to understand process dynamics and to train operators from an industrial prospective. This chapter covers another application of the dynamic simulators in designing a neural network based controller. Process control is a well-established technique used in mineral industry to ensure efficient performance of the process and smooth working of the equipment. However, the development of the controllers requires process knowledge to model the relationships between the manipulated and control variables. This becomes a challenging task when there are large amounts of variables involved. The problem lies not only in identifying the variables truly affecting process and control variables, but how to encapsulate the relationships for a wide range of operating conditions, which are mostly non-linear.

For this study only the SAG mill was considered for controller design. Because of their high susceptibility to changes in feed rate and ore characteristics they are critical equipment from a control viewpoint. SAG mill controllers are designed to maintain the mill power within acceptable limits. Conventional controllers such as PID have failed to perform effectively as they are based on feedback logic. In some cases, the response of PID was implemented when the situation had gone out of control. Thus, information of control variable (mill power) in advance is needed which may take necessary action beforehand for smooth working of the process by maximizing equipment availability.

The application of neural network for such continuous systems have been practiced before in the field of control and system engineering and signal processing. The applicability of one such special class of neural network known as non-linear auto regressive with exogenous inputs (NARX) was studied for non-linear dynamic systems such as grinding. Pani and Mohanta (2015) demonstrated the application of

time delay neural network (TDNN; a class of NARX) to fine tune SAG mill feed particles size. For this study, the NARX structure was used to predict mill power based on feed data and mill power data of previous time steps. The dynamic simulator was used in generating data for different operating conditions. The performance of the network using different numbers of neurons, training algorithms, and TDL was also studied.

5.1 Modeling

A neural network based time series auto-regressive model was developed. Feed rate and power data of previous time steps were used to predict mill power at future time steps. The modeling strategy and network architecture are described below.

5.1.1 Neural Network Modeling

Neural networks are the computing systems made up of highly interconnected functions, known as neurons, which process information by dynamic state response to external inputs. Neural networks have a wide applicability in system identification and process control and can be used for pattern classification and function approximation to map any nonlinear functions. Figure 50 shows typical structure of a single neuron, consisting of inputs as a weighted sum of each other. The sum is passed through a transfer function, which can be linear, hyperbolic, sigmoid, etc., chosen on the applicability for which the network is to be designed. As this study was focused on modeling a time series, the network was used for function approximation. Several neurons are selected and arranged in different layers to lay the network architecture based on complexity of the problem.

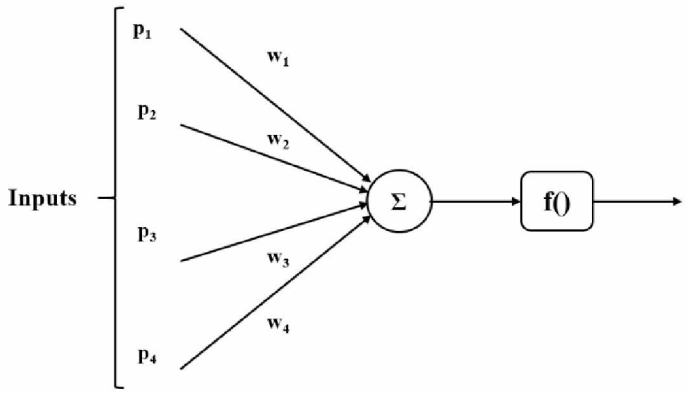

Figure 50: Structure of a Neuron

Once the network architecture is chosen they are trained on the data. Training involved iteratively adjusting weights and biases assigned to various inputs by comparing them with the targets, thereby minimizing the objective function. The comparison can be of any form such as mean square error, sum of square error, mean absolute percent error, etc. Eq (65) describes the functional form of mean square error (MSE) which was used for this problem. The method can be regarded as an estimation of parameters in a regression model by minimizing MSE.

$$F(x) = \sum_{q=1}^{Q} e^T e \tag{65}$$

$$e = (t_q - a_q) \tag{66}$$

where e is the error, t_q represent target, a_q is the network output, and Q is the number of data targets

The network structure 2-20-1 (1 hidden layer and 1 output layer) was used to model a multiple input single output (MISO) SAG system. Tangent hyperbolic functions were used as a transfer function in a hidden layer with a pure linear function in the output layer (Figure 51). The inputs consisted of the feed rate to the mill and the mill power to predict the power at next time step.

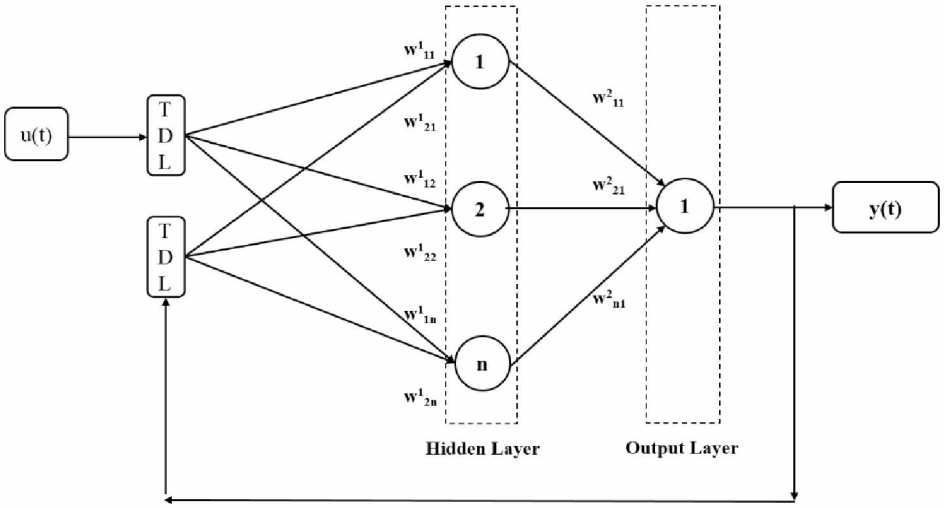

Figure 51: Network architecture used

The network was trained on the generated data using two different training algorithms; Levenberg Marquardt Back Propagation (LMBP) and Bayesian Regularization (BR). Both algorithms vary on the method they employ to adjust network parameters (i.e., weight and bias) to minimize the error function. LMBP is based on a modified version of the Gauss-Newton method in which the weights are updated as per the following rule:

$$w_{k+1} = w_k - [J^T J + \mu_k I]^{-1} J^T E_k \quad (67)$$

where w_{k+1} is the weight update at k+1-time step using previous weight w_k, Jacobian matrix; J, learning rate; μ_k, error vectors E_k at k step and the identity matrix I. The advantage of LMBP is, that it has faster convergence because it doesn't require computation of a Hessian matrix. However, one limitation of the use of LMBP is that they are focused on minimizing the error function which results in overfitting of the network. As there exist no fixed rule to determine the number of neurons in a network, the problem was resolved by use of the BR method. BR method penalizes for more neurons in the network to prevent overfitting by using the objective function as a weighted sum of MSE and squared parameters (Eq (68)). The parameter α/ß is called the regularization parameter, determined using

Bayesian analysis, Eq (69). The posterior distribution of weights is determined assuming a Gaussian density function for the likelihood and priors.

$$F(x) = \alpha \sum_{i=1}^{n} w_i^2 + \beta \sum_{q=1}^{Q} e^T e \quad (68)$$

where α, ß are the regularization parameters, w_i is the weight, and e is the error derived using Eq (66)

$$P(\boldsymbol{w}|\, Data, \alpha, \beta, M) = \frac{P(\, Data|\boldsymbol{w},\alpha,\beta,M)P(\boldsymbol{w}|\alpha,\beta,M)}{P(\, Data|\alpha,\beta,M)} \quad (69)$$

where P (**w** | Data, α, ß, M) is the posterior distribution of weights, P (Data **|** **w,** α, ß, M) is the likelihood function, P (**w |** α, ß) is prior distribution for weights, P (Data **|** α, ß, M) in the denominator is a normalizing constant, and M is the network structure.

5.1.2 NARX Modeling

The non-linear auto-regressive model with exogenous inputs (NARX) is a class of non-linear technique employed to model any non-linear dynamic system. They are also considered an extended version of linear ARX models which offer advantage over the conventional ARX method to model any chaotic and noisy time series (Becerikli & Oysal, 2007). The general form of equation describing a NARX model is given by:

$$y(t) = f\left(y(t-1), y(t-2), \ldots y\left(t-n_y\right), u(t-1), u(t-2), \ldots u(t-n_u)\right) + w(t) \quad (70)$$

where u(t) and y(t) denote the input and output variables of the system, respectively. n_u and n_y are the delay order for both input and output provided, nu < n_y. f() is the non-linear mapping function dependent upon the choice of network architecture and transfer functions used, and w is the random error (Menezes & Barreto, 2008). There are different variations of this technique when laying the network architecture such as series-parallel mode and parallel mode. The underlying difference between the two is that in the series mode the estimated

output is regressed upon the incoming input signal, whereas in series-parallel mode, the incoming input signals are regressed upon the original output of previous time steps. For mill power prediction model series-parallel mode of network architecture was used at different tapped delay lengths (TDL) of 2, 4 and 6 minutes (Figure 51). Typical representation of the input vector to network for the TDL of 2 minutes is given as:

$$\boldsymbol{p} = \begin{bmatrix} u(t) \\ u(t-1) \\ y(t-1) \\ y(t-2) \end{bmatrix} \tag{71}$$

It can also be seen from Eq (71) that the complexity of the network is increased as the TDL is increased, which will cause the input vector to grow and require more parameters to fit the network. The entire network parameters are summarized in Table 6.

Table 6: Network summary

Parameters	Description
Inputs	• Feed rate at current time, f(t) • Predicted mill power of previous time steps, p(t-2) …. p(t-4) … p(t-6)
Output	• Mill power at current time, p(t)
Training algorithm	• Levenberg Marquardt Back Propagation (LMBP) • Bayesian Regularization (BR)
Cost function	• For LMBP $F(x) = \sum_{q=1}^{Q} e^T e$ • For BR $F(x) = \alpha \sum_{i=1}^{n} w_i^2 + \beta \sum_{q=1}^{Q} e^T e$
Number of data points	4200

5.2 Discussion

The network described in the previous section was trained on simulated data and the network performance was evaluated at different numbers of neurons, TDL and training algorithm. It was found that network performance was higher when the LMBP was used as the training algorithm when compared to BR, which is well justified as it focuses completely on minimizing the objective function. The network performance for LMBP was better when the network was trained on 40 neurons when compared to 20; however, the difference was not that significant (Figure 52). The network performance also improved with increase in delay length from 2 to 4

indicating the process to be 4th order. Further increasing the delay length did not produce much change in MSE.

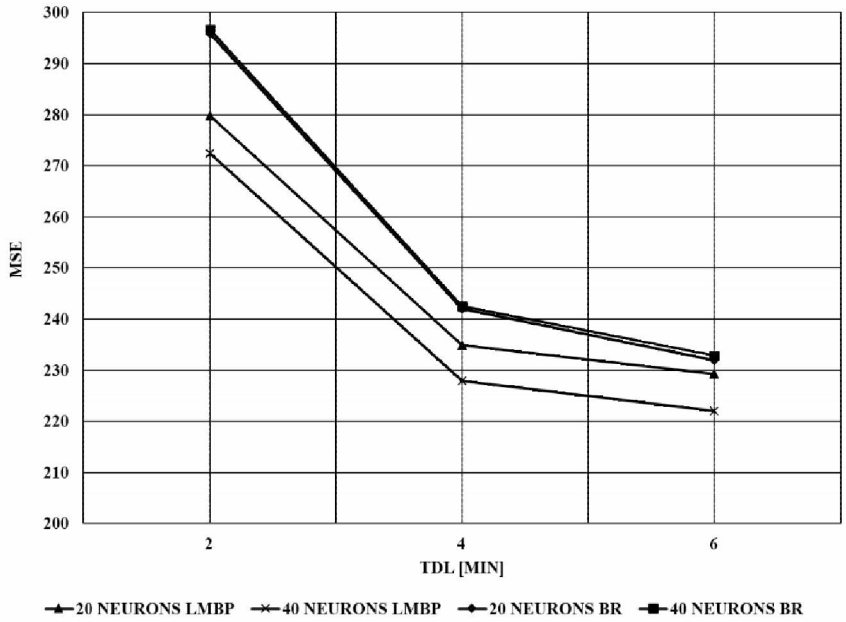

Figure 52: MSE using different algorithm at different TDL

In case of BR algorithm, the network performance improved when the TDL was increased from 2 to 4 resembling the same order obtained using LMBP. However, there was no change in the network performance with variation in number of neurons indicating that 20 neurons are sufficient to fit the above model to prevent overfitting of the network. Another observation when training using the BR algorithm was that the effective number of parameters for TDL of 4 was in the range of 30 to 40 from a total of 201 and 401, for 20 and 40 neurons, respectively. This shows that the network can be mapped with less number of neurons with considerable degree of accuracy.

The network was tested on an independent data set generated from the simulator at different operating conditions. Figure 53 and Figure 54 show a plots of network prediction with actual operating data and error for BR algorithm indicating that the

network was able to predict the mill power with good accuracy with error lying in the range of $\pm$ 5 percent of maximum operating power.

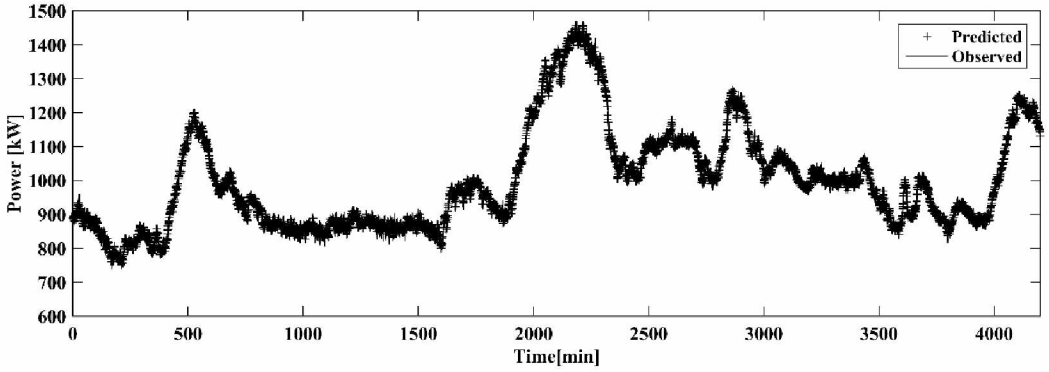

Figure 53: Response Plot

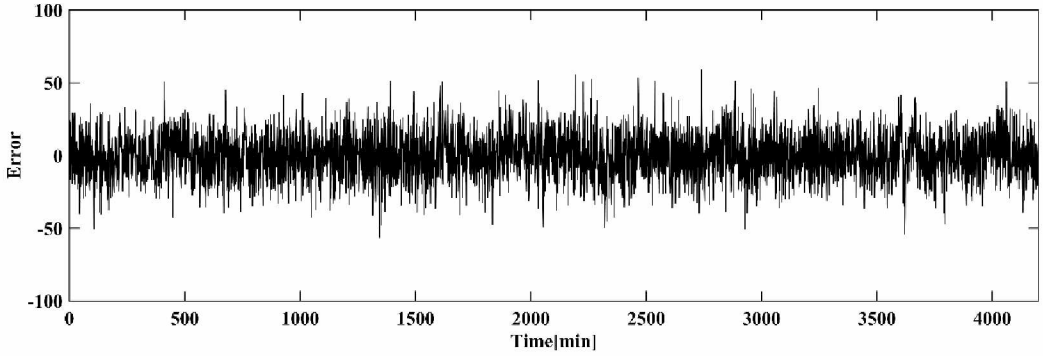

Figure 54: Error Plot

The designed network can be implemented as feedback controller to control the mill power to a desired reference point by changing feed rate to the mill. In reality, the network prediction may not be as accurate as tested on simulated data. As mentioned earlier, in a real situation the feed characteristics are not constant with time. Hence, for more accurate performance in industries the network training using simulated data should include variable feed size distribution and hardness parameter coupled to Whiten's content based model.

5.3 Conclusion

Steady state simulators which exist in the mineral industry have limited usage and cannot be used in studying transient response of the system or for practicing control strategy. A library of dynamic mathematical models was developed in this research with an intent to simulate mineral processing operations in real time. Process variables crucial from an operational point of view were identified for all equipment. Models were developed to predict response of such variables for different operating conditions. The parameters of the models were evaluated utilizing design and process data obtained from the mine. The models of the equipment were validated by simulating under the same condition as that of the plant. The validated model library was later interlinked in specific order to produce the flowsheet of the mine in consideration.

Simulation runs were performed for various operating conditions by changing manipulated variables and introducing disturbance to the system. The effect of introduced changes and disturbances were analyzed. The complexity of the process escalated as changes progressed to subsequent equipment of the flowsheet. In the case presented changes were introduced in one variable at a time which may even become more complex when introduced to multiple variables. The models also provided the information of the variables which cannot be measured directly in the industry. This can be used for inferring such variables and may provide a new insight to the process. The developed model library was kept generic and can be tuned to any other operating mill plant. Thus, it can be utilized for training purposes by producing flowsheets of any configuration.

Finally, the application of the simulator in development of a controller for the SAG mill was presented. A neural network based controller was designed using the simulated data to predict mill power by varying the feed rate from 85 tph to 125 tph. NARX neural network architecture was chosen which utilizes the past values of mill power and feed rate to predict the future values. The network was trained

using two different training algorithms Levenberg-Marquardt and Bayesian regularization algorithm. Network performance and relative convergence using both training algorithms showed LM performed better. The controller was then implemented to the SAG mill. The controller performed well and was able to limit SAG mill power close to the reference point supplied by the user by varying the feed rate. The simulator demonstrated the possibility of designing and testing a predictive controller for a mineral processing operation. Similar networks can be designed for controlling other process variables as well and in practicing different control strategies.

Other salient features which were drawn from the study are listed below:

1. Dynamic simulation provided a new approach to determine the conditions prevailing in the mills. It helped in understanding how the changes in ore characteristics and operating conditions affect the breakage process within the mill which in turns affects the other response variables essential from control objective such as power draw.
2. Consequently, the effect of increase in water flow rate to the mill caused an increase in the discharge rate parameter. This resulted in a coarser grind and deterioration of the product quality.
3. The dynamic simulation provided information about variables such as the amount of rock charge (mill load) for the SAG mill which are not readily accessible or cannot be measured directly in the industries (Wei and Craig, 2009).
4. Dynamic simulation also helped in understanding interactions among variables which often pose challenges in designing multivariable control schemes in the form of coupling.
5. The choice of training algorithm can aid in determining the number of neurons required to train the network which is a contentious topic in neural network modeling.

6. NARX neural networks are advantageous in comparison to conventional ARX models as they easily allow incorporation of an external input variable (rather than regressing on past values of the same variable) as a predictor, feed rate in this case, thereby increasing the predictability of the model.
7. The BR algorithm provides a tradeoff between MSE and number of parameters (weights and biases) thereby making the network more robust and less susceptible to failure. The predictive capability and network computation time can be greatly improved if the algorithm can be used in a unified framework.
8. The controller implementation demonstrated that dynamic simulation can be used in designing and implementing controllers offline in a safe environment. Thus, using a dynamic simulator can prevent control engineers from going through a rigorous task of data collection without actually operating the equipment in different conditions.

5.4 Scope for future work

The scope for further research in this area includes:

1. The model library can be enriched in terms of ore characteristic data in collaboration with various mines. This can help in replacing the generic appearance function with true ore breakage distribution functions specific to a mine, thereby improving the model performance.
2. There exists no direct procedure for estimation of breakage rate within the mill, which is still estimated using a back-calculation procedure. This accounts for any uncertainty in other parameters (i.e., breakage distribution and discharge rate) and may not result in a true value of breakage rate. A careful study on different mills can help in identifying a functional form of breakage rate.
3. The ore parameter in the Whiten model equation, i.e. appearance function was kept constant during the simulation. This parameter changes with

respect to the ore work index and it is recommended for the future work as a variable to be updated with change in ore characteristics. The appearance function has already been related to specific energy and family of t-curves which provides breakage distribution of particles at different specific energy supplied (Napier-Munn, 1996), incorporating multiple distributions to the simulator and updating it with respect to change in ore-characteristics. An alternate can be the incorporation of a hardness parameter coupled with appearance function. This is expected to improve the predictive capabilities of the simulator.

4. The model library is restricted to the grinding circuit which can be expanded to other equipment and processes.

REFERENCES

Apelt, T., Asprey, S., & Thornhill, N. (2001). Inferential measurement of SAG mill parameters. *Minerals engineering, 14*(6), 575-591.

Apelt, T., & Thornhill, N. (2009). Inferential measurement of SAG mill parameters V: MPC simulation. *Minerals Engineering, 22*(12), 1045-1052.

Asbjörnsson, G. (2013). *Modelling and Simulation of Dynamic Behaviour in Crushing Plants* (Doctoral dissertation, Chalmers University of Technology, Göteborg, Sweden). Retrieved from http://chalmers.summon.serialssolutions.com/#!/

Austin, L. G. (1971). Introduction to the mathematical description of grinding as a rate process. *Powder Technology, 5*(1), 1-17.

Austin, L. G., & Luckie, P. T. (1972). Methods for determination of breakage distribution parameters. *Powder Technology, 5*(4), 215-222.

Becerikli, Y., & Oysal, Y. (2007). Modeling and prediction with a class of time delay dynamic neural networks. *Applied Soft Computing, 7*(4), 1164-1169.

Bond, F. C. (1961). *Crushing and grinding calculations*: Allis-Chalmers Manufacturing Company.

Chen, W., Zydek, N., & Parma, F. (2000). Evaluation of hydrocyclone models for practical applications. *Chemical Engineering Journal, 80*(1), 295-303.

Chen, X.-s., Zhai, J.-y., Li, S.-h., & Li, Q. (2007). Application of model predictive control in ball mill grinding circuit. *Minerals Engineering, 20*(11), 1099-1108.

Epstein, B. (1948). Logarithmico-normal distribution in breakage of solids. *Industrial & Engineering Chemistry, 40*(12), 2289-2291.

Flament, F., Thibault, J., & Hodouin, D. (1993). Neural network based control of mineral grinding plants. *Minerals engineering, 6*(3), 235-249.

Ganguli, R., Dutta, S., & Bandopadhyay, S. (2006). Determining relevant inputs for SAG mill power draw modeling. *Advances in Comminution*, 161-168.

Herbst, J., & Fuerstenau, D. (1980). Scale-up procedure for continuous grinding mill design using population balance models. *International journal of mineral processing, 7*(1), 1-31.

Hodouin, D. (2011). Methods for automatic control, observation, and optimization in mineral processing plants. *Journal of Process Control, 21*(2), 211-225.

Hukki, R. (1961). Proposal for a solomonic settlement between the theories of von Rittinger, Kick and Bond. *Trans. AIME, 220*, 403-408.

Kick, F. (1885). Das Gesetz der proportonalen Winderstande und Wissenschaftsanwendung. *Felix, Leipzig*.

Klimpel, R., & Austin, L. (1977). The back-calculation of specific rates of breakage and non-normalized breakage distribution parameters from batch grinding data. *International journal of mineral processing, 4*(1), 7-32.

Liu, Y., & Spencer, S. (2004). Dynamic simulation of grinding circuits. *Minerals engineering, 17*(11), 1189-1198.

Lynch, A., & Bush, P. (1977). *Mineral crushing and grinding circuits: their simulation, optimisation, design, and control* (Vol. 1): Elsevier Scientific Pub. Co.

Lynch, A., & Rao, T. (1975). *Modelling and scale-up of hydrocyclone classifiers.* Paper presented at the Proceedings of the 11th International Mineral Processing Congress, Cagliari.

Menezes, J. M. P., & Barreto, G. A. (2008). Long-term time series prediction with the NARX network: An empirical evaluation. *Neurocomputing, 71*(16), 3335-3343.

Morrell, S. (1992). Prediction of grinding-mill power. *Institution of Mining and Metallurgy Transactions. Section C. Mineral Processing and Extractive Metallurgy, 101.*

Morrell, S. (1996). Power draw of wet tumbling mills and its relationship to charge dynamics. Pt. 1: a continuum approach to mathematical modelling of mill power draw. *Transactions of the Institution of Mining and Metallurgy. Section C. Mineral Processing and Extractive Metallurgy, 105.*

Moys, M. (1972). The control of autogenous and semi-autogenous mills: the relationship between measurements of bearing pressure and parameters describing the mill load. *Journal of the Southern African Institute of Mining and Metallurgy, 72*(11), 401-408.

Moys, M. (1993). A model of mill power as affected by mill speed, load volume, and liner design. *Journal of the Southern African Institute of Mining and Metallurgy, 93*(6), 135-141.

Mular, A. L., & Bhappu, R. B. (1978). *Mineral processing plant design*: Society of Mining Engineers of the American Institute of Mining, Metallurgical, and Petroleum Engineers.

Mular, A. L., Halbe, D. N., & Barratt, D. J. (2002). *Mineral processing plant design, practice, and control proceedings*: SME.

Nageswararao, K. (1999). Reduced efficiency curves of industrial hydrocyclones-an analysis for plant practice. *Minerals engineering, 12*(5), 517-544.

Nageswararao, K., Wiseman, D., & Napier-Munn, T. (2004). Two empirical hydrocyclone models revisited. *Minerals Engineering, 17*(5), 671-687.

Napier-Munn, T. J. (1996). *Mineral comminution circuits ; their operation and optimisation*. Queensland, Australia: Julius Kruttschnitt Mineral Research Centre.

Napier-Munn, T. J., & Lynch, A. (1992). The modelling and computer simulation of mineral treatment processes—current status and future trends. *Minerals engineering, 5*(2), 143-167.

Pani, A. K., & Mohanta, H. K. (2015). Online monitoring and control of particle size in the grinding process using least square support vector regression and resilient back propagation neural network. *ISA transactions, 56*, 206-221.

Plitt, L. (1976). A mathematical model of the hydrocyclone classifier. *CIM bulletin, 69*(776), 114-123.

Pomerleau, A., Hodouin, D., Desbiens, A., & Gagnon, É. (2000). A survey of grinding circuit control methods: from decentralized PID controllers to multivariable predictive controllers. *Powder Technology, 108*(2), 103-115.

Ramasamy, M., Narayanan, S., & Rao, C. D. (2005). Control of ball mill grinding circuit using model predictive control scheme. *Journal of Process Control, 15*(3), 273-283.

Reid, K. (1971). Derivation of an equation for classifier-reduced performance curves. *Canadian Metallurgical Quarterly, 10*(3), 253-254.

Salazar, J.-L., Valdés-González, H., Vyhmesiter, E., & Cubillos, F. (2014). Model predictive control of semiautogenous mills (sag). *Minerals Engineering, 64*, 92-96.

Salazar, J., Magne, L., Acuna, G., & Cubillos, F. (2009). Dynamic modelling and simulation of semi-autogenous mills. *Minerals Engineering, 22*(1), 70-77.

Sbárbaro, D. (2010). Dynamic Simulation and Model-based Control System Design for Comminution Circuits *Advanced control and Supervision of Mineral Processing plants* (pp. 213-247): Springer.

Sedlatschek, K., & Bass, L. (1953). Contribution to the theory of milling processes. *Powder Metall. Bull, 6*, 148-153.

Stange, W. (1993). Using artificial neural networks for the control of grinding circuits. *Minerals engineering, 6*(5), 479-489.

von Rittinger, R. (1867). Textbook of mineral dressing. *Ernest and Korn.*

Wei, D., & Craig, I. K. (2009). Grinding mill circuits—a survey of control and economic concerns. *International journal of mineral processing, 90*(1), 56-66.

Whiten, W. (1972). The simulation of crushing plants with models developed using multiple spline regression. *Journal of the Southern African Institute of Mining and Metallurgy, 72*(10), 257-264.

Whiten, W. (1973). Simulation and model building for mineral processing.

Whiten, W. (1974). A matrix theory of comminution machines. *Chemical Engineering Science, 29*(2), 589-599.

Wills, B. A., & Finch, J. (2015). *Wills' mineral processing technology: an introduction to the practical aspects of ore treatment and mineral recovery*: Butterworth-Heinemann.

APPENDICES

Appendix A. Design Data of Process Units Used in Models

SAG Mill

Mill diameter [m]	6.679
Mill length [m]	2.21
Center Line Length [m]	3.47
Belly Length [m]	2.51
Mill speed fraction of critical	0.7338
Fractional filling of mill with balls	0.05-0.1
True density of balls [t/m3]	7.86
Mill Maximum power [kilowatts]	1678
Mill-No-Load Power [kW]	147
Grate Aperture Size [mm]	15
Operating Feed Range [tph]	90-120
Percent Solids	65-75

Appearance Function					
	-16 + 13.2	-22.4 + 19.0	31.5 + 26.0	-45.0 + 37.5	-63.0 + 53.0
t10	Ecs (kWh/t)				
10	0.24	0.2	0.18	0.15	0.13
20	0.51	0.44	0.38	0.33	0.28
30	0.82	0.71	0.62	0.53	0.46

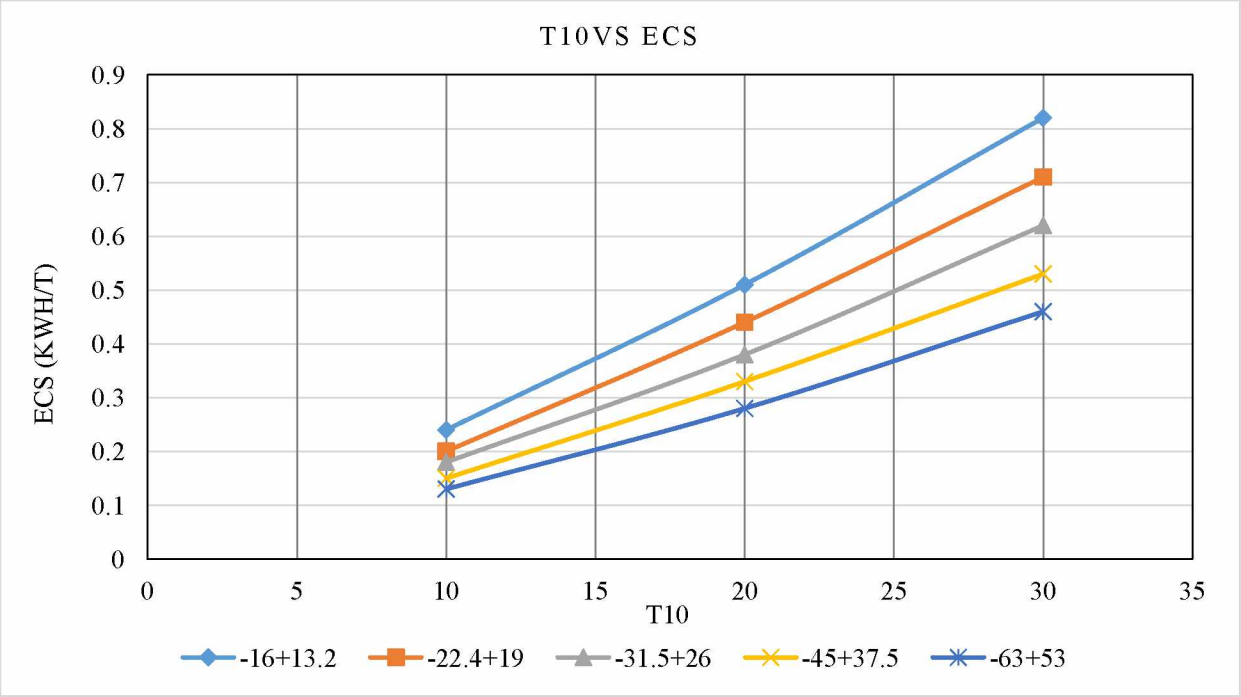

Figure 55: Plot OF t10

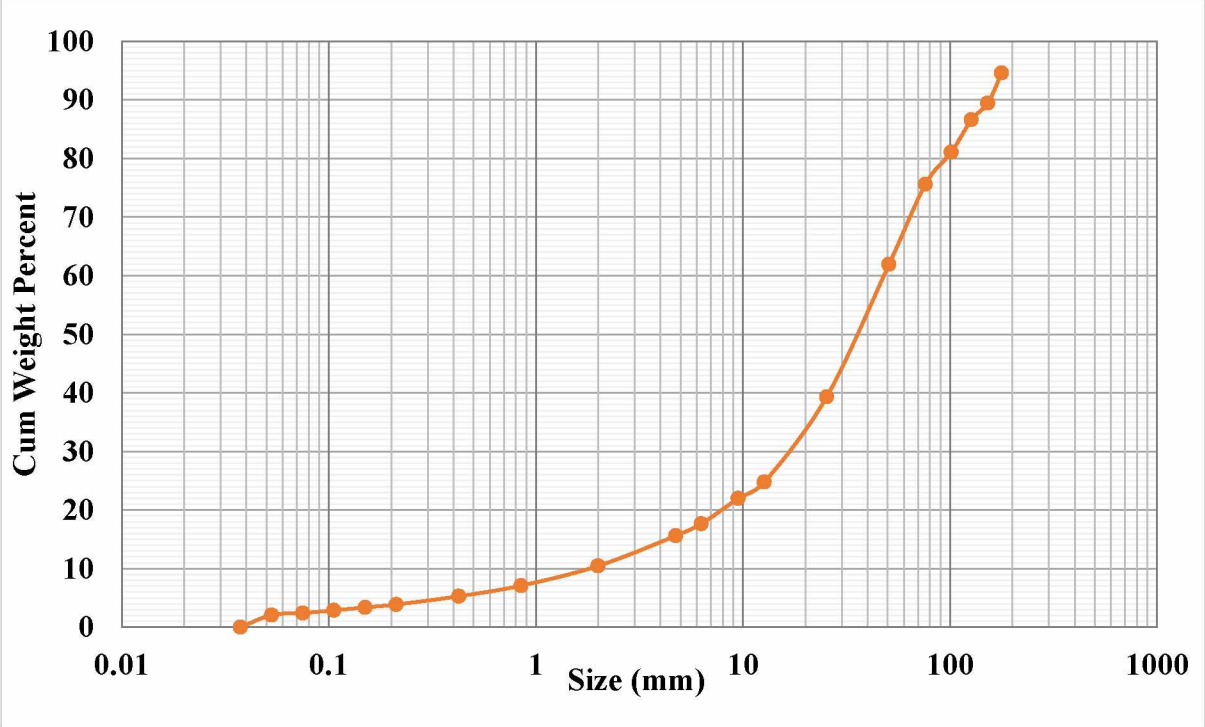

Figure 56: SAG Feed Size Distribution

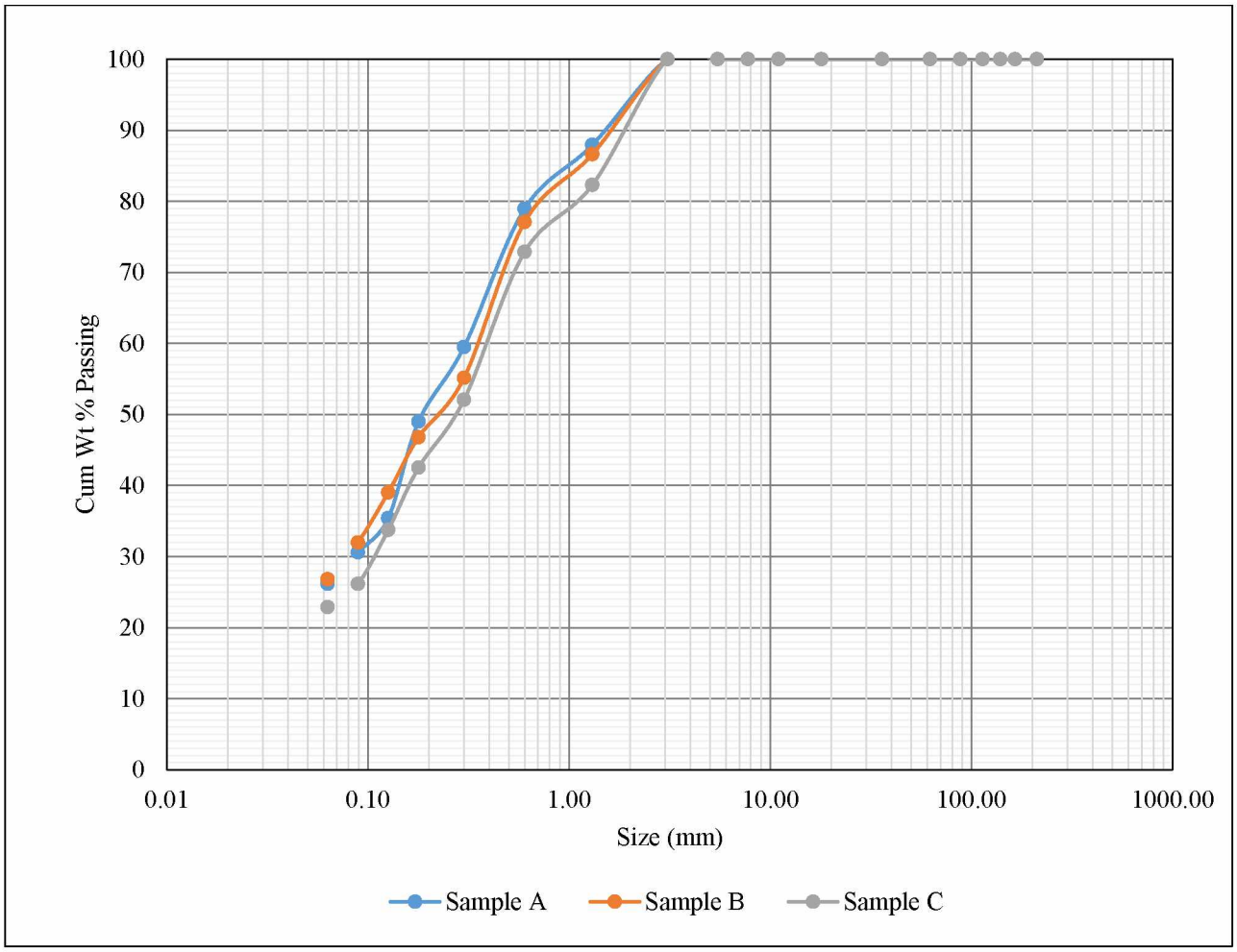

Figure 57: SAG Product size distribution of three different samples obtained during the circuit survey

Ball Mill

Mill diameter [m]	5.0
Mill length [m]	8.7
Mill speed fraction of critical	0.66
Fractional filling of mill with balls	0.35
True density of balls [t/m3]	7.86
Mill power [kilowatts]	3430
Operating Feed Range [tph]	90-120
Percent Solids	65-72

Screen

Screen Aperture Size [Mesh]	16
Alpha	4.00
R_f	0.40
d_{50C} [mm]	1.00

Hydrocyclone

Number of cyclones in parallel	5 or 6
Cyclone Cylinder Diameter - Dc [m]	0.254
Equivalent Inlet Diameter - Di [m]	0.1
Vortex Finder Diameter - Dv [m]	0.063
Spigot (Apex) Diameter - Ds [m]	0.057
Free vortex height - h [m]	1.732
Hydrodynamic exponent (0.5 for laminar) - k	1
Liquid Viscosity - ɳ [cP]	1-10
d50c scaling - F1	1
P scaling - F2	1
S scaling - F3	1
m scaling - F4	1

Appendix B. Code for Mill Model

```
function y = appearance_fcn(aij)

% The function accepts the appearance function vector provided by user and

% converts to nxn matrix where, n is the length of size class.

n = length(aij);      % Calculate length of a appearance vector

ii  =  diag(aij)*ones(n);          % converting it to a matrix of symmetric matrix of size nxn

 for i = 2: n

   for j = 2 : n

      ii(j,i) = ii(j-1,i-1);

      j = j + 1;

   end

   i = i + 1;

end

y = tril(ii);              % final aij
```

Breakage function calculation from spline parameter

```
function y = breakage_rate(size_range, knots, r,f)

 % knots = size knots where breakage values are known

% r = Breakage rate at size knots

% size_range = mean of size class
```

```
lnsize_range = log(knots);

ln_r = log(r);

spline_cal = spline(lnsize_range, ln_r,log(size_range));          % Spline
Interpolation

br = exp(spline_cal);

brate_matrix = k*diag(br);                                % Final Selection Matrix

y = brate_matrix ;
```

Appendix B. Code for Mill Model Cont

Discharge rate function

```
function y = discharge_rate(alpha,size_range,d50c,dmax)

% The function evaluates discharge rate matrix

n = length(size_range);

rs = 1:n;                % Intermediate variable to store values of d/d50c

Eu = 1:n;                % Partition Number array to discharge stream

for j = 1:n

   rs(j) = size_range(j)/d50c;

   Eu(j) = 1 - ((exp(alpha*rs(j))-1)/(exp(alpha*rs(j))+exp(alpha)-2));

   j = j+1;

end

disc_rate = dmax*Eu;

y = disc_rate;
```

Appendix C. Mill solid content architecture

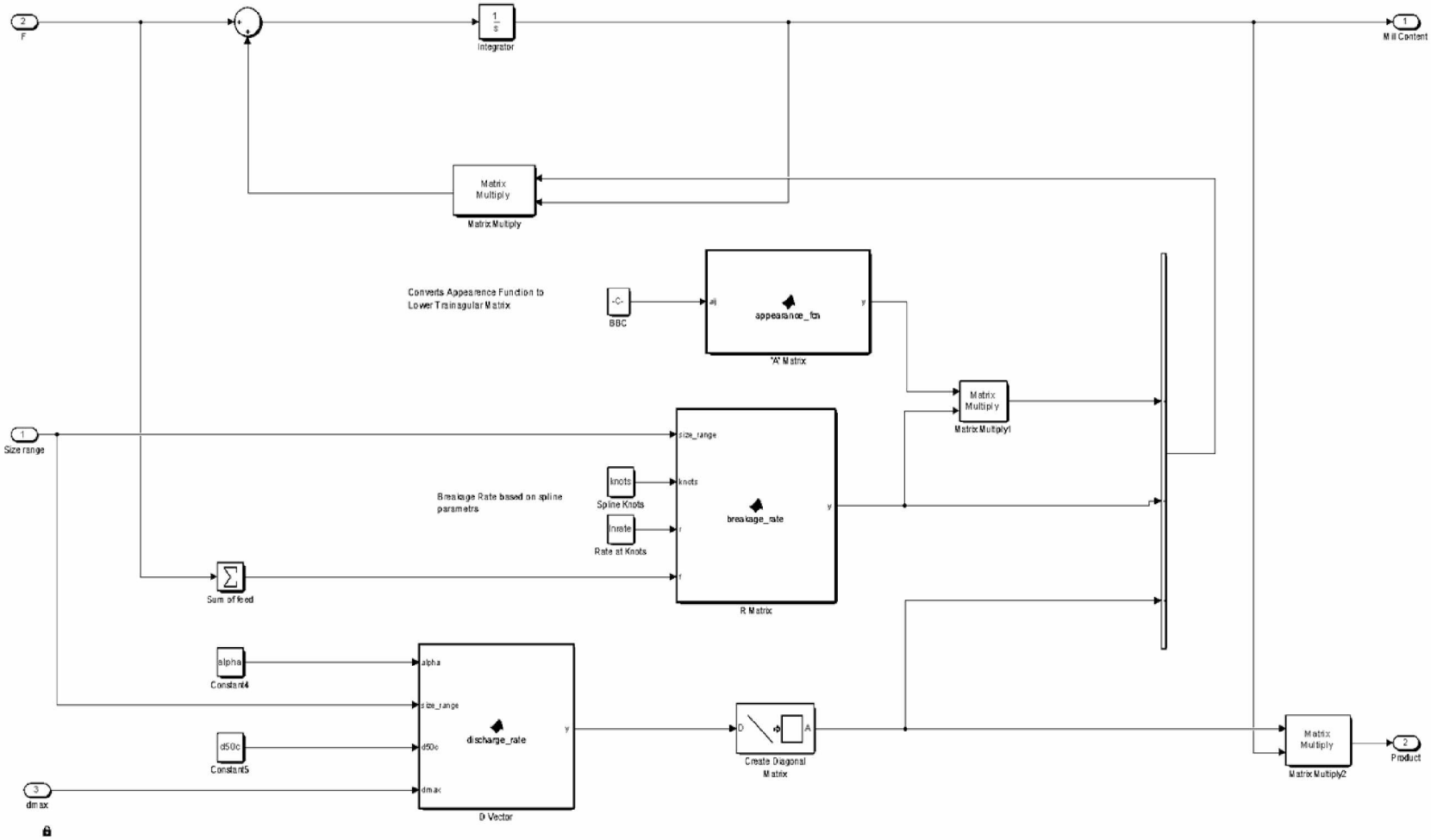

Appendix D. Code for Cyclone

```
function [d50c,m , Rv ,Cv,P] = Plitts_cyclone(solid_tph,water_tph, des_par,mod_par,NN)

%% Cut size prediction

% Design Parameters

% NN = number of cyclones

Di = des_par(1) ;                    % Inlet Diameter in cm

Do = des_par(2) ;                    % Overflow Diameter in cm

Dc = des_par(3) ;                    % Cyclone Diameter in cm

Du = des_par(4) ;                    % Apex Diameter in cm

h =  des_par(5) ;                    % Distance b/w apex and vortex

n =  des_par(6) ;                    % Liquid Viscosity in centiPoise, I have assumed 1 which is of water

k =  des_par(7) ;                    % Hydrodyanamic expoent, Default value of 0.5 for Laminar Flow, To be estimated from data

ps = des_par(8) ;                    % Density of solids

F1 = mod_par(1);                     % Parameter

% Cv, percent solid by volume

Qf = ((solid_tph/ps) + water_tph)/NN ;      % Feed Volumetric Flow rate per cyclone

Qf1 = Qf*16.667 ;                    % Flow rate of feed converted to L/Min (from m3/hr)

pp = (solid_tph + water_tph)/(Qf*NN);        % Pulp Specific Gravity
```

```
Cv = (solid_tph/ps)*100/(Qf*NN) ;                % Percent Solids by Volume

d50c=
(F1*39.7*(Dc^0.46)*(Di^0.6)*(Do^1.21)*(sqrt(n))*exp(0.063*Cv))/(1000*(Du^0.71)*(
h^0.38)*(Qf1^0.45)*((ps-1)/1.6)^k);

%%

%% Pressure Drop, Fraction Bypass & Efficiency Curve Parameter

F2 = mod_par(2) ;                                % Parameter

F3 = mod_par(3) ;                                % Parameter

F4 = mod_par(4) ;                                % Parameter

P  =  (F3*1.88*(Qf1^1.8)*exp(0.0055*Cv))/((Dc^0.37)*(Di^0.94)*(h^0.28)*(Du^2  +
Do^2)^0.87);

% pp

S  =  (F4*3.29*(pp^0.24)*((Du/Do)^3.31)*h^0.54*(Du^2  +  Do^2)^0.36*
exp(0.0054*Cv))/(Dc^1.11 * P^0.24);

Rv = S/(1+S);                                    % volumetric flow rate in the
underflow / volumetric flow rate in the feed

m = F2*1.94*((Dc^2*h/Qf1)^0.15)*exp(-1.58*Rv);

%%

function [psd_uf, psd_of,Yield_uf, alpha] = Plitts_efficiency( d50c, m,Rv, Cv, fsd,
size)

% Efficiency Curve

% Number of Size class
```

```
n = length(size);
Eu = 1:n;                          % Partiton Number array
Wu = 1:n;                          % Underflow Weight
Wo = 1:n;                          % Overflow Weight
 % Size is weight distribution in different size class
% Partition Number Calculation
for j = 1:n
    Eu(j) = 1 - exp(-log(2)*(size(j)/d50c)^m);
    Wu(j) = fsd(j)*Eu(j);
    Wo(j) = fsd(j) - Wu(j);
    j = j+1;
end
% Solids Calculation
Yield_uf = sum(Wu);                % Yield to underflow
Yield_of = sum(Wo);                % Yield to overflow
psd_uf = Wu*100/Yield_uf;          % Particle Size distribution of product
psd_of = Wo*100/Yield_of;
% Water Calculation
% alpha = (Rv - (Yield_uf*Cv/10000))/(1-Cv/100);        % Water to u/f /
% was giving wrong results updated on 05/31/2017 as
```

```
alpha = Rv - ((Yield_uf*Cv/10000)/(1-Cv/100));
```

Appendix E. Cyclone architecture

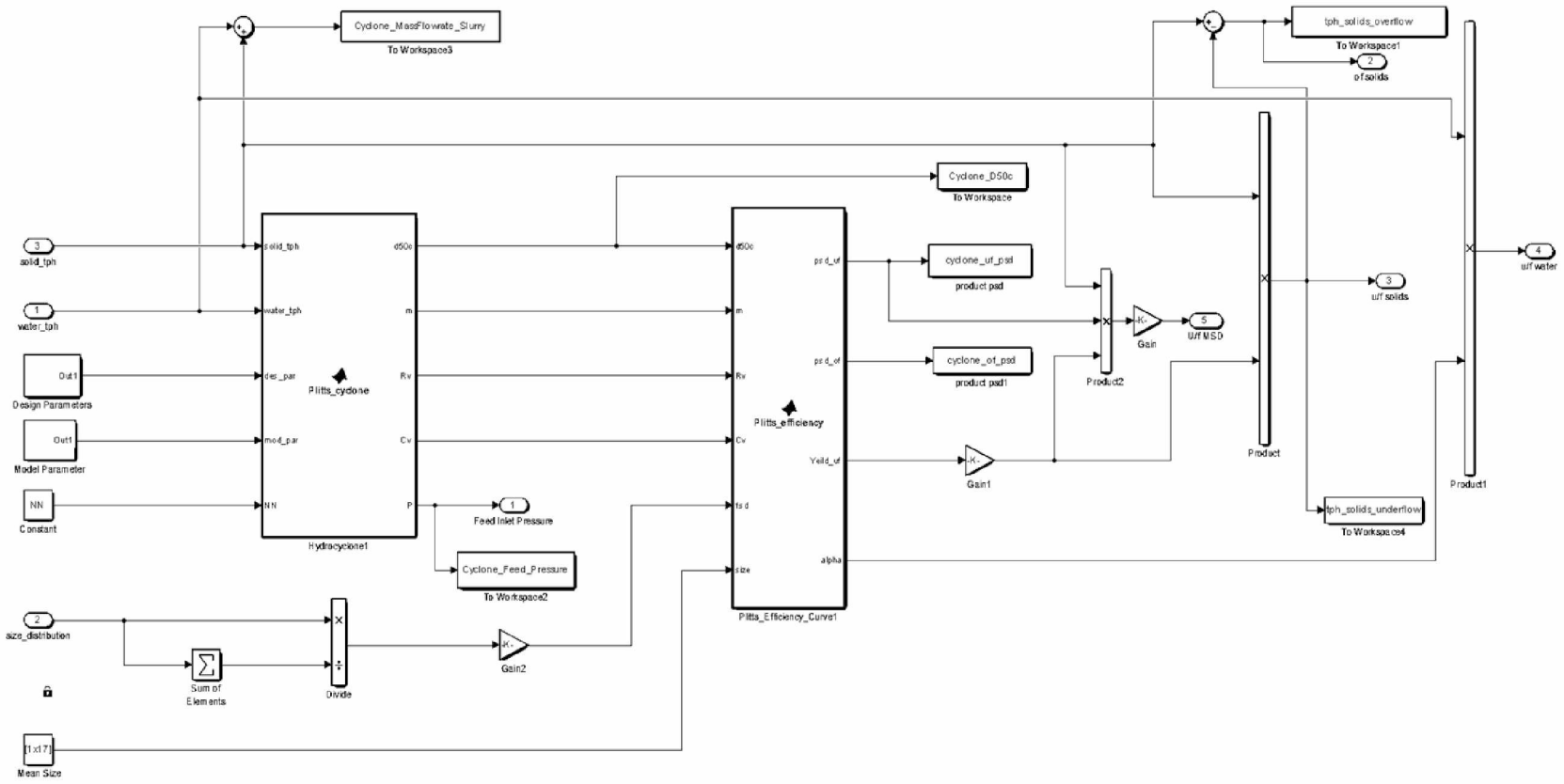

Appendix F. Code for Screen

```
function [psd_os,Yield_os,Yield_us, psd_us,water_us] = screen(size,fsd, water_tph,alpha,d50c,Rf)

% Efficiency Curve

% Number of Size class

n = length(size);

AEos = 1:n;                 % Corrected Partiton Number array to oversize stream

Eos = 1:n;                  % Partiton Number array to oversize stream

Wos = 1:n;                  % Oversize Weight

Wus = 1:n;                  % Undersize Weight

x = size/d50c;

% Partition Number Calculation (Eu) based on Whiten's Equation

for j = 1:n

   Eos(j) = (exp(alpha*x(j))-1)/(exp(alpha*x(j))+exp(alpha)-2);

   j = j+1;

end

% % Actual Partitopn Number (AEu)

for k = 1:n

   AEos(k) = (Eos(k) - Eos(n))/(1-Eos(n));

   Wos(k) = fsd(k)*AEos(k);

   Wus(k) = fsd(k) - Wos(k);
```

```
    k = k+1;
end
% Solids Calculation
Yield_os = sum(Wos);                    % Yield to oversize
Yield_us = sum(Wus);                    % Yield to undersize
psd_os = Wos*100/Yield_os;              % Particle Size distribution of undersize
psd_us = Wus*100/Yield_us;              % Particle Size distribution of oversize
water_os = Rf*water_tph;
water_us = water_tph - water_os;
```